ISSN 2188-286X

マス・フォア・インダストリ研究　No.11

結晶転位の先進数理解析

Institute of Mathematics for Industry
Kyushu University

編　集　松谷　茂樹
佐伯　修
中川　淳一
濵田　裕康
上坂　正晃

九州大学マス・フォア・インダストリ研究所

About the Mathematics for Industry Research

The Mathematics for Industry Research was founded on the occasion of the certification of the Institute of Mathematics for Industry (IMI), established in April 2011, as a MEXT Joint Usage/Research Center – the Joint Research Center for Advanced and Fundamental Mathematics for Industry – by the Ministry of Education, Culture, Sports, Science and Technology (MEXT) in April 2013. This series publishes mainly proceedings of workshops and conferences on Mathematics for Industry (MfI). Each volume includes surveys and reviews of MfI from new viewpoints as well as up-to-date research studies to support the development of MfI.

October 2018
Osamu Saeki
Director
Institute of Mathematics for Industry

Advanced Mathematical Investigation for Dislocations

Mathematics for Industry Research No.11, Institute of Mathematics for Industry, Kyushu University

ISSN 2188-286X

Editors: Shigeki Matsutani, Osamu Saeki, Junichi Nakagawa, Hiroyasu Hamada, Masaaki Uesaka

Date of issue: 7 January 2019

Publisher:

Institute of Mathematics for Industry, Kyushu University

Motooka 744, Nishi-ku, Fukuoka, 819-0395, JAPAN

Tel +81-(0)92-802-4402, Fax +81-(0)92-802-4405

URL http://www.imi.kyushu-u.ac.jp/

Printed by

Social Welfare Service Corporation Fukuoka Colony

1-11-1, Midorigahama, Shingu-machi Kasuya-gun, Fukuoka, 811-0119, Japan

TEL +81-(0)92-962-0764 FAX +81-(0)92-962-0768

結晶転位の先進数理解析

編集　：　松谷　茂樹
佐伯　修
中川　淳一
濵田　裕康
上坂　正晃

Table of contents

はじめに i

プログラム iii

集合写真 iv

数学と物質・材料との連携への展開―転位と回位の数学的記述を事例に― 1
(Propulsion of Collaboration between Mathematics and Materials
-Topics regarding Mathematical Description for Dislocation and Disclination-)
中川淳一 *Junichi Nakagawa (Nippon Steel & Sumitomo Metal Co.)*

結晶中の転位観察と塑性変形現象：現状と課題 11
(On observation of dislocations and phenomena of plastic deformation in crystals)
東田賢二 , *Kenji Higashida (Nat. Inst. Tech. Sasebo)*

液晶における転位と準周期性 55
(Quasi-periodicity and dislocation in liquid crystals)
時弘哲治 , *Tetsuji Tokihiro（The University of Tokyo）*

先進数理解析と結晶の転位問題 77
(Advanced mathematical investigation and dislocations in crystal lattice)
松谷茂樹 , *Shigeki Matsutani (Nat. Inst. Tech. Sasebo)*

結晶構造の数学的記述 Growth 115
(Mathematical Description of Crystal Lattice Structure, Growth)
中川淳一 *Junichi Nakagawa (Nippon Steel & Sumitomo Metal Co.)*
社会数理実践研究
(FMSP mathematical research on real world problems of the University of Tokyo)

転位の連続体の動的理論：微分幾何によるアプローチ 129
(Space-Time Theory of Continuously Distributed Dislocations:
Differential-Geometrical Approach)
甘利俊一 , *Shun-ichi Amari（RIKEN）*

Certain Arithmetic Quasicrystals 147
砂田利一 , *Toshikazu Sunada（Meiji University）*

はじめに

本研究集会 II「結晶転位の先進数理解析」は，研究集会 II「結晶のらせん転位の数理」(2016 年 9 月 3-4 日）と，研究集会 I「結晶の界面，転位，構造の数理」(2017 年 8 月 28-30 日）の成果を発展させるものとして 2018 年 9 月 10 日—11 日に開催した.

結晶は，特殊ユークリッド変換群 SE(3)の離散部分群の作用によって不変である集合として特徴づけられる．2016 年 9 月の研究集会では，らせん転位をこの離散群の対称性の破れとして捉え，代数的な考察による離散幾何の表示とζ関数との関係や，Γ 収束によるモデル化に関する話題にフォーカスし，議論を行った．また，2017 年 8 月の研究集会では，最近の分析装置を用いた観察データや数値解析結果に関する講演などを基に，キンク現象・界面成長・粒界の結晶構造・構造と離散群の関係などについて，多分野の研究者が幅広く議論を行った.

これらの結晶の問題に関しては, 計算機が発達した 90 年代後半から(古典及び第一原理）分子動力学法を使って計算機上で原子を並べ転位を再現することなどが可能となり，また 2000 年頃からは分析装置・観察装置・実験技術が急激に発展し，連続描像から結晶構造まで様々なものが可視化されている．また，これらの微細構造をマルチスケールに制御したいという，産業界からの要望も顕著となっている.

これらの結晶の問題，特に，転位の問題を解決するには，様々な連続描像の性質と，離散的性質との両方を上手く取り扱う枠組みが必要である．しかし，現在そうした枠組みは出来上がっていない.

連続描像に関しては，1950 年代より近藤一夫先生，甘利俊一先生が微分幾何的な考察を行い，70－80 年代に現代数学（主に代数的位相幾何，微分幾何）の物理現象への応用が盛んに研究された際に，机上で可能な考察はほぼ達成できたと思われる.

他方，離散群の 20 世紀後半の発展の影響を受け，20 世紀前半に発展し完成した，従来の結晶群や分子の対称性を表す群構造の理論を再考しようとする動きが，今世紀に入って現れている.

本研究集会は，様々な分野の専門家をお迎えして開催することとした．尚，北海道地震のために，とても残念なことではあるが，予定していた北海道大学の上坂正晃氏が出席できず，講演が中止となってしまった.

初日の１０日は，新日鐵住金（株）の中川淳一氏より産業界の要望と数学と物質・材料との連携への展開について転位と回位の数学的記述を中心とした講演を問題提起も兼ねして頂いた．その後，転位の観察・観測に関して長年実験的研究に携われてきた東田賢二先生より，昨年に引き続き，近年の観察，実験に関する状況を解説・報告して頂いた．また，物理現象の離散的な定式化を深く研究されている時弘哲治先生からは，液晶における転位と回位，またその準周期性との関わりを通じて，現実の系の数学的記述について講演して頂いた. 数学と物理の連携研究のあり方のスコープを提示すると共に，先の東田先生の講演の実験

事実に対する理論的研究の方向性をも想起させるものであったと考えている．それに引き続き，松谷が本研究会の名称でもある先進数理解析の意味とその重要性をオイラー・ベヌーイの弾性曲線の研究を通して提示し，その立場で行われた転位に関わる研究，二例の報告を行った．

11 日は，東京大学数理科学研究科の数理社会数理実践研究において実施されている「Growth」と称する結晶構造の新たな数学的記述に関する講演を中川淳一氏にして頂いた後に，結晶転位の微分幾何に基づく理論を構築された甘利俊一先生から，先生が構築された理論の解説と，数理工学及び、数学と他分野との連携、またその最近の成果について，先生のご経験を基に講演をして頂いた．近藤先生，甘利先生が構築した理論は従来，微分幾何の枠組みで捉えられてきたものであるが，塑性変形の本質を抉ったもので，現状の離散的枠組みに対しても指導方針を提示する緻密なものであり，講演は極めて示唆的なものとなった．また，位相的結晶論により現代数学的視点から結晶を研究されている砂田利一先生からは，Gauss の日記の記述から始まり数の幾何に関わる実に primitive でかつ数学的に深い問題の紹介とその最近の進展結果について解説して頂いた．最終結果は，準結晶ひいては結晶とは何かという素朴な問いにも繋がり，本研究会の締めくくりの講演としても意味深いものとなった．

これらの講演とそれに続く質問や議論により，本研究集会を通して，結晶の転位の新たな数学的定式化に対して大きな方向性を与えることができたと考えている．特に，実験を基にした物理的な本質を提示した講演や，物理的本質とその数学的表現（あるいは数学的本質）について（応用側面からと数学側面から）長年研究に携わってきた研究者からの講演があり，通常の数学の研究会とは大きく異なる広がりを持つ研究会となった．物理的（数理的）本質を捉えながら数学分野を横断した課題の解析は，科学全体としても数学の枠内でも困難を伴うものであるが，本研究集会において，大きな飛躍の種が生まれたと考えている．異分野融合の一つのケーススタディとなる事を願っている．

組織委員代表　松谷茂樹

2018 年 11 月 9 日

組織委員

松谷茂樹	佐世保高専
佐伯修	九州大学 IMI
中川淳一	新日鐵住金(株)
濵田 裕康	佐世保高専
上坂正晃	北海道大学

2018.9.10 version

IMI Workshop II: 結晶転位の先進数理解析

(Advanced Mathematical Investigation for Dislocations)

at IMI オーディトリアム（W1-D413） 九州大学伊都キャンパス
(2018 年 9 月 10 日（月）-11 日（火）)

Program

9 月 10 日（月）

13:00-13:05	オープニング	
13:05-13:55	中川淳一（新日鐵住金）	数学と物質・材料との連携への展開 -転位と回位の数学的記述を事例に-
14:10-15:00	東田賢二（佐世保高専）	結晶中の転位観察と塑性変形現象：現状と課題
15:00-15:30	休憩	
15:30-16:20	時弘哲治（東京大学)	液晶における転位と準周期性
16:30-17:15	松谷茂樹（佐世保高専）	先進数理解析と結晶の転位問題

9 月 11 日（火）

10:00-10:30	社会数理実践研究 (東大数理)	- 結晶構造の数学的記述 Growth -
10:45-12:15	甘利俊一（理化学研究所）	転位の連続体の動的理論：微分幾何によるアプローチ
12:15-14:00	昼休憩	
14:00-15:30	砂田利一（明治大学）	Certain Arithmetic Quasicrystals
15:30-15:35	クロージング	
15:35-	（時間の余裕がある方でフリーの	ディスカッションを行います）
~~15:30-16:00~~	~~ティータイム~~	
~~16:00-16:50~~	上坂正晃 (北海道大学)	(震災のため講演中止)
~~16:50-16:55~~	~~クロージング~~	

集合写真　2018. 9. 11

数学と物質・材料との連携への展開 -転位と回位の数学的記述を事例に-
(Propulsion of Collaboration between Mathematics and Materials -Topics regarding Mathematical Description for Dislocation and Disclination-)

中川淳一, Junichi Nakagawa
新日鐵住金 (株) Nippon Steel & Sumitomo Metal Co.

Disordered structures in a crystal, such as lattice defects, are a primary factor in determining the mechanical properties of materials. For example, the plasticity observed in the macro-scale world is caused by lattice defects called dislocations in the micro-scale world. We have been focusing on the mathematical properties of lattice defects in the Study Group Workshop and the FMSP mathematical research on real world problems of the University of Tokyo. In these activities, the behavior of the screw dislocation observed by material scientists was described by a simple formula. It was found that the mathematical essence of the formula was monodromy. Then, the monodromy was described using a bundle whose fibers constitute a discrete group, such as $\mathbb{Z}$. Furthermore, both the screw and edge dislocations, moreover, disclination were described by encoding the symmetry arising from the original lattice using Thurston's monodromy, which was composed of local charts of the graph corresponding to the lattice defects, and a coordinate change of these charts. The topics described above are problems in mathematics originating from problems in materials and industry. Progress on the problem is advancing mathematically year by year through interdisciplinary discussions among the fields of mathematics, materials and industry, as well as among different fields of mathematics. In this workshop, I hope to move to the next stage where their theories make consistent mathematical and pragmatic progress with the social cooperation of mathematics.

IMI Workshop: 結晶転位の先進数理解析

数学と物質・材料との連携への展開
-転位と回位の数学的記述を事例に-

Propulsion of Collaboration
between Mathematics and Materials
-Topic regarding Mathematical Description of Line Defects-

2018.9.10-21
Institute of Mathematics for Industry
Kyushu University

Nippon Steel & Sumitomo Metal Corporation
Advanced Technology Research Laboratories
Mathematical Science & Technical Research Lab.

Junichi Nakagawa

Behavior of Dislocation in Different View Scale

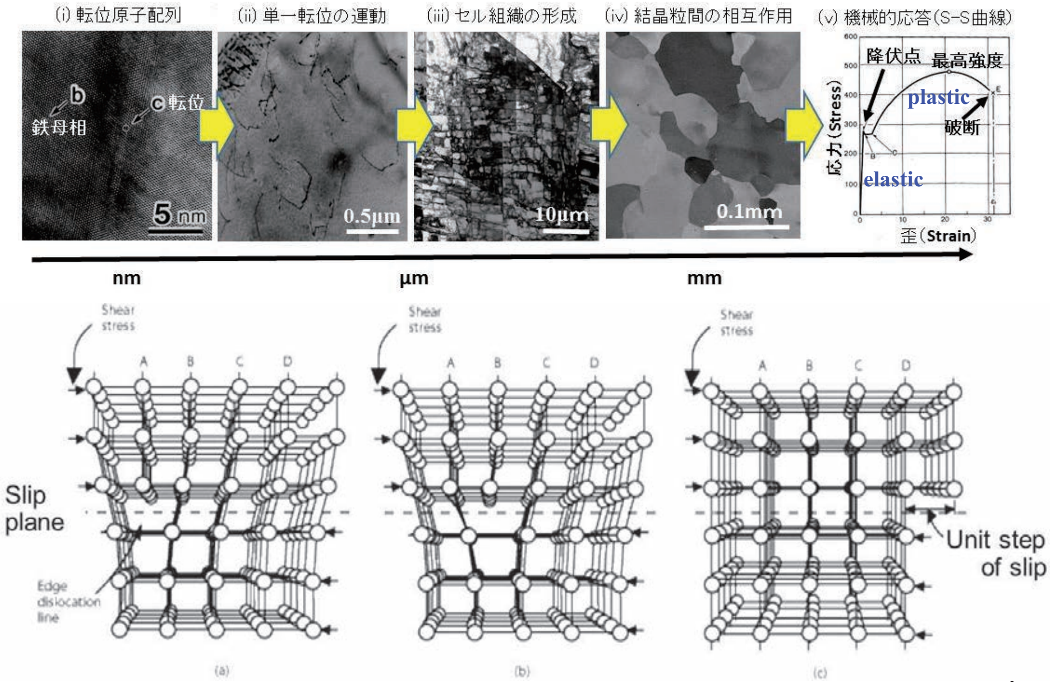

Study Group 2014, 東大

Observed Result by Material Scientists

Screw Dislocation in BCC Lattice

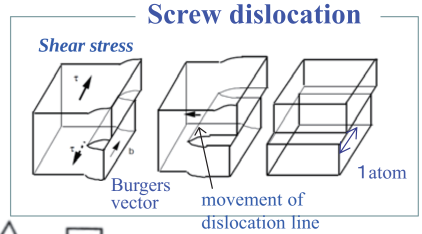

1. The Burgers vector is 1/2[111].
2. A dislocation starts at a boundary.
3. The dislocation is more likely to occur at a circuit around Circuit B rather than Circuit A.
4. When the dislocation line is in Triangle B, the arrangement of atoms of Circuit B changes Circuit A.
5. After the dislocation line passes Circuit B, the arrangement of atoms becomes Circuit B.

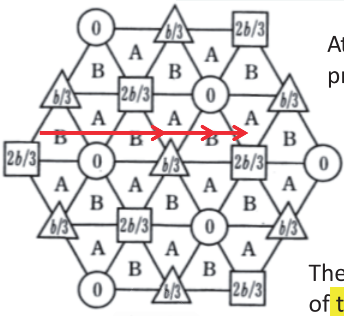

Atomic configuration projected on a (111) plane.

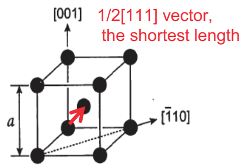

The arrangement of atoms of the circuit B in CCW:
0 -> b/3 -> 2b/3

The arrangement of atoms of the circuit A in CCW:
0 -> 2b/3 -> 1b/3

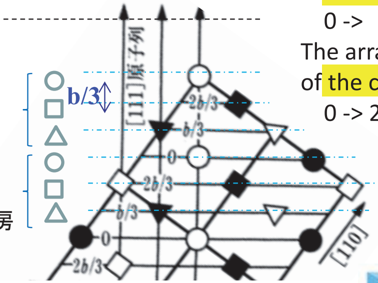

projected on a (1$\bar{1}$0) plane.

加藤雅治, 入門転位論(1998), 裳華房

3

新日鐵住金 NIPPON STEEL & SUMITOMO METAL

Study Group 2014, 東大

Derived Formula for Describing the Behavior of Screw Dislocation

[111] direction of atom's movement due to screw dislocation

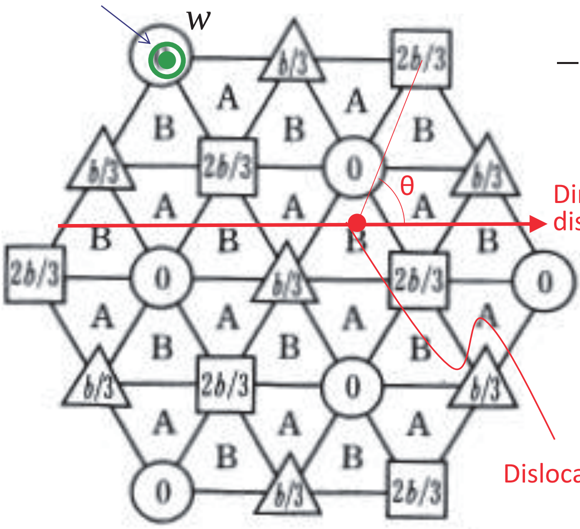

$$w = w_0 + f(x - x_0)\frac{\theta}{2\pi} e_{[111]},$$

$$-\pi \le \theta \le \pi,\ x \in \{\mathit{dislocation\ line}\}$$

$$f(t) = f(-t),\quad t \in R$$

$$f(t) \ge 0,$$

$e_{[111]}$: *unit vector of the* $[111]$ *direction*

4

新日鐵住金 NIPPON STEEL & SUMITOMO METAL

Validation of the Formula Using Computer Simulation

Dislocation at Circuit B in the case of $f(x-x_0)=|x-x_0|$

The arrangement of B — The arrangement of A — The arrangement of B

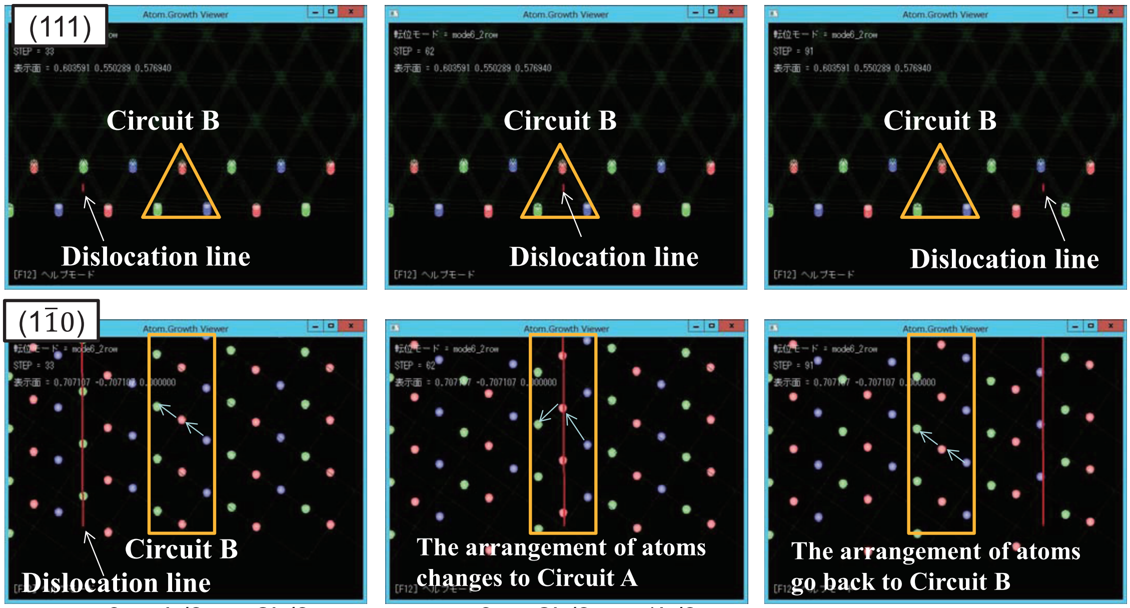

0 -> b/3 -> 2b/3
B R G

0 -> 2b/3 -> 1b/3
B R G

Monodromy of Screw Dislocation in BCC Lattice

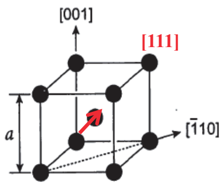

P : atomic configuration projected on (111)
:= base space
L : fiber on the base space

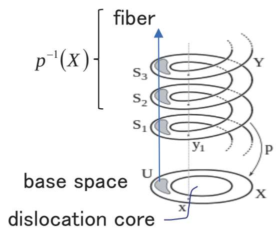

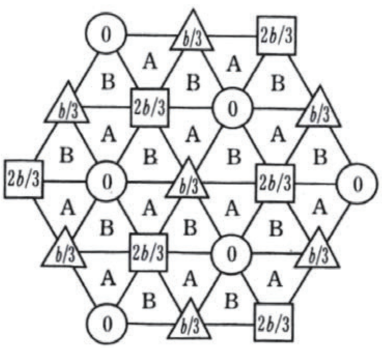

$$\{\pi_1(P) \to Aut(L)\} = Hom(\pi_1(P), \mathbb{Z}) \cong H^1(P;\mathbb{Z}) \supset S$$

$$S = \{\varphi \in H^1(P;\mathbb{Z}) \mid \varphi(\Delta) \in \{+1, -1, 0\}\}$$

P: Atomic configuration projected on a (111) plane.

SGW 2015を契機に生まれた論文

Pacific Journal of Mathematics for Industry manuscript No.
(will be inserted by the editor)

An algebraic description of screw dislocations in SC and BCC crystal lattices

Hiroyasu Hamada · Shigeki Matsutani ·
Junichi Nakagawa · Osamu Saeki ·
Masaaki Uesaka

Received: date / Accepted: date

Abstract We give an algebraic description of screw dislocations in a crystal, especially simple cubic (SC) and body centered cubic (BCC) crystals, using free abelian groups and fibering structures. We also show that the energy of a screw dislocation based on the spring model is expressed by the Epstein zeta function approximately.

Keywords Crystal lattice · screw dislocation · topological defect, monodromy · group ring of abelian group · dislocation energy · Epstein zeta function

新日鐵住金
NIPPON STEEL & SUMITOMO METAL

Commutative Diagram for Screw Dislocation in BCC Lattice

$\mathcal{S} = \{z_0\}$ corresponds to
the position of the dislocation line

$$
\begin{tikzcd}
\mathbb{E}_{\mathcal{B}(c)} \arrow[r, "\hat{\iota}_{\breve{\delta}}^{\mathrm{BCC},c}"] \arrow[d] \arrow[dd, bend right, "\widehat{\psi}"'] & \mathbb{E}_{\mathbb{E}^2\setminus\mathcal{S}} \arrow[d] \arrow[dd, bend left, "\widehat{\psi}"] \\
\mathcal{B}(c) \arrow[r, "\iota_{\breve{\delta}}^{\mathrm{BCC},c}"] & \mathbb{E}^2 \setminus \mathcal{S} \\
S^1_{\mathcal{B}(c)} \arrow[r, "\hat{\iota}_{\breve{\delta}}^{\mathrm{BCC},c}"] \arrow[u] & S^1_{\mathbb{E}^2\setminus\mathcal{S}} \arrow[u]
\end{tikzcd}
$$

Proposition 6 *Set* $\gamma = \exp(4\pi\sqrt{-1}\delta_3/(\sqrt{3}a)) \in S^1$ *and consider the global sections*

$$\breve{\sigma}_{\gamma,c} \in \Gamma(\mathcal{B}^{(c)}, S^1_{\mathcal{B}^{(c)}}), \quad c = 0, 1, 2,$$

that constantly take the values $\gamma\zeta_3^{-c}$, *where* $\zeta_3 = \exp(2\pi\sqrt{-1}/3)$. *Then, we have*

$$\iota_{\breve{\delta}}^{\mathrm{BCC}}(\mathbb{B}^a) = \bigcup_{c=0}^{2} \hat{\iota}_{\breve{\delta}}^{\mathrm{BCC},c}\left(\widehat{\psi}^{-1}\left(\breve{\sigma}_{\gamma,c}(\mathcal{B}^{(c)})\right)\right) \subset \mathbb{E}^3.$$

$$\mathcal{B} := \mathcal{B}^{(0)} \coprod \mathcal{B}^{(1)} \coprod \mathcal{B}^{(2)},$$

BCC格子を3枚のシートで表現

$$
\left.\begin{aligned}
\mathcal{B}^{(0)} &:= \{\ell_1(a_1 - a_3) + \ell_2(a_2 - a_3) \,|\, \ell_1, \ell_2 \in \mathbb{Z}\},\\
\mathcal{B}^{(1)} &:= \{\ell_1(a_1 - a_3) + \ell_2(a_2 - a_3) + a_1 - b \,|\, \ell_1, \ell_2 \in \mathbb{Z}\},\\
\mathcal{B}^{(2)} &:= \{\ell_1(a_1 - a_3) + \ell_2(a_2 - a_3) + a_1 + a_2 - b \,|\, \ell_1, \ell_2 \in \mathbb{Z}\}.
\end{aligned}\right\}
$$

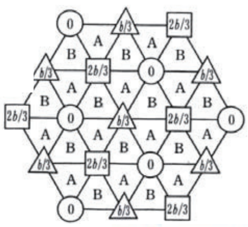

新日鐵住金
NIPPON STEEL & SUMITOMO METAL

LATTICE DEFECTS FROM MONODROMY

HOKUTO KONO, TSUKASA ISHIBASHI, AND SHO EJIRI

Earlier works

(a) Single screw dislocations are described in terms of the **monodromy of a fiber bundle** by Hamada et. al [5].

(b) There are many works on lattice defects in terms of **singular Riemannian manifolds**.

We shall first consider a "topological version" of the approach (b), which generalizes the basic part of (a) to edge dislocations and disclinations. Our tool is the monodromy of a (singular) affine manifold.
It much simplifies the Riemannian geometry calculations.

[5] H.Hamada, S.Matsunami, J.Nakagawa, O.Saeki, M.Uesaka, An algebraic description of screw dislocations in SC and BCC crystal lattices, arXiv:1605.09550

9

To describe monodromy in the sense of Thurston, we need the notion of (G, X)-*manifold*.

Basic Setting

X : a topological space
G : a group
Assume that G continuously acts on X: we have a group homomorphism $\rho : G \to \mathrm{Homeo}(X)$, where
$\mathrm{Homeo}(X) := \{ f : X \to X \mid f \text{ is a homeomorphism} \}$.

Actually we will only use the case that

- X is a C^ω-manifold, and
- $G \subset \mathrm{Diff}^\omega(X) := \{ f : X \to X \mid f \text{ is a } C^\omega\text{-diffeomorphism} \}$

for our main purpose.

10

Definition ((G, X)-manifold)

M : a topological space
(1) $\{(U_\alpha, \phi_\alpha)\}_\alpha$ is a (G, X)-*atlas* on M if

- $\{U_\alpha\}_\alpha$ is an open covering of M,
- each $\phi_\alpha : U_\alpha \to X$ is a homeomorphism onto its image, and
- $\phi_\alpha \circ \phi_\beta^{-1}|_{\phi_\beta(U_\alpha \cap U_\beta)} : \phi_\beta(U_\alpha \cap U_\beta) \to \phi_\alpha(U_\alpha \cap U_\beta)$ is the restriction of an element of $\rho(G)$.

(2) M equipped with a (G, X)-atlas is called a (G, X)-*manifold*.

Each (U_α, ϕ_α) is called a (G, X)-*chart*.

11

今野，石橋，江尻，FMSP社会数理実践研究(2017Fy)

For each (G, X)-manifold M, we can define a group homomorphism which is called the *monodromoy*

$$\mathrm{Mon} : \pi_1(M, p_0) \to G$$

if we fix a point $p_0 \in M$ and a (G, X)-chart (U_0, ϕ_0) near p_0. (If we change the initial data p_0 and (U_0, ϕ_0), the map is changed by conjugation.)

12

© 2018 NIPPON STEEL & SUMITOMO METAL CORPORATION All Rights Reserved.

新日鐵住金
NIPPON STEEL & SUMITOMO METAL

(1) Take a loop $\gamma : [0,1] \to M$ with a base point p_0.
(2) Take (G,X)-charts $(U_1,\phi_1),\ldots,(U_n,\phi_n)$ that cover the image of γ. (Note that the neighborhood of the base point is already covered by U_0.) Take the covers such that $U_i \cap U_{i+1}$ is non-empty and connected for each $i \in \{0,\ldots,n-1\}$.
(3) There exists a unique $g_i \in G$ such that g_i gives the coordinate change of (U_i,ϕ_i) and (U_{i+1},ϕ_{i+1}). (Here, for the uniqueness we need to assume that X is C^ω.)
(4) One can show that $\mathrm{Mon}_M([\gamma]) := g_0 \cdots g_{n-1} \in G$ depends only on the homotopy class of γ (for the fixed chart (U_0,ϕ_0)).

In the following examples, we use $G = \mathrm{aff}(\mathbb{R}^2) := GL(\mathbb{R}^2) \propto \mathbb{R}^2$.
The group operation is $(A,x)\cdot(B,y) := (AB, Ay + x)$.

Example (No defects)

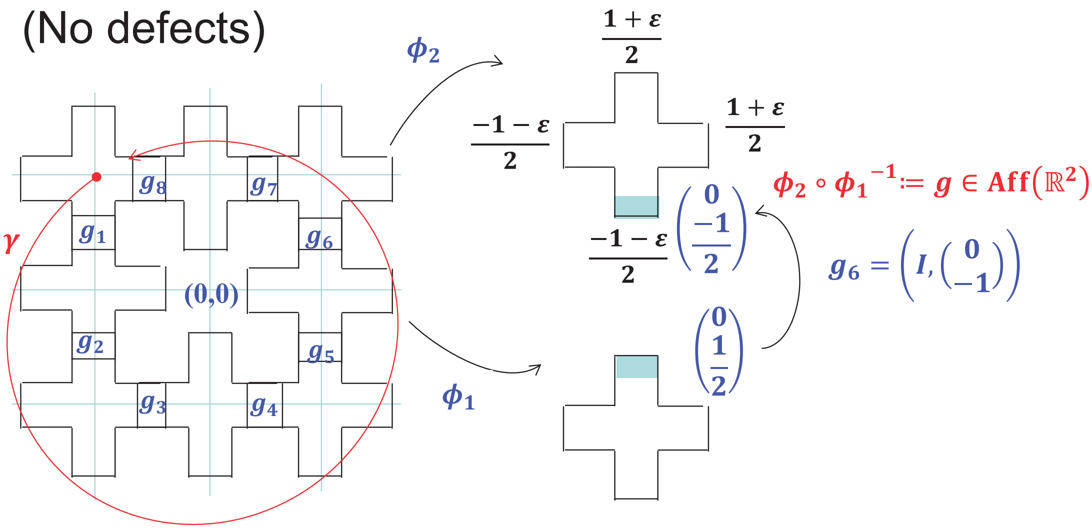

$\mathrm{Mon}_M(\gamma) = g_8\, g_7\, g_6\, g_5\, g_4\, g_3\, g_2\, g_1$

$= \left(I, \begin{pmatrix} 1 \\ 0 \end{pmatrix}\right) \left(I, \begin{pmatrix} 1 \\ 0 \end{pmatrix}\right) \left(I, \begin{pmatrix} 0 \\ -1 \end{pmatrix}\right) \left(I, \begin{pmatrix} 0 \\ -1 \end{pmatrix}\right) \left(I, \begin{pmatrix} -1 \\ 0 \end{pmatrix}\right) \left(I, \begin{pmatrix} -1 \\ 0 \end{pmatrix}\right) \left(I, \begin{pmatrix} 0 \\ 1 \end{pmatrix}\right) \left(I, \begin{pmatrix} 0 \\ 1 \end{pmatrix}\right)$

$= \left(I, \begin{pmatrix} 0 \\ 0 \end{pmatrix}\right) \in \mathrm{Aff}(\mathbb{R}^2)$

Example
(Edge dislocation)

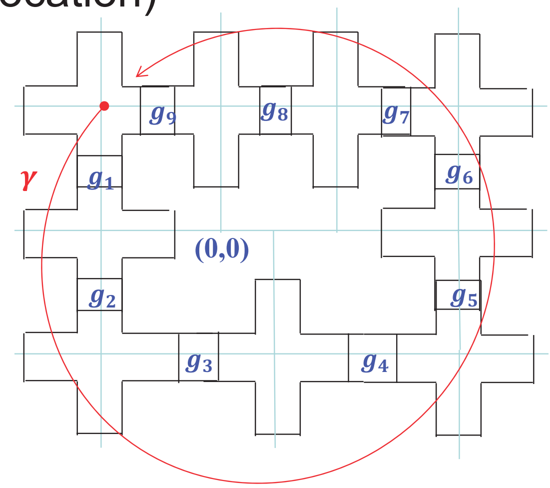

$\mathbf{Mon}_M(\gamma) = g_9\, g_8\, g_7\, g_6\, g_5\, g_4\, g_3\, g_2\, g_1$

$$= \left(I, \begin{pmatrix}1\\0\end{pmatrix}\right) \left(I, \begin{pmatrix}1\\0\end{pmatrix}\right) \left(I, \begin{pmatrix}1\\0\end{pmatrix}\right) \left(I, \begin{pmatrix}0\\-1\end{pmatrix}\right) \left(I, \begin{pmatrix}0\\-1\end{pmatrix}\right) \left(I, \begin{pmatrix}-1\\0\end{pmatrix}\right) \left(I, \begin{pmatrix}-1\\0\end{pmatrix}\right) \left(I, \begin{pmatrix}0\\1\end{pmatrix}\right) \left(I, \begin{pmatrix}0\\1\end{pmatrix}\right)$$

$$= \left(I, \begin{pmatrix}1\\0\end{pmatrix}\right) \in \mathrm{Aff}$$

This corresponds to Burgers vector with respect to the edge dislocation.

Burgers Vector

(a) Burgers circuit round a dislocation with positive line sense in the direction.
(b) The same circuit in a perfect crystal; closure failure is the Burgers vector.

Edge dislocation

The Burgers vector of a dislocation is normal to the dislocation line.

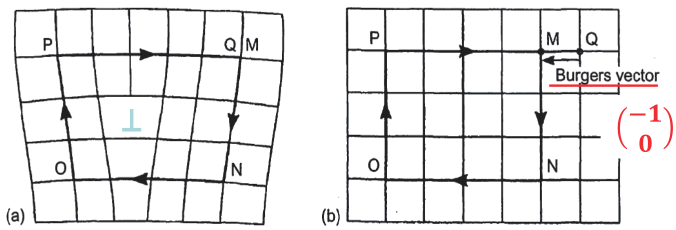

Screw dislocation

The Burgers vector of a dislocation is parallel to the dislocation line.

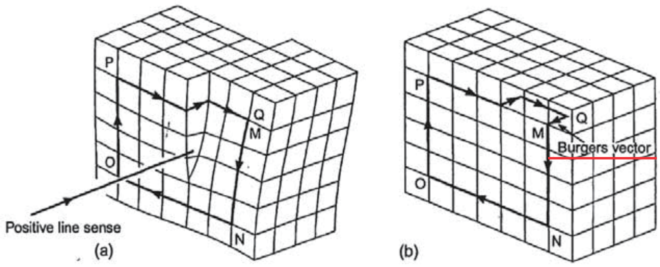

D. Hull and D. J. Bacon, Introduction to Dislocation, Butterworth-Heinemann (2011)

Example (Disclination)

石橋さん，FMSP社会数理実践研究(2018Fy)

The coordinate neighborhoods are set to be parallel to the coordinate axes.

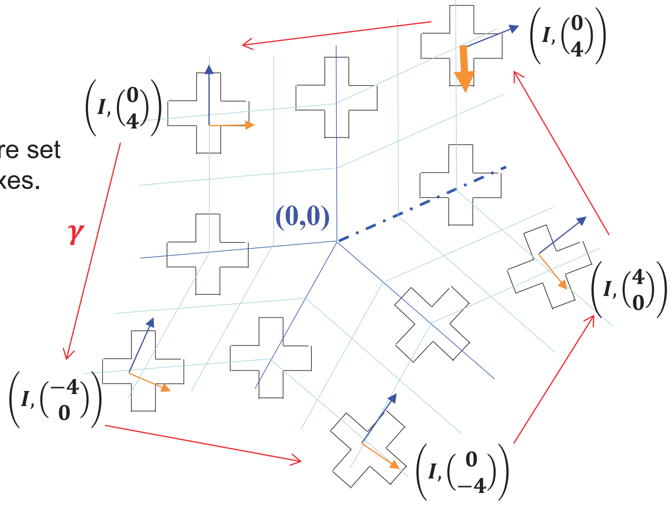

$$\mathrm{Mon}_M(\gamma)=\left(\begin{pmatrix}\cos(-\pi/2) & -\sin(-\pi/2)\\ \sin(-\pi/2) & \cos(-\pi/2)\end{pmatrix},\begin{pmatrix}0\\0\end{pmatrix}\right)\left(I,\begin{pmatrix}0\\4\end{pmatrix}\right)\left(I,\begin{pmatrix}4\\0\end{pmatrix}\right)\left(I,\begin{pmatrix}0\\-4\end{pmatrix}\right)\left(I,\begin{pmatrix}-4\\0\end{pmatrix}\right)\left(I,\begin{pmatrix}0\\4\end{pmatrix}\right)$$

$$=\left(\begin{pmatrix}0 & 1\\ -1 & 0\end{pmatrix},\begin{pmatrix}0\\0\end{pmatrix}\right)\left(I,\begin{pmatrix}0\\4\end{pmatrix}\right)=\left(\begin{pmatrix}0 & 1\\ -1 & 0\end{pmatrix},\begin{pmatrix}1 & 0\\ 0 & 1\end{pmatrix}\begin{pmatrix}0\\4\end{pmatrix}+\begin{pmatrix}0 & 1\\ -1 & 0\end{pmatrix}\begin{pmatrix}0\\0\end{pmatrix}\right)$$

$$=\left(\begin{pmatrix}0 & 1\\ -1 & 0\end{pmatrix},\begin{pmatrix}4\\0\end{pmatrix}\right)\in \mathrm{Aff}(\mathbb{R}^2)$$

17

新日鐵住金 NIPPON STEEL & SUMITOMO METAL

Points under Discussion at SGW 2018 regarding Topic 2

A monodromy map can be regarded as a geometric invariant of lattice defects such as disclination as well as dislocations.

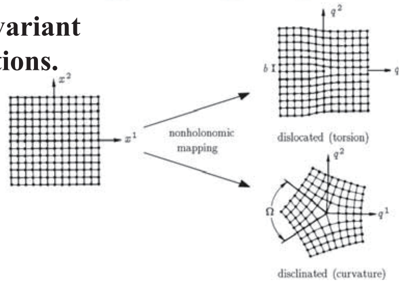

1. Describing lattice defects using a monodromy map that has the singular affine structure
2. Giving a physical interpretation of the mathematical theory

Σ : Riemann surface

$\omega=\mathcal{F}(z)dz^k$ Meromorphic k differential

$\omega \xrightarrow{\text{yields}}$ singular affine structure on Σ

$$\boxed{\omega=\left(\frac{1}{z}\cdot(z-t)\right)dz^4}$$

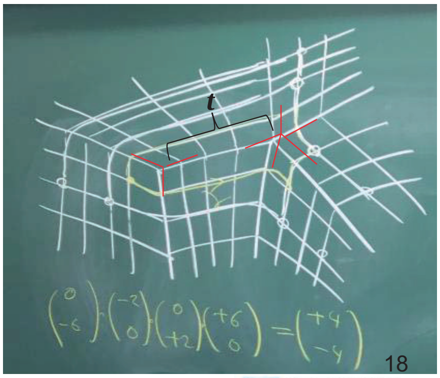

石橋さん，東大FMSP社会数理実践研究 (2018Fy)

18

新日鐵住金 NIPPON STEEL & SUMITOMO METAL

結晶中の転位観察と塑性変形現象：現状と課題
(On observation of dislocations and phenomena of plastic deformation in crystals)

東田賢二, Kenji Higashida
佐世保工業高等専門学校
National Institute of Technology, Sasebo College

In this talk, several observation results of dislocations and phenomena of plastic deformation in crystals are reported. The experimental results exhibit that dislocations essentially control the mechanical behaviours of crystals such as plastic deformation and fracture. A plastic deformation phenomenon called “kink deformation” is introduced, since it attracts interests not only from materials engineering but also from mathematical field. The properties of dislocations and related phenomena play important roles for the next generations.

結晶中の転位観察と塑性変形現象:現状と課題

K. Higashida
National Institute of technology, Sasebo College,
Sasebo, Japan
(Department of Materials Science & Engineering, Kyushu University)

IMI Workshop II: 結晶転位の先進数理解析
at IMI オーディトリアム（W1-D413） 九州大学伊都キャンパス (2018.9.10)

Outline

１. 転位と塑性変形
Dislocations and plastic deformation

２. 種々の転位観察
Observations of various dislocation configurations

３. キンク変形について
Observations of Kink Deformation

Lattice Image of a slicon crystal observed by HR-TEM

Perfect crystal without defects

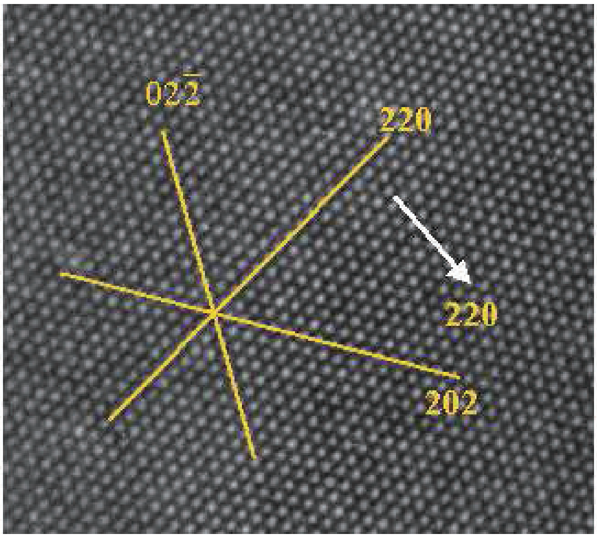

Electron Diffraction Pattern

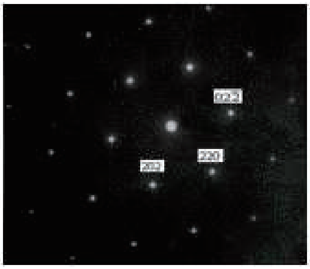

http://www.ion-eng.co.jp

Lattice image of a silicon crystal irradiated by electron beam

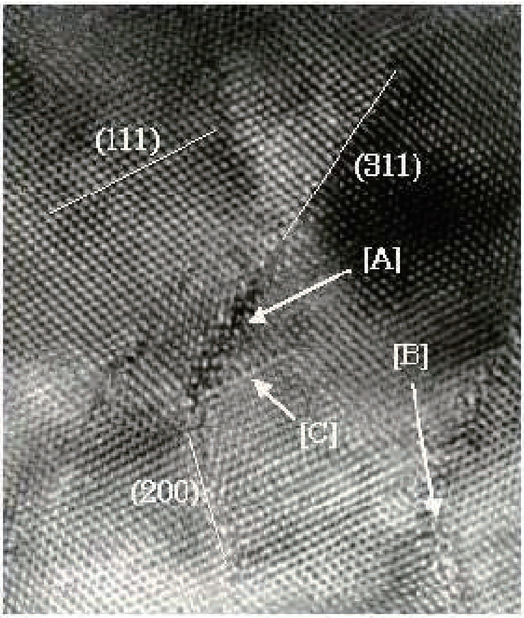

lattice defects

http://www.ion-eng.co.jp

Crystal lattice defects (結晶格子欠陥)

Point defect: vacancy, interstitial atom

点欠陥: 原子空孔, 格子間原子

Line defect: Dislocation

線欠陥: 転 位

Plane defect: Stacking fault, free surface

面欠陥: 積層欠陥 自由表面

Volterra distortions in an elastic cylinder

Linear defects in structure-less continuum. There are no low bound restrictions on the strength of disclinations and dislocations in the continuum.

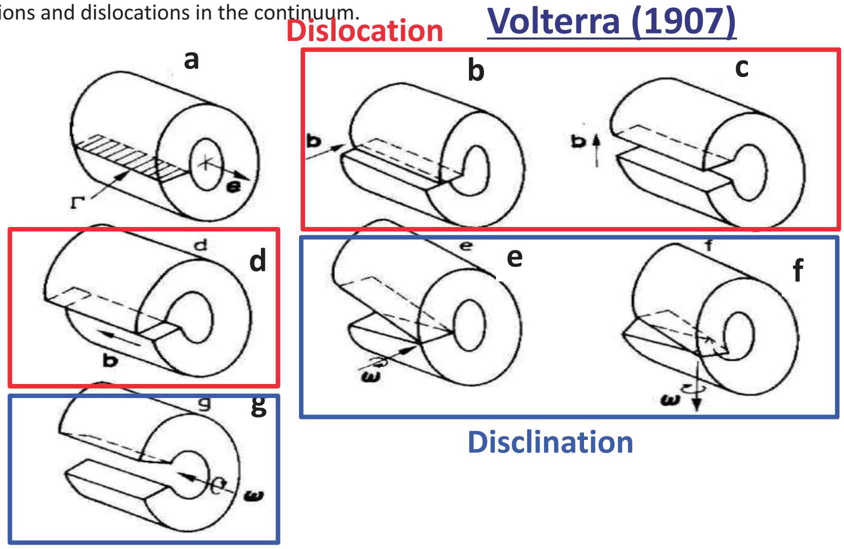

Volterra dislocations. (a) Initial hollow cylinder with a cut Γ, **e** is the unit vector along cylinder axis. (b, c) Edge dislocations of Burgers vector $\boldsymbol{b}$. (d) A screw dislocation. (e, f) Twist disclinations of Frank vector $\boldsymbol{\omega}$. (g) A wedge disclination.

どのようにして転位の存在は認識され始めたのか？

Crystal growth

X-ray diffraction spot

Mechanical properties

Mechanism of plastic deformation

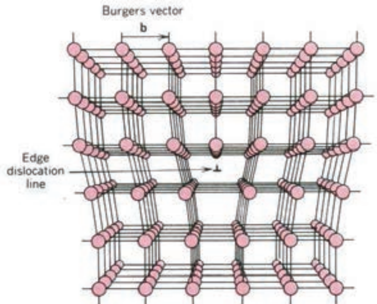

W.D. Callister, Materials Science and Engineering, An Introduction

Stress-strain relation (応力ーひずみ関係) when a metal rod is deformed in tension

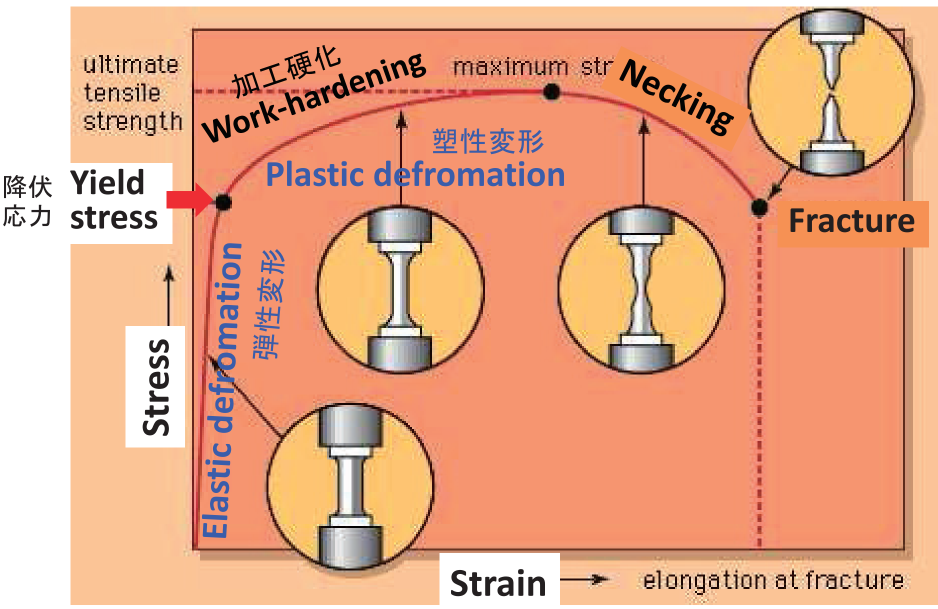

Mechanism of plastic deformation in a crystal

Slip deformation すべり変形

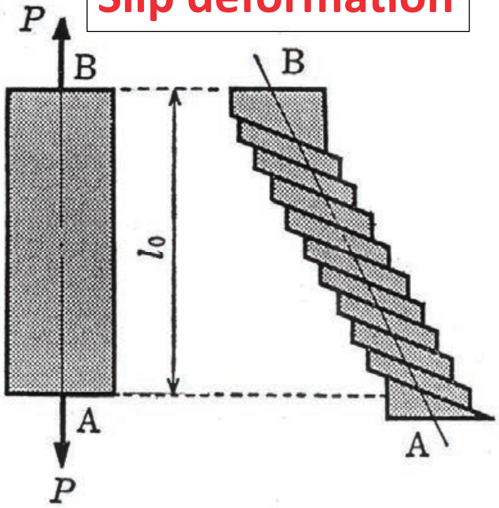

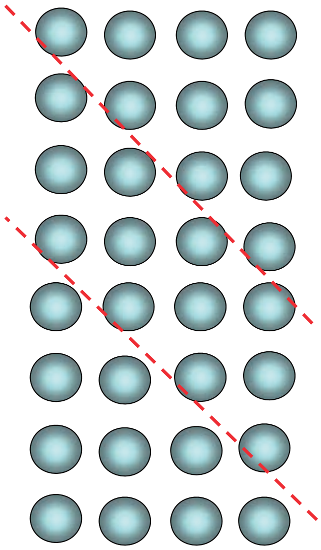

Mechanism of plastic deformation in a crystal

Slip deformation

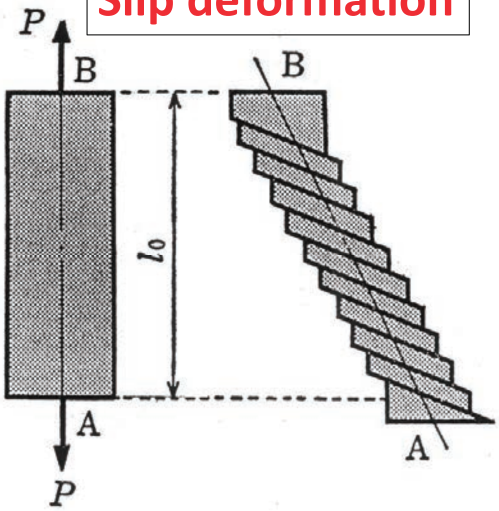

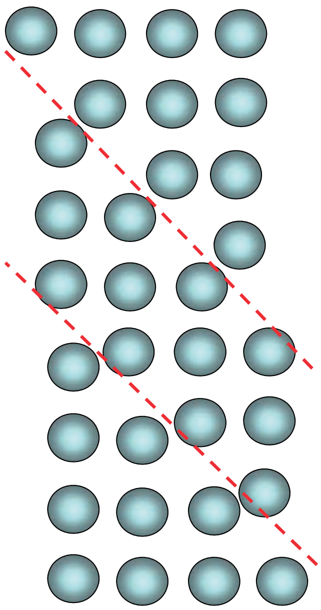

Mechanism of plastic deformation in a crystal

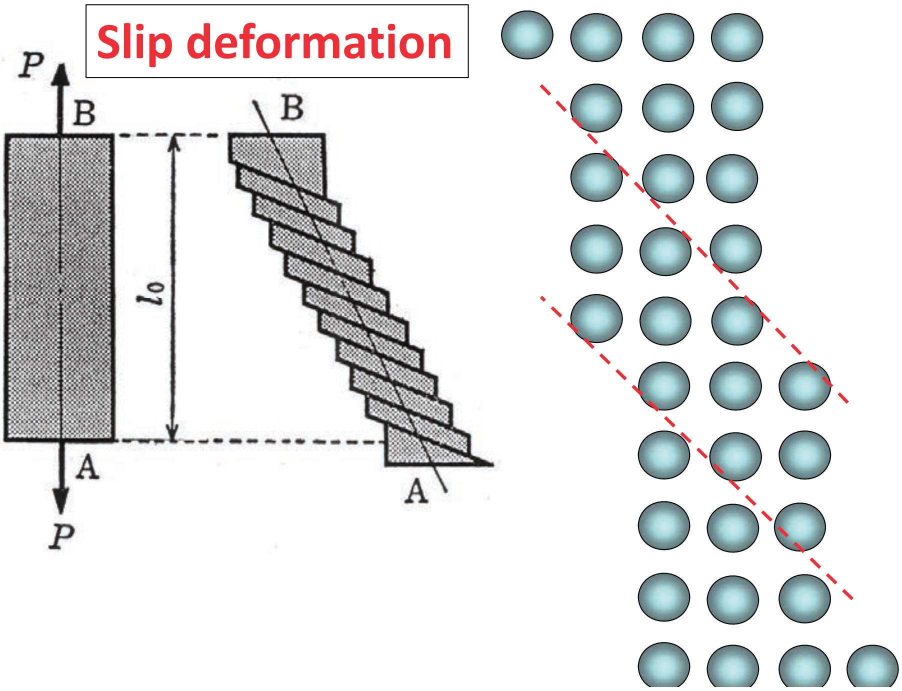

Slip bands

すべり帯

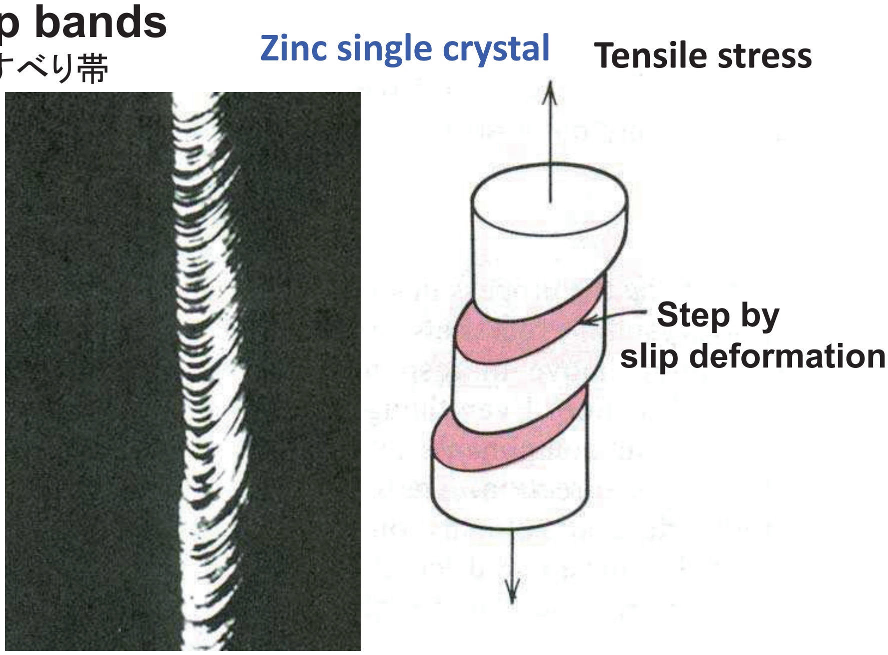

(From C. F. Elam, *The Distortion of Metal Crystals*, Oxford University Press, London, 1935.)

Slip deformation in crystals

Slip system すべり系 : slip plane ________ **slip direction** ________

depends on crystal structure

Face-centered cubic crystal
{111}plane, <110>direction

Body-centered cubic crystal
{110}plane, <111>direction

Closed-packed hexagonal lattice
(0001)plane, <11$\bar{2}$0> direction

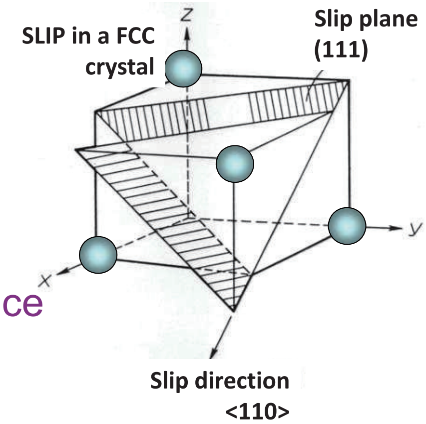

Proceedings of the Royal Society of London Series A(1934)

362

The Mechanism of Plastic Deformation of Crystals.
Part I.—Theoretical.

By G. I. Taylor, F.R.S., Royal Society Yarrow Profes

(Received February 7, 1934.)

Experiments on the plastic deformation of single crystals, of rock salt have given results which differ in detail but possess cer characteristics.

In general the deformation of a single crystal in tension or consists of a shear strain in which sheets of the crystal paralle plane slip over one another, the direction of motion being some si lographic axis. The measure of this strain, which will be repr is the ratio of the relative lateral movement of two parallel planes distance between them. Thus it is defined in the same way as th considered in the theory of elasticity.

G.I. Taylor (1934)

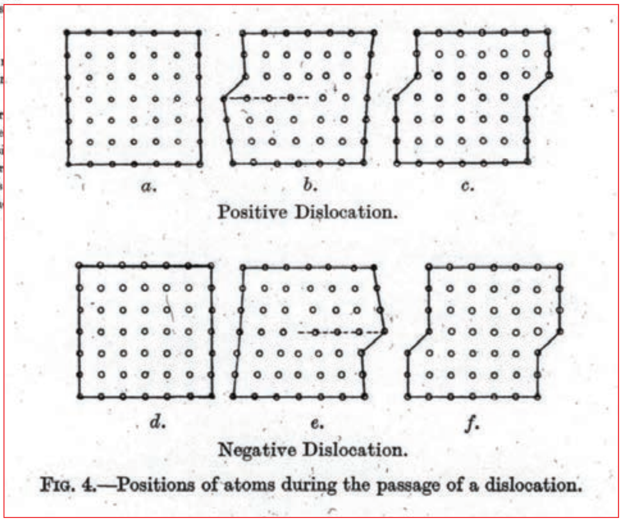

Fig. 4.—Positions of atoms during the passage of a dislocation.

1886-1975

British physicist and mathematician,
and a major figure in fluid dynamics and wave theory.

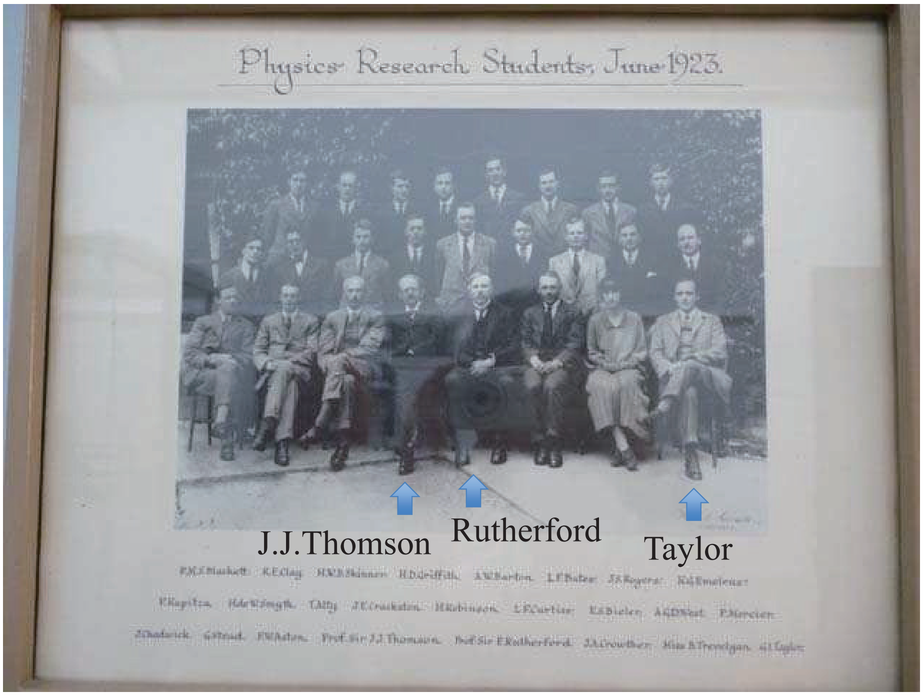

Cambridge University

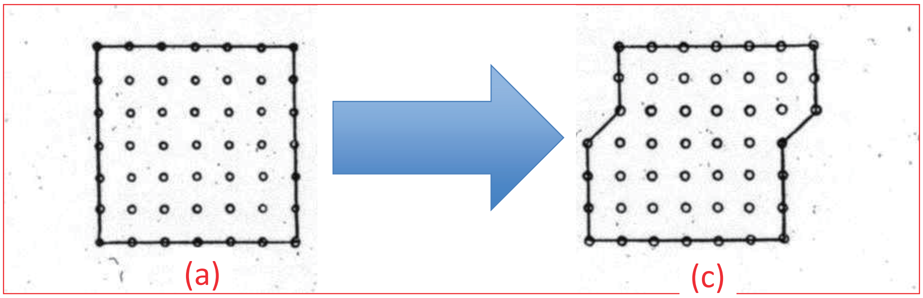

The mechanism of slipping may be like the simple shift from fig.(a) to (c), in which the whole of the material on one side of a definite plane shifts through the length of one lattice cell.

The mechanism of this simple shift differs from what is observed in real materials.

Differences from real materials:

(1) This ideal slipping would leave the material in the form of a perfect crystal and the strength would be unaltered by the distortion.

(2) To shift the whole of the upper row of atoms simultaneously over the lower row would necessitate the application of a stress comparable with the elastic moduli of the material (1000 times larger than the real strength)

(3) No room for explanation of the large observed effect of temperature on plastic distortion.

Illustration of stress – strain curves in fcc, bcc and hcp crystals

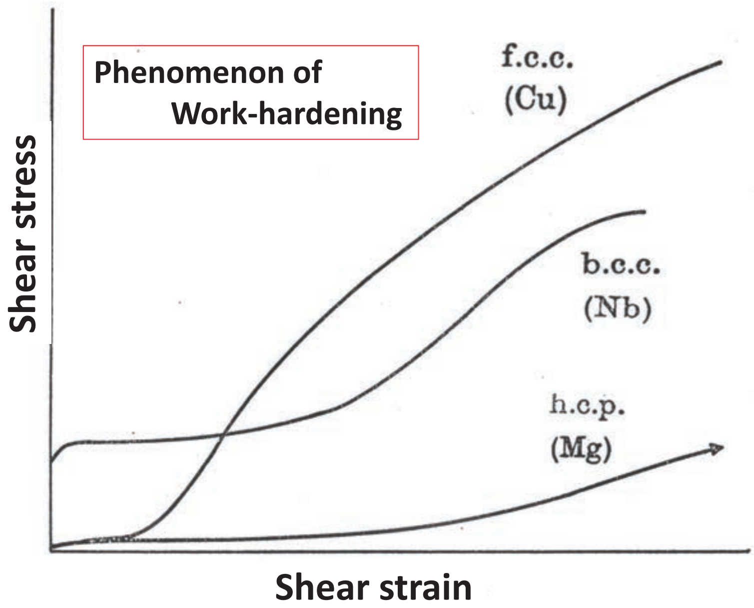

Differences from real materials:

(1) This ideal slipping would leave the material in the form of a perfect crystal and the strength would be unaltered by the distortion.

(2) To shift the whole of the upper row of atoms simultaneously over the lower row would necessitate the application of a stress comparable with the elastic moduli of the material (1000 times larger than the real strength)

(3) No room for explanation of the large observed effect of temperature on plastic distortion.

Ideal strength for slip deformation

Simple shear along the whole of the slip plane

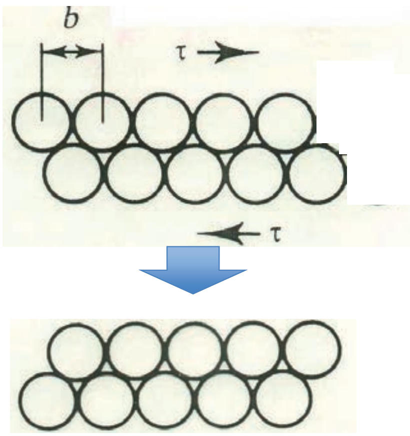

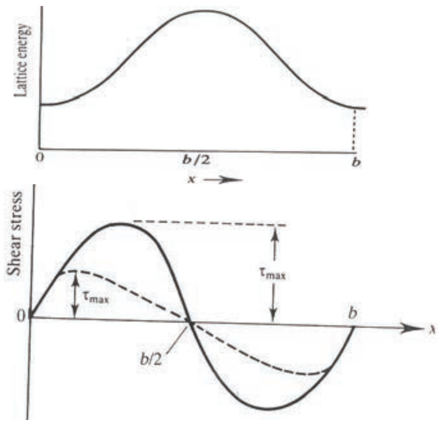

$$\tau_{ideal} \doteqdot G$$

Shear modulus

1000 times larger than the real strength

Differences from real materials:

(1) This ideal slipping would leave the material in the form of a perfect crystal and the strength would be unaltered by the distortion.

(2) To shift the whole of the upper row of atoms simultaneously over the lower row would necessitate the application of a stress comparable with the elastic moduli of the material (1000 times larger than the real strength)

(3) No room for explanation of the large observed effect of temperature on plastic distortion.

Temperature dependence of s-s relations

Nb crystals

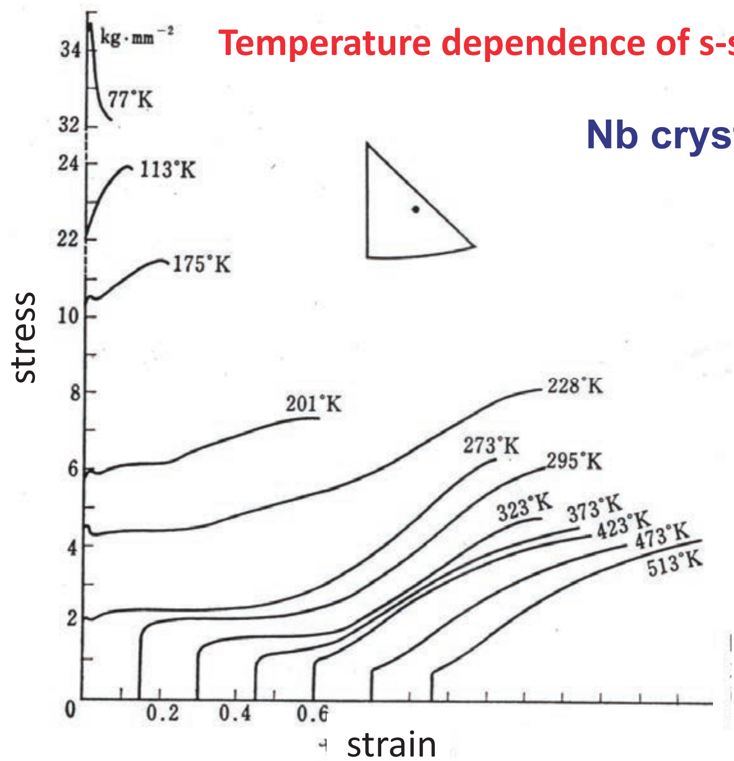

P.B.Hirsch *et.al*

Slip by dislocatios

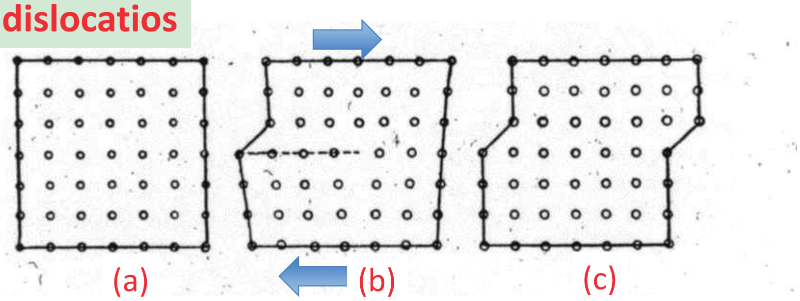

The slipping is considered to occur not simultaneously over all atoms in the slip plane but over a limited region which is propagated from side to side of the crystal.

(a) The atoms in the lattice of a crystal block,
(b) A slip of one atomic spacing has been propagated from left to right into the middle.
(c) The block after the unit slip (dislocation) has passed through from left to right.

A looper

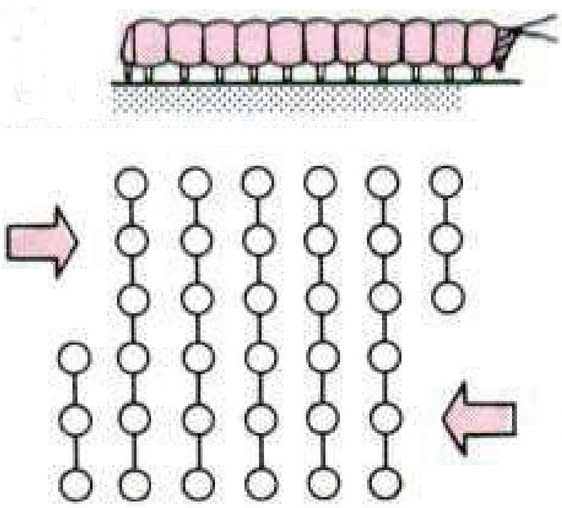

Outline

1. 転位と塑性変形
   Dislocations and plastic deformation

2. 種々の転位観察
   Observations of various dislocation configurations

3. キンク変形について
   Observations of Kink Deformation

High voltage Transmission Electron Microscope at Kyushu University

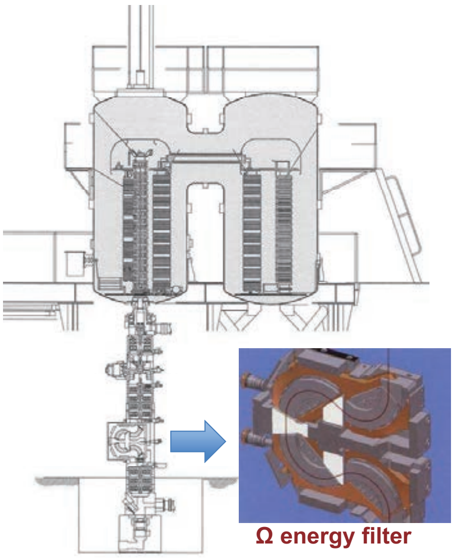

Ω energy filter

Accelerating voltage
1250kV

JEM-1300NEF with Ω energy filter

In-situ observation in silicon crystals

deformed at 700ºC

0.3μm

Characters of dislocations in crystals

defined by two vectors

1. Burgers vector ***b***
2. Dislocation line vector ***t***

Edge dislocation: $\boldsymbol{b} \perp \boldsymbol{t}$

Screw dislocation: $\boldsymbol{b} // \boldsymbol{t}$

Mixed dislocation: combination of two components of edge and screw dislocs.

Edge Dislocation

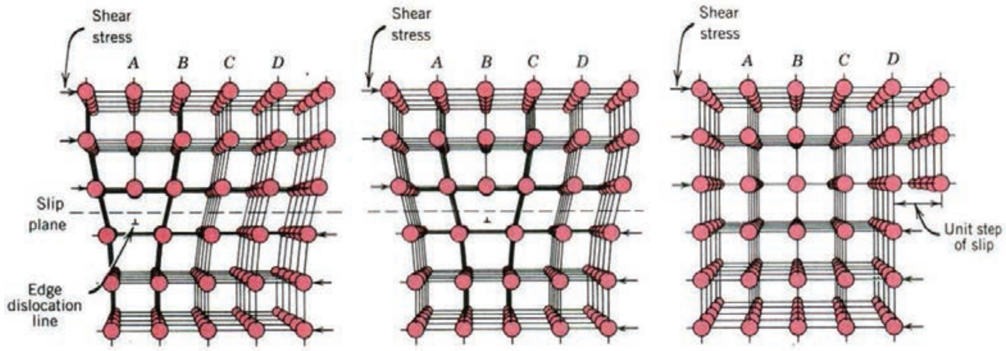

Edge dislocation

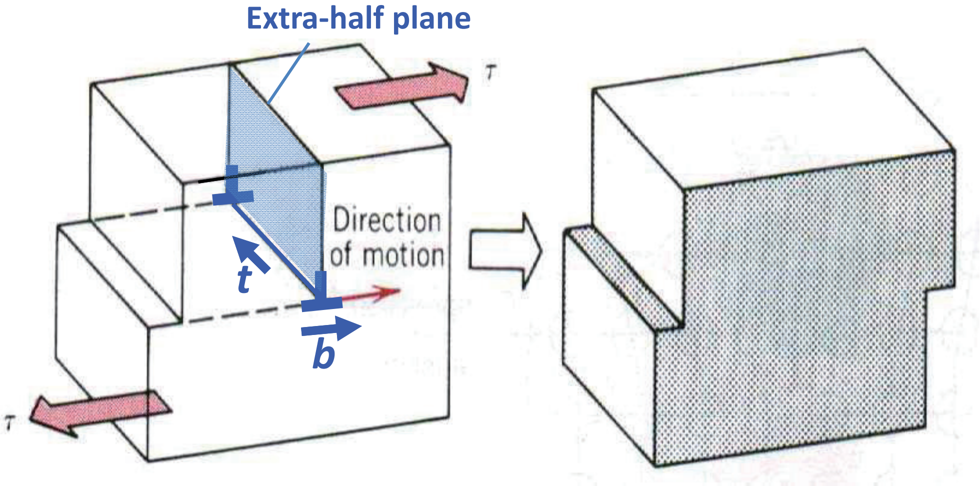

Signs of edge dislocations

determined by the direction of extra-half plane

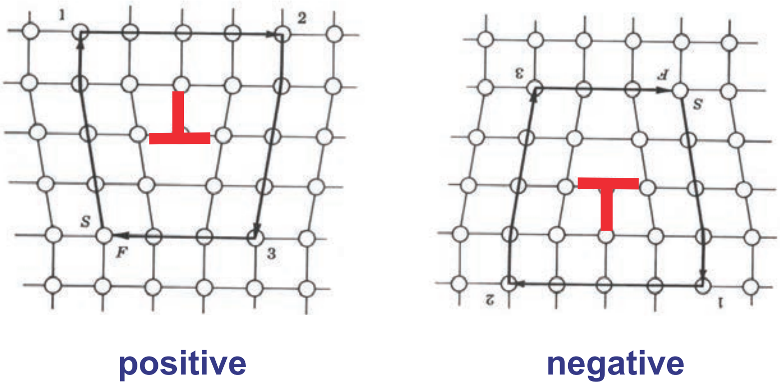

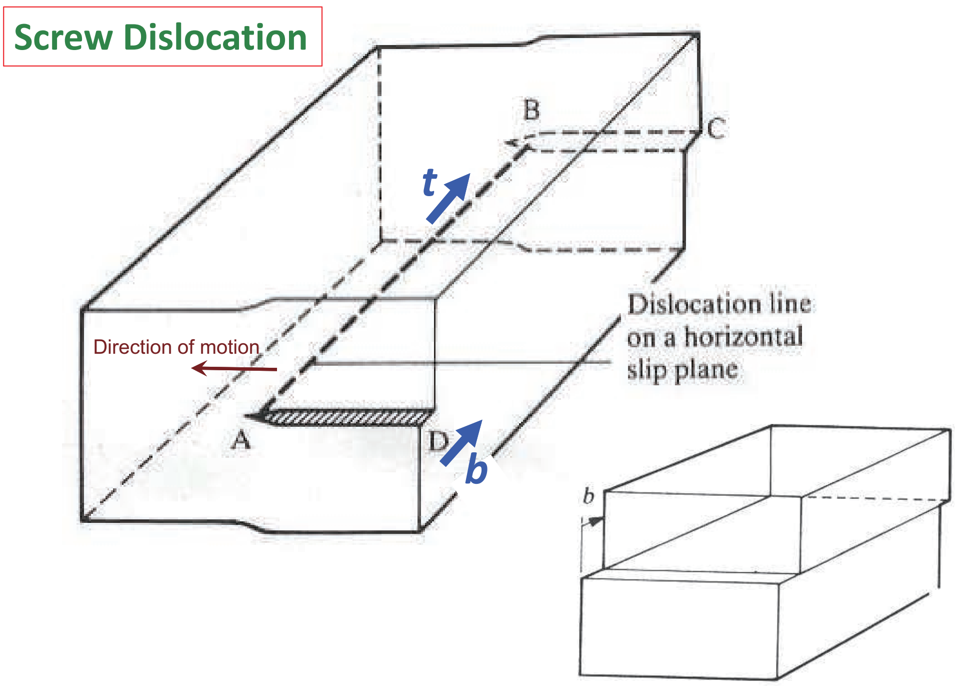

Screw Dislocation

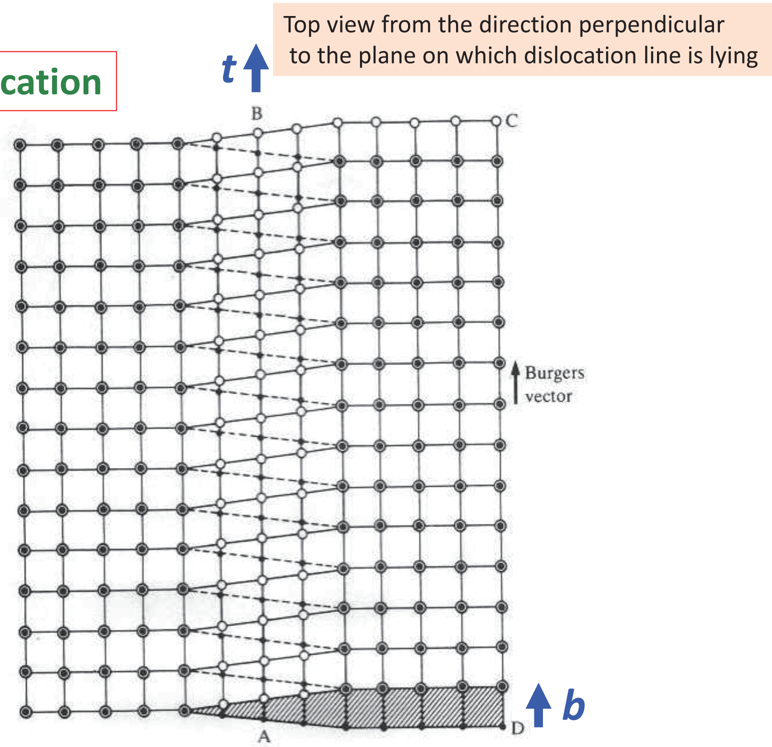

Signs of screw dislocations

determined by the direction of spiral configuration of atoms

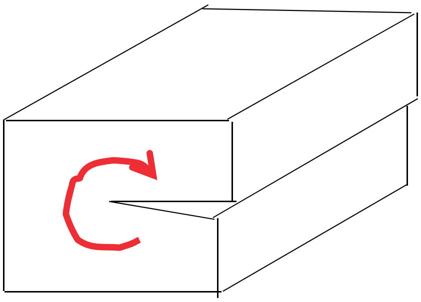

Right-handed (R-H) Screw dislocation

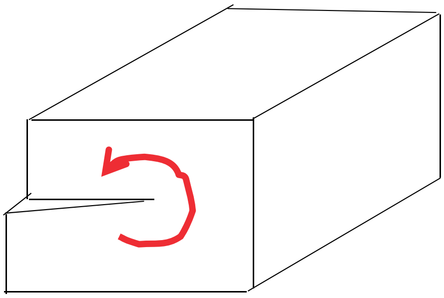

Left-handed (L-H) Screw dislocation

Mixed Dislocation

Burgers vector is conservative on one dislocation line

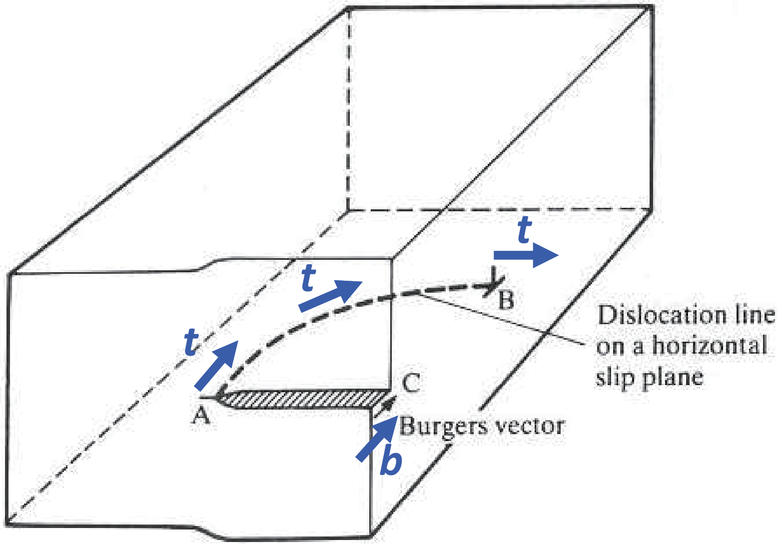

Mixed Dislocation

Top view from the direction perpendicular to the plane on which dislocation line is lying

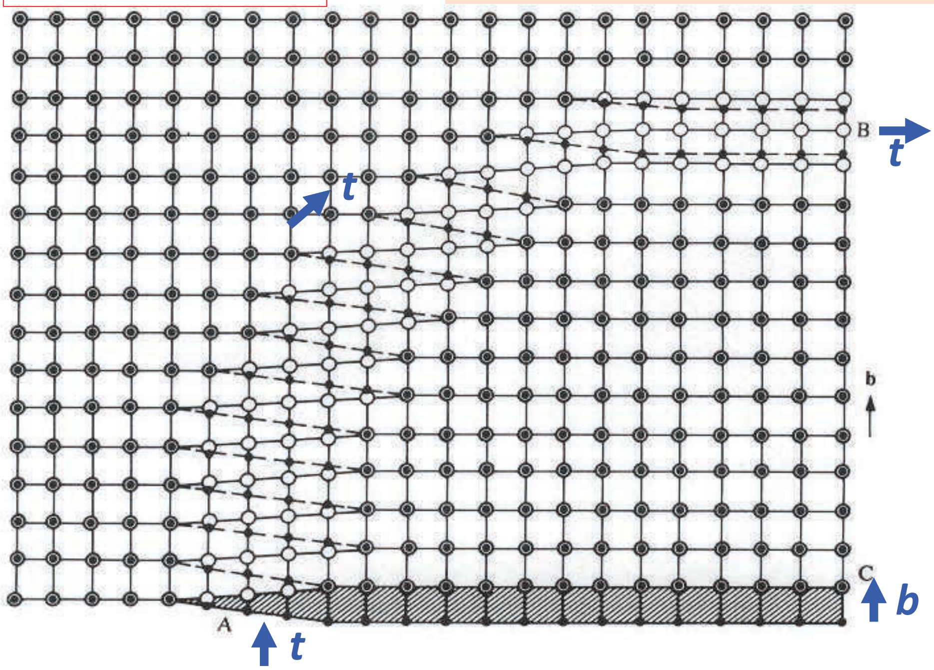

Dislocation loop

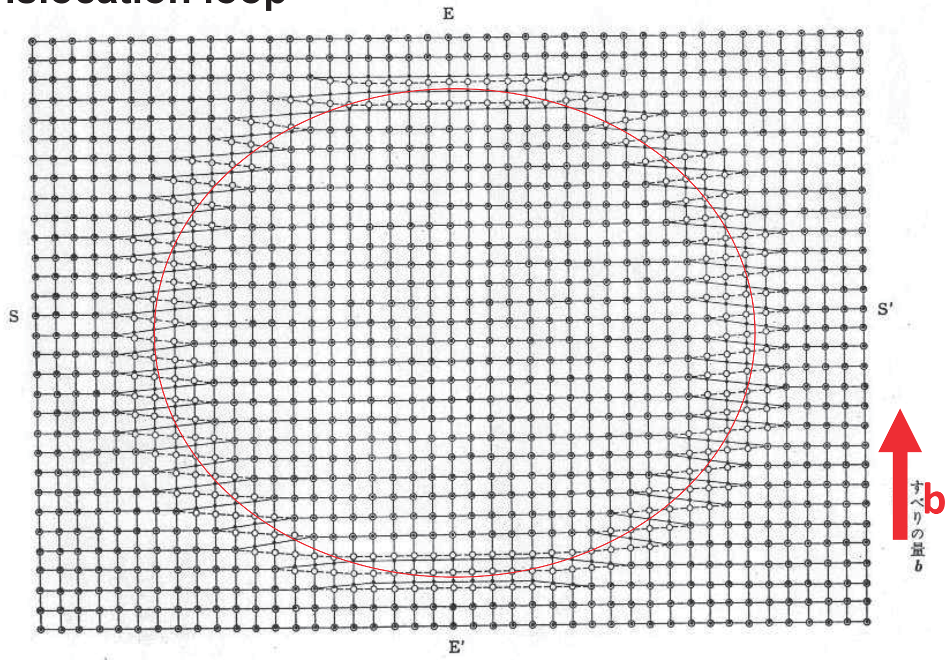

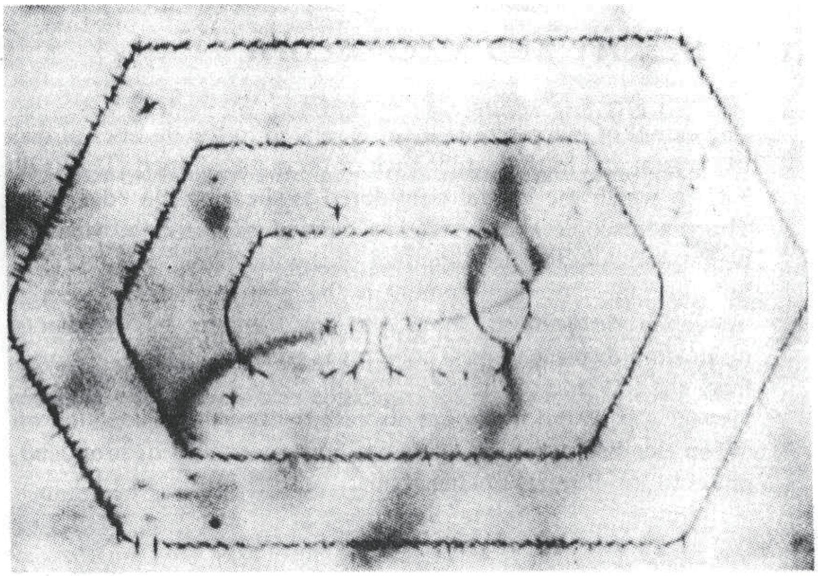

An example of a Frank–Read source in silicon. The dislocation loops have been delineated by chemical etching. In silicon, the loops are not circular; the anisotropic bonding of Si creates "loops" composed of approximately straight segments. (*From W. G. Dash, Dislocations and Mechanical Properties of Crystals. ed. J. C. Fisher, Wiley, New York, 1957.*)

Frank−Read Source

Dislocation source in a crystal

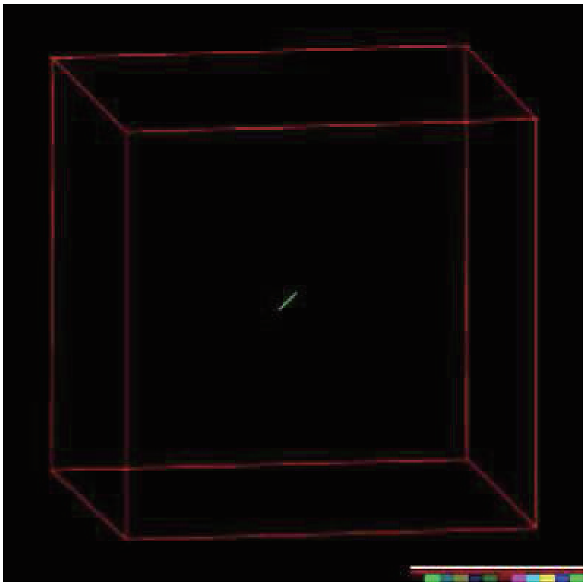

http://zig.onera.fr/DisGallery/

Frank-Read source in silicon crystals

deformed at 700°C

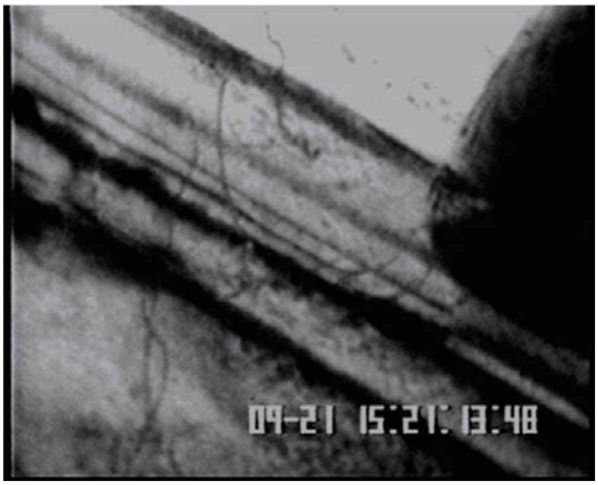

0.3μm

K. Higashida

Role of dislocations on mechanical properties

Not only the mechanism of plastic deformation
but also
strengthening

Work-hardening: To increase flow stress with
加工硬化 increasing dislocation density

Toughening: To suppress crack extension
強靭化 by dislocation emission
from the crack-tip

種々の転位構造
Dislocation Configurations

1．亀裂先端近傍の転位構造
Dislocation Configurations around a crack-tip
電子顕微鏡像
Transmission electron microscopy images

2．加工硬化を引き起こす転位構造
Dislocation Configurations causing
work-hardening
転位腐食孔による転位分布の観察
Dislocation distribution observed by etch-pits

Dislocation configuration in front of a crack-tip in a MgO crystal

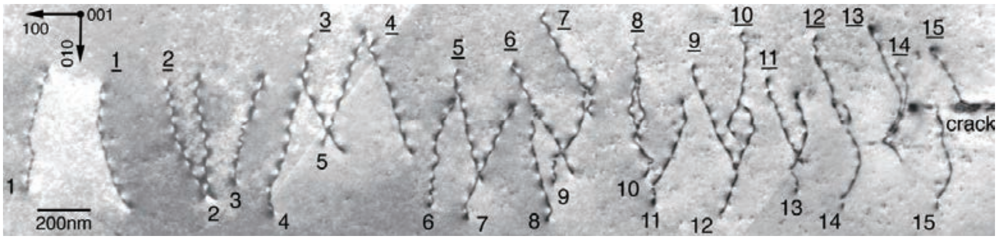

{001} incidence, g=020

Simulated image of screw disloc.

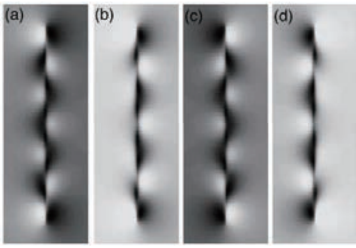

RH screw **LH screw**

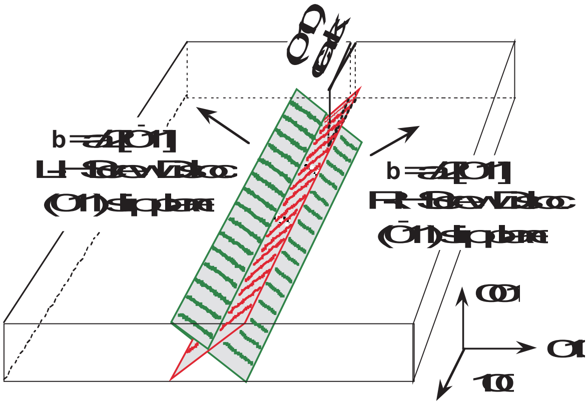

Simulated image of screw dislocations Inclining to the foil surface

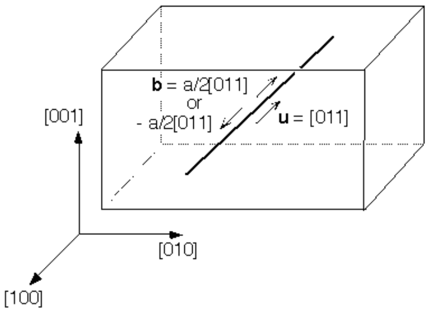

Under just Bragg condition

Right-handed screw disloc.

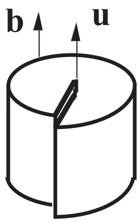

Left-handed screw disloc.

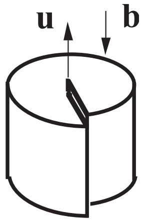

Dislocation configuration in front of a crack-tip in a MgO crystal

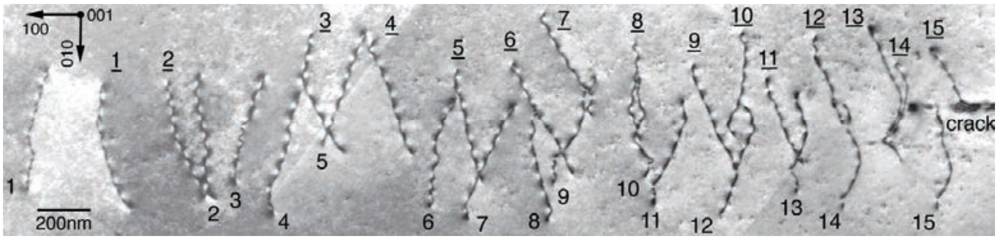

{001} incidence, g=020

Simulated image of screw disloc.

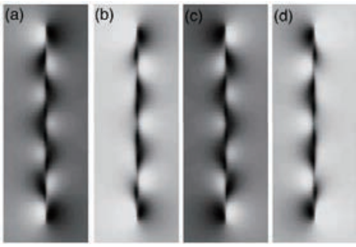

RH screw LH screw

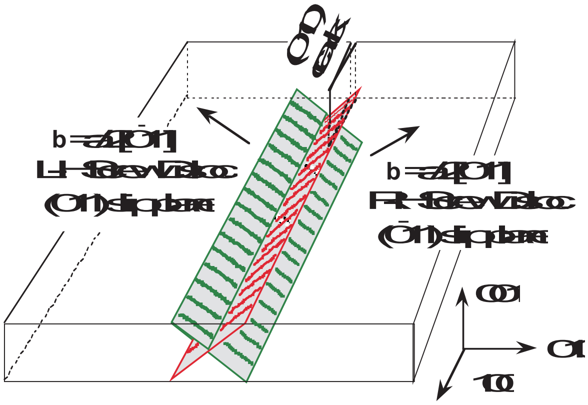

Local Stress Intensity Factor k_D due to a Screw Dislocation

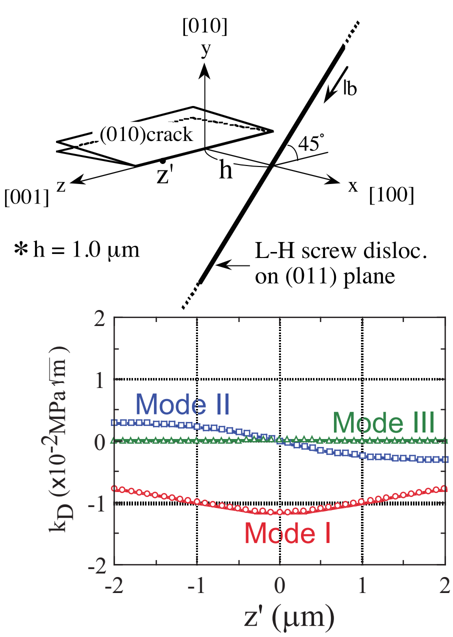

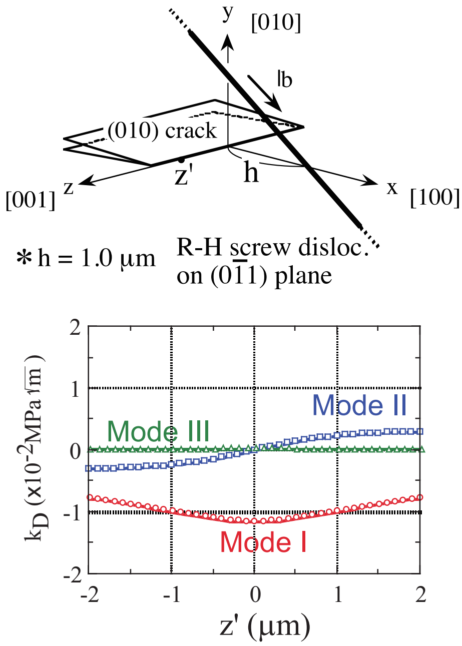

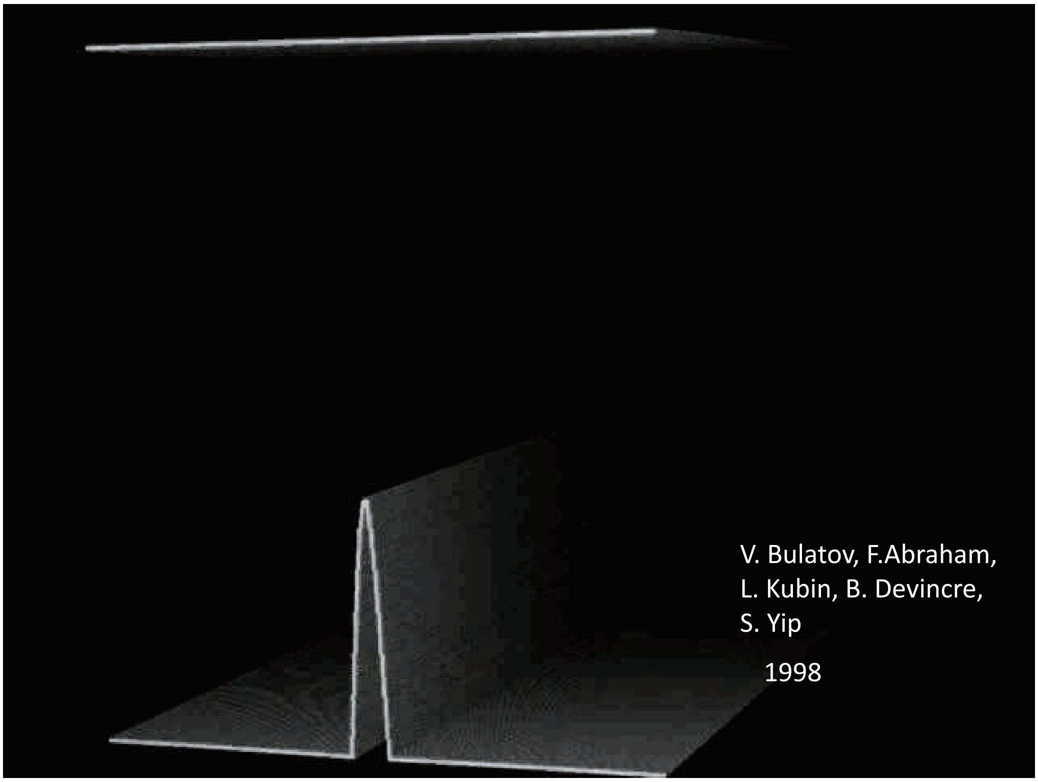

Crack and dislocations in Si crystal

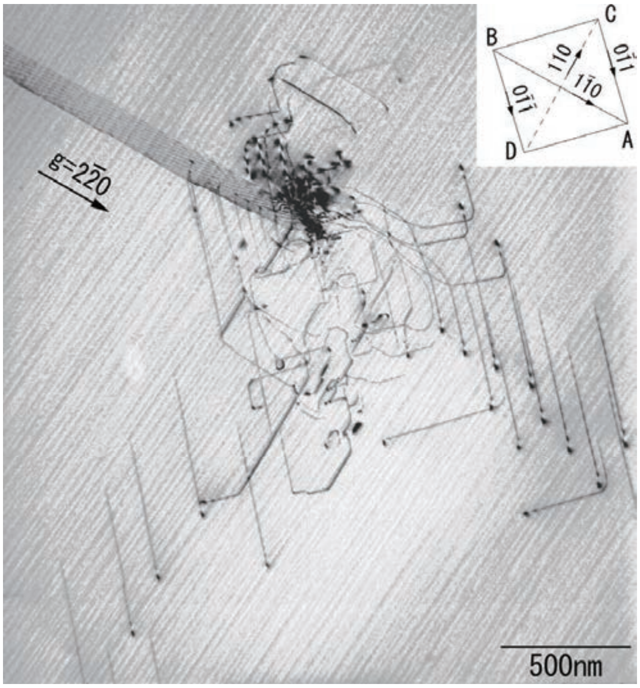


[1̄10]
[110]
[001]
g=220

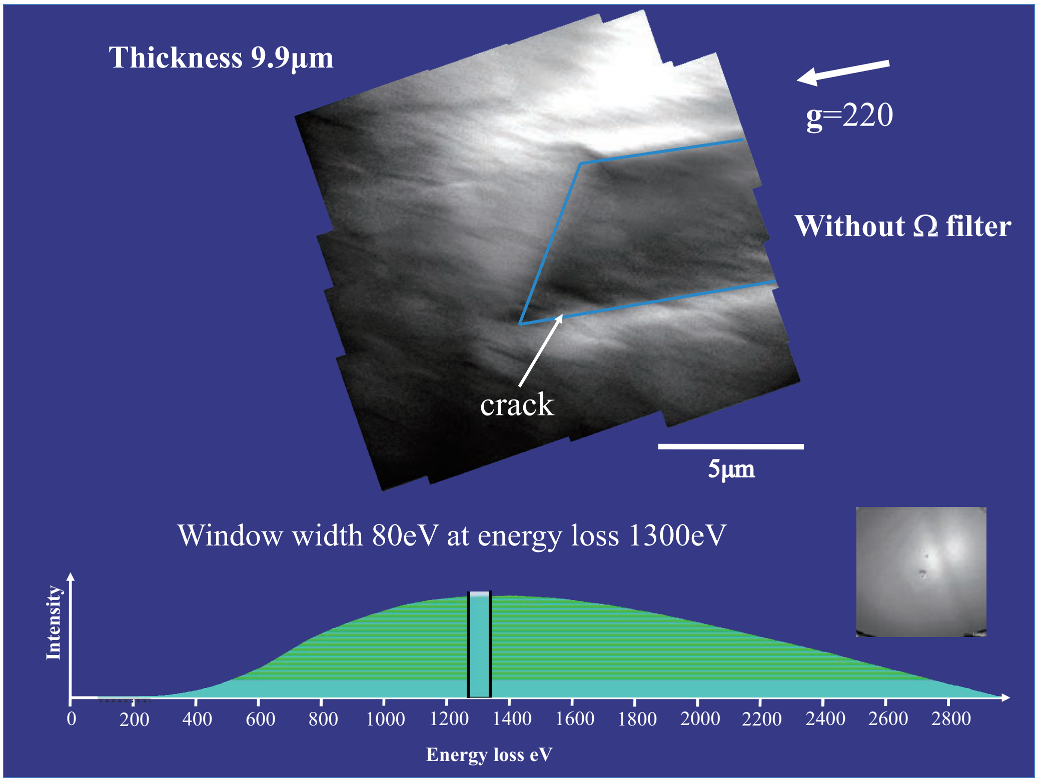
Thickness 9.9μm
g=220
Without Ω filter
crack
5μm
Window width 80eV at energy loss 1300eV
Intensity
0
200
400
600
800
1000
1200
1400
1600
1800
2000
2200
2400
2600
2800
Energy loss eV

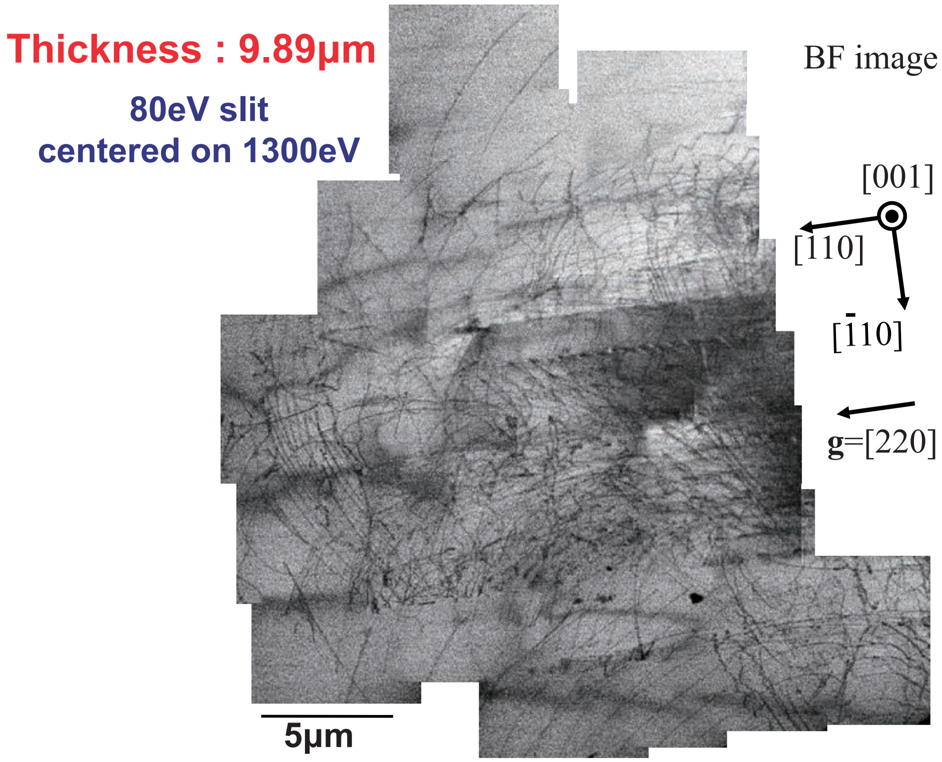

種々の転位構造
Dislocation Configurations

1．亀裂先端近傍の転位構造
Dislocation Configurations around a crack-tip
電子顕微鏡像
Transmission electron microscopy images

2．加工硬化を引き起こす転位構造
Dislocation Configurations causing work-hardening
転位腐食孔による 転位分布の観察
Dislocation distribution observed by etch-pits

A. H. Cottrell:

Dislocations and Plastic Flow in Crystals (1953), P.151より

14. WORK HARDENING

14.1. Introduction

Few problems of crystal plasticity have proved more challenging than work hardening. It is a spectacular effect, for example enabling the yield strengths of pure copper and aluminium crystals to be raised a hundred fold. Also, it occupies a central place in the subject, being related both to the nature of the slip process and to processes such as recrystallization and creep. It was the first problem to be attempted by the dislocation theory of slip and may well prove the last to be solved.

Etch Pits on {111} Plane

エッチピット法による転位分布観察

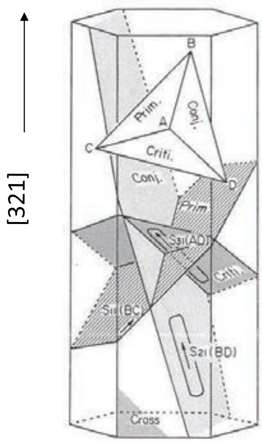

Cu-1at.%Ge Crystal

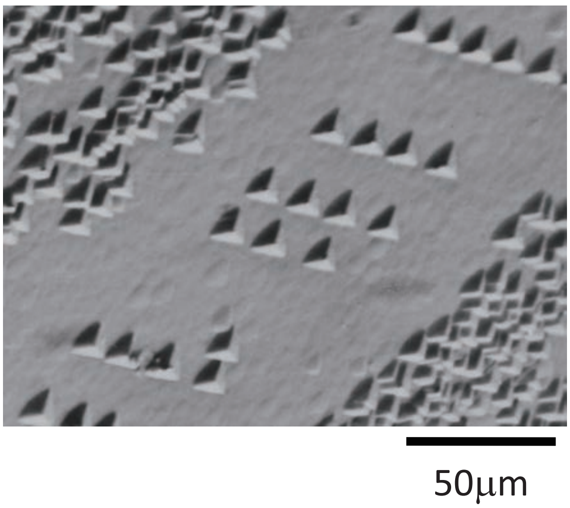

Dislocation Distribution Revealed by Etch-Pits

Cu-1at.%Ge
Deformed at RT
Stage I

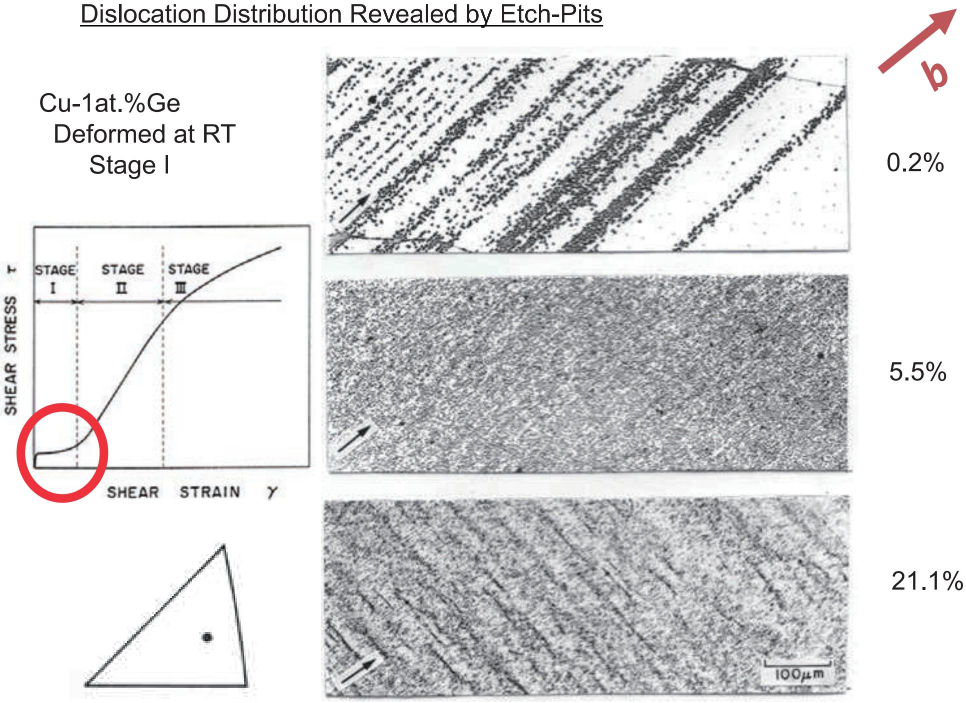

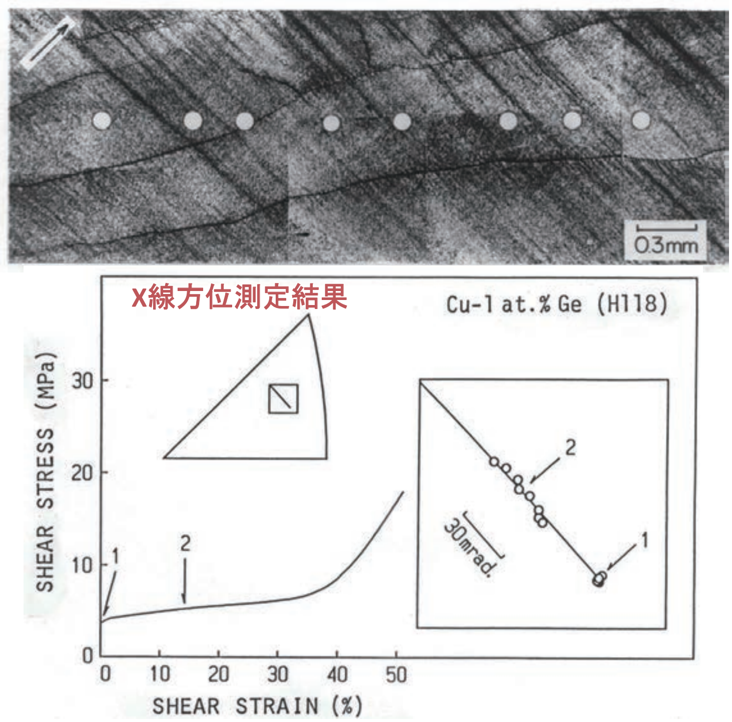

彎曲すべり（Bend Gliding）

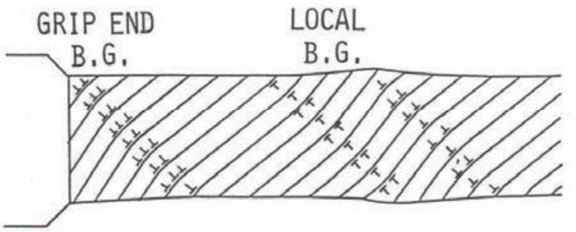

過剰転位（Excess Dislocation）

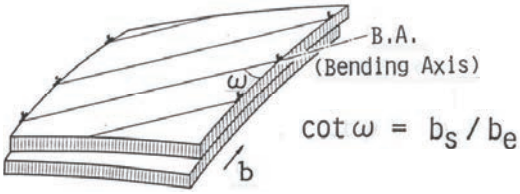

J. Takamura (1955)

主すべり活動の
不均質

Geometrically Necessary Dislocation

Cu Crystal

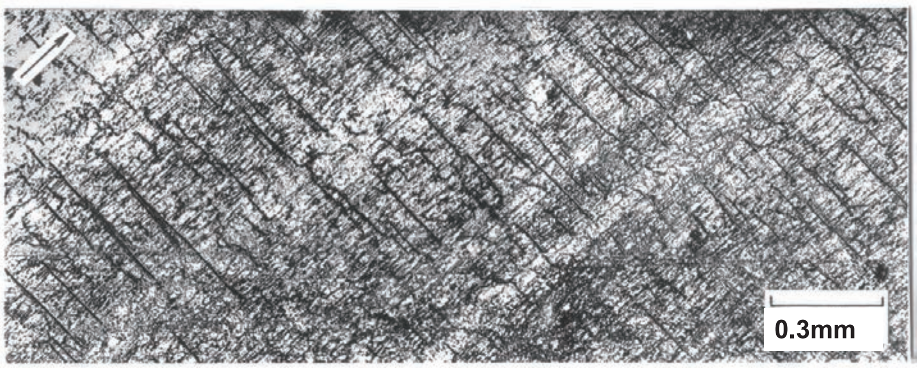

Primary Slip Direction

Transition from Stage I to II

Dislocation Accumulation due to Kink Bands in Early Stage II

Revealed by Etch-Pits in Cu Crystal Deformed at RT

変形帯
Kink Bands

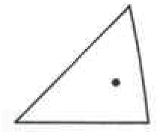

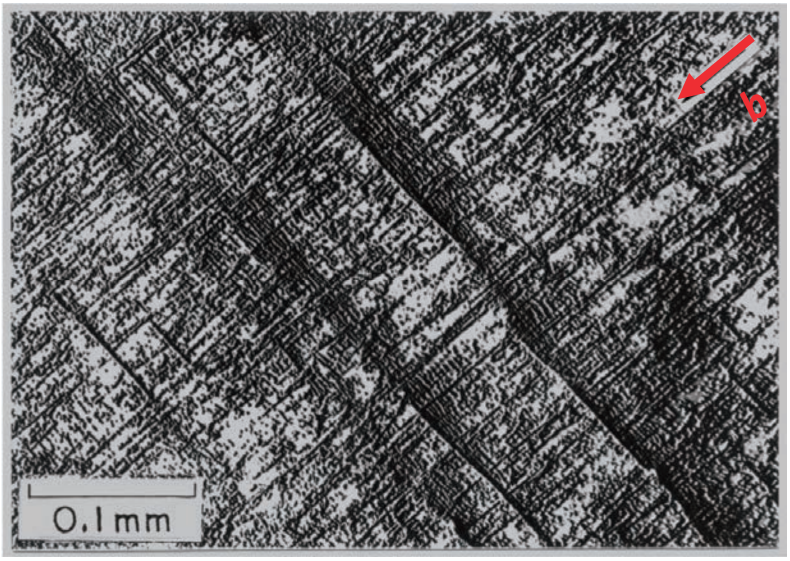

Outline

1. 転位と塑性変形
   Dislocations and plastic deformation

2. 種々の転位観察
   Observations of various dislocation configurations

3. キンク変形について
   Observations of Kink Deformation

Outline

1. Characteristic behaviors in plastic deformation of HCP crystals.

2. Origin of high strength and good ductility in Mg-Zn-Y alloy with a synchronized LPSO structure

3. Kink bands contribute not only to plastic deformation but also to an essential strengthening mechanism.

Mg Alloy containing Zn and Rare Earth Elements

High strength and sufficient ductility for plastic working

$Mg_{97}Zn_1Y_2$

Synchronized Long period stacking order (LPSO) phase(18R) in $Mg_{97}Zn_1Y_2$

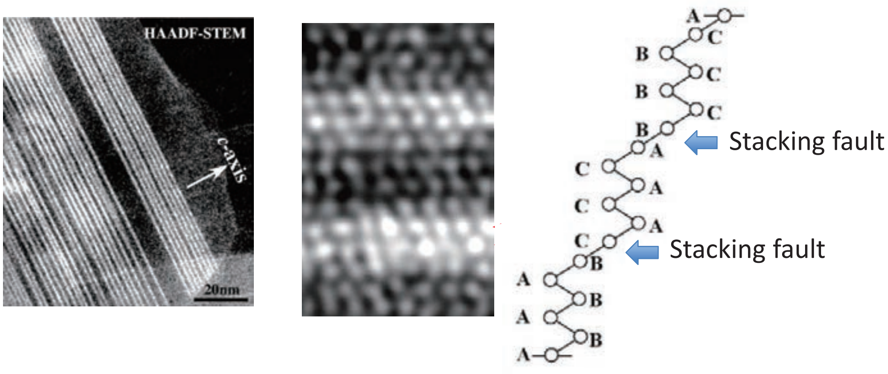

HAADF-STEM Image（E. Abe, Y.Kawamura, K.Hayashi and A.Inoue : Acta Mater., 50(2002),3845）

Slip system in HCP crystals

$\{0001\}\langle 1\bar{1}\bar{2}0\rangle$ 2 independent slip systems
$\{1\bar{1}00\}\langle 1\bar{1}\bar{2}0\rangle$ 2 independent slip systems] a slip

To satisfy the arbitrary deformation by slip

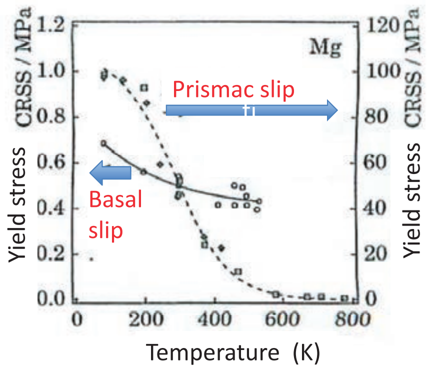

H. Numakura, vol.37（1998）

Von Mises criterion : five independent slip systems

a + c slip

$\{11\bar{2}2\}\langle\bar{1}\bar{1}23\rangle$, $\{10\bar{1}1\}\langle\bar{1}\bar{1}23\rangle$

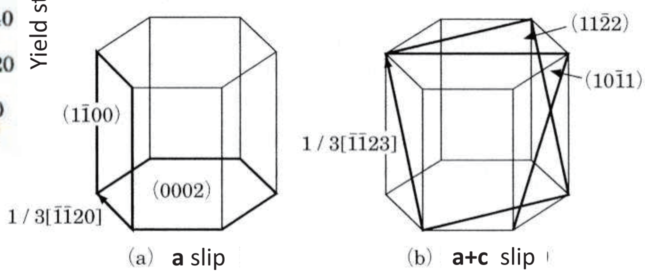

Stress-strain curves of single crystals （deformed in tension at RT）

P.B.Hirsch and T.E.Mitchell, 1967

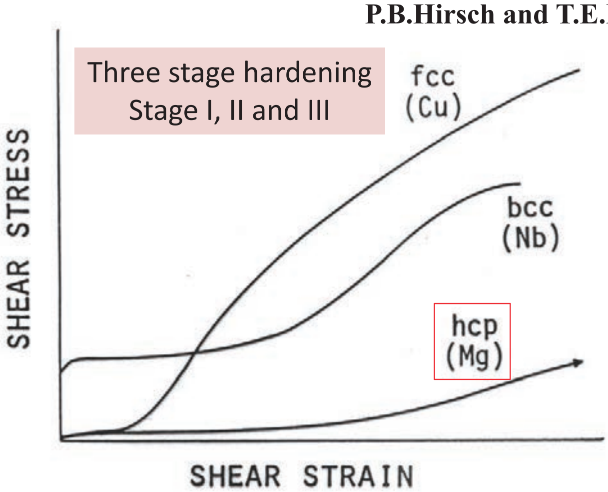

In HCP crystal, large extent of stage I
dominant operation of basal slip
and no activation of secondary

Remarkable Anisotropy
of slip system

Orientation dependence of Stress-strain curves （compressed at RT ）

Mg-5at.Zn-7at.%Y DS crystals (18R LPSO structure)　Hagihara et al.

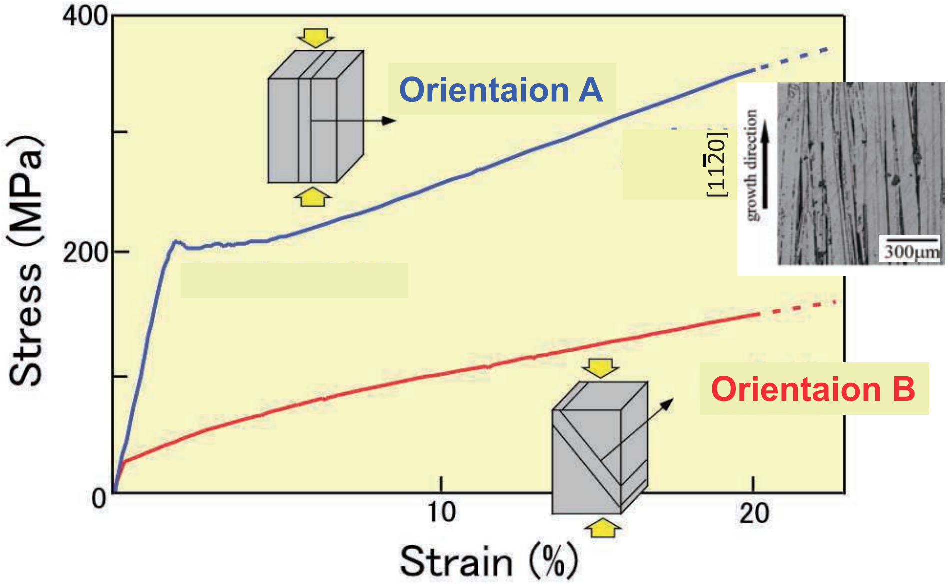

Temperature dependence of yield stress

Mg-5at.Zn-7at.%Y DS crystals (18R structure)　Hagihara et al.

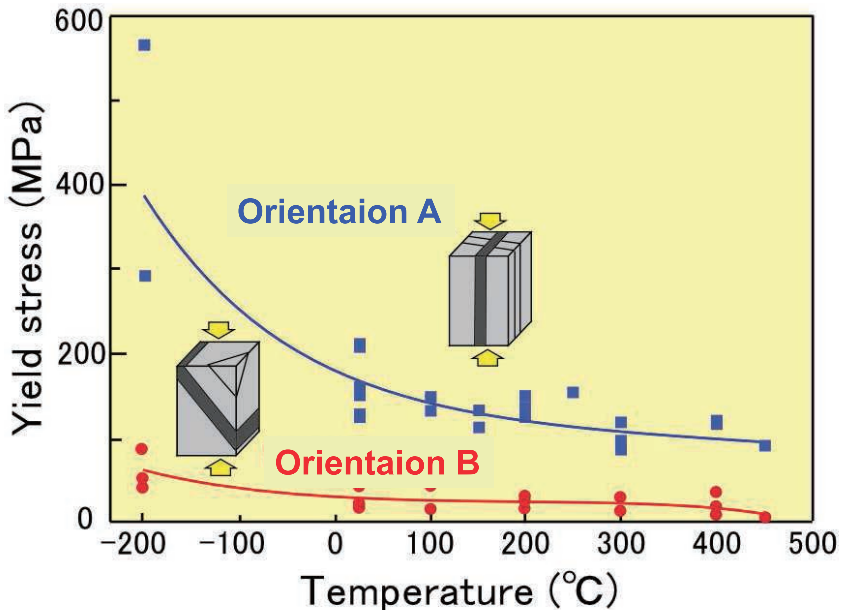

Slip bands in orientation B

Mg-5at.Zn-7at.%Y DS crystals (18R structure) Hagihara et al.

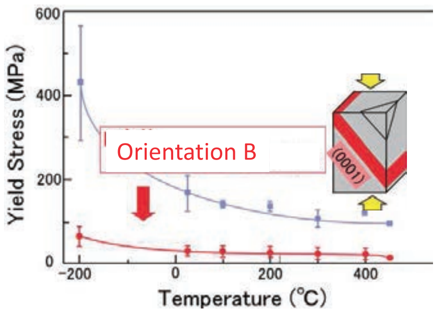

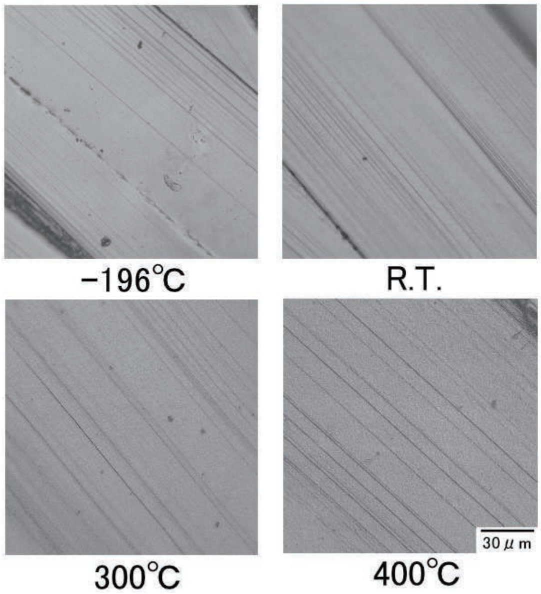

(0001) basal slip bands
are observed
at every temp.

Orientation B : Basal plane is inclined to compressive axis by

Surface undulation in orientation A

Hagihara et al.

Mg-5at.Zn-7at.%Y
DS crystals (18R)

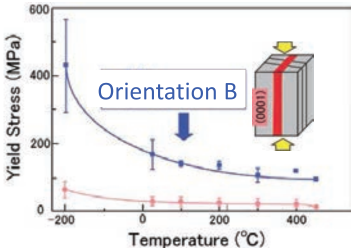

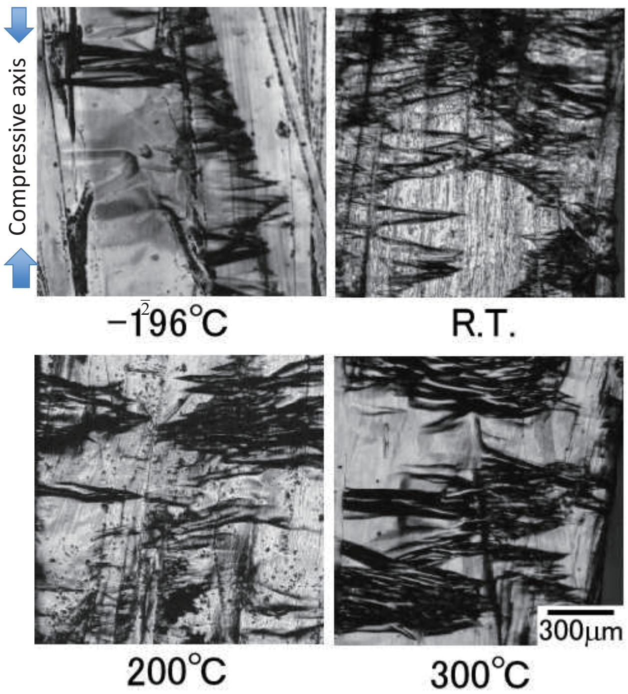

Kink bands
are observed
at every temp.

Orientation A :
compressive axis is <1120>

In-Situ observation of kink bands formation

Hagihara et al.

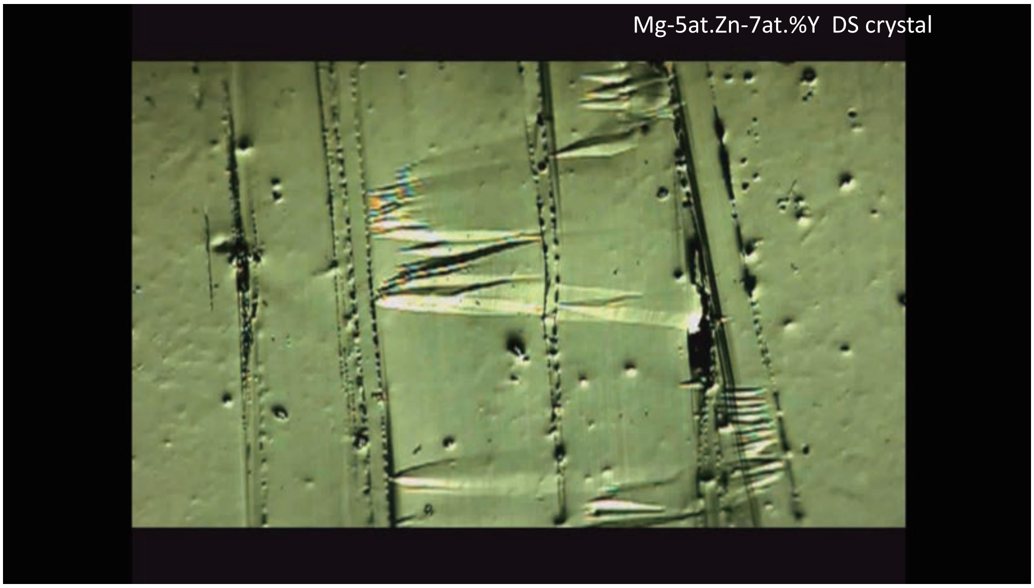

Crystal rotation due to kink bands

Hagihara et al.

Mg-5at.Zn-7at.%Y DS crystals (18R)

Orientation A

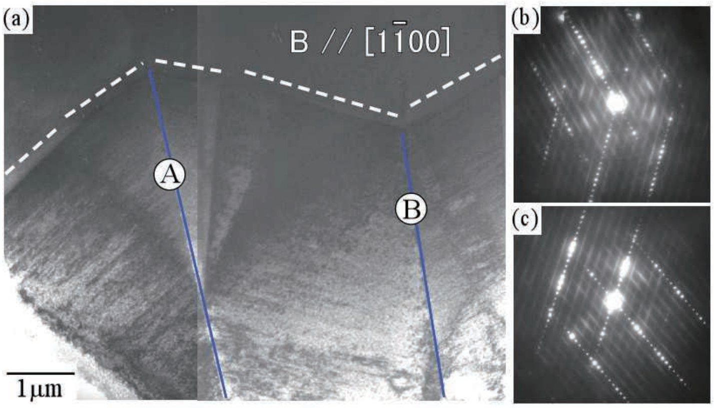

Rotation axis: <1100>

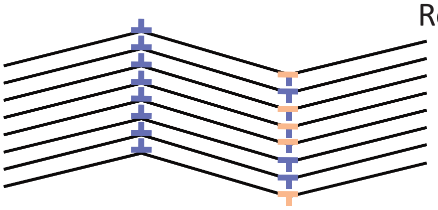

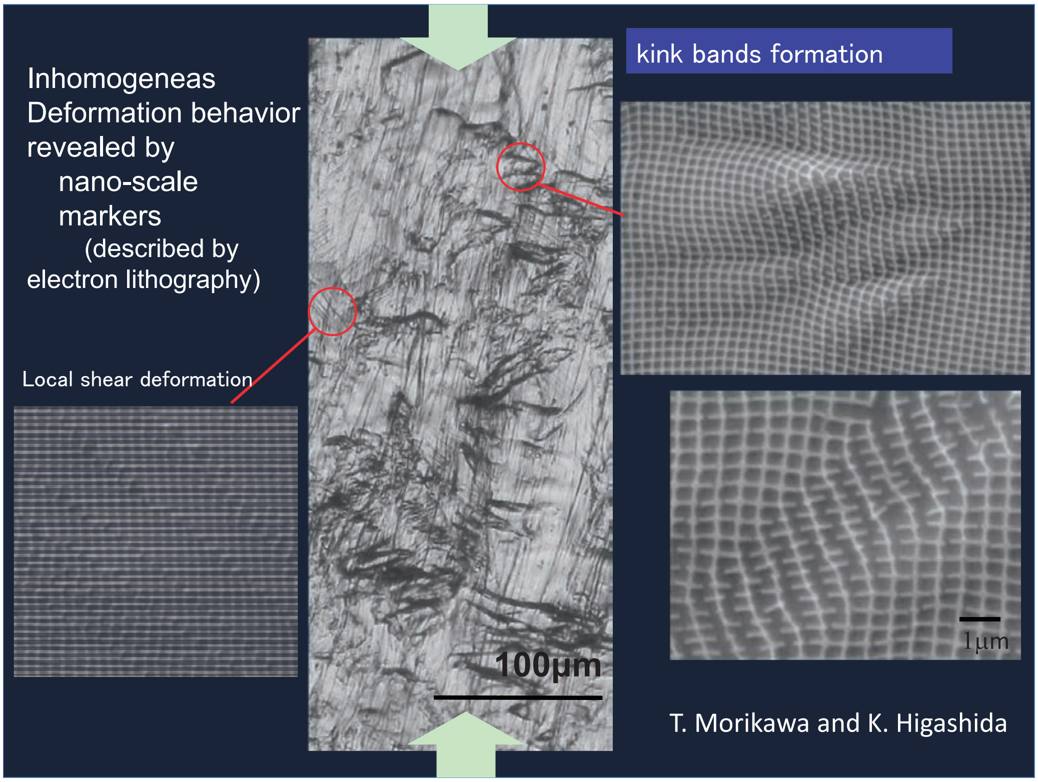
Inhomogeneas
Deformation behavior
revealed by
nano-scale
markers
(described by
electron lithography)
Local shear deformation
100μm
kink bands formation
1μm
T. Morikawa and K. Higashida

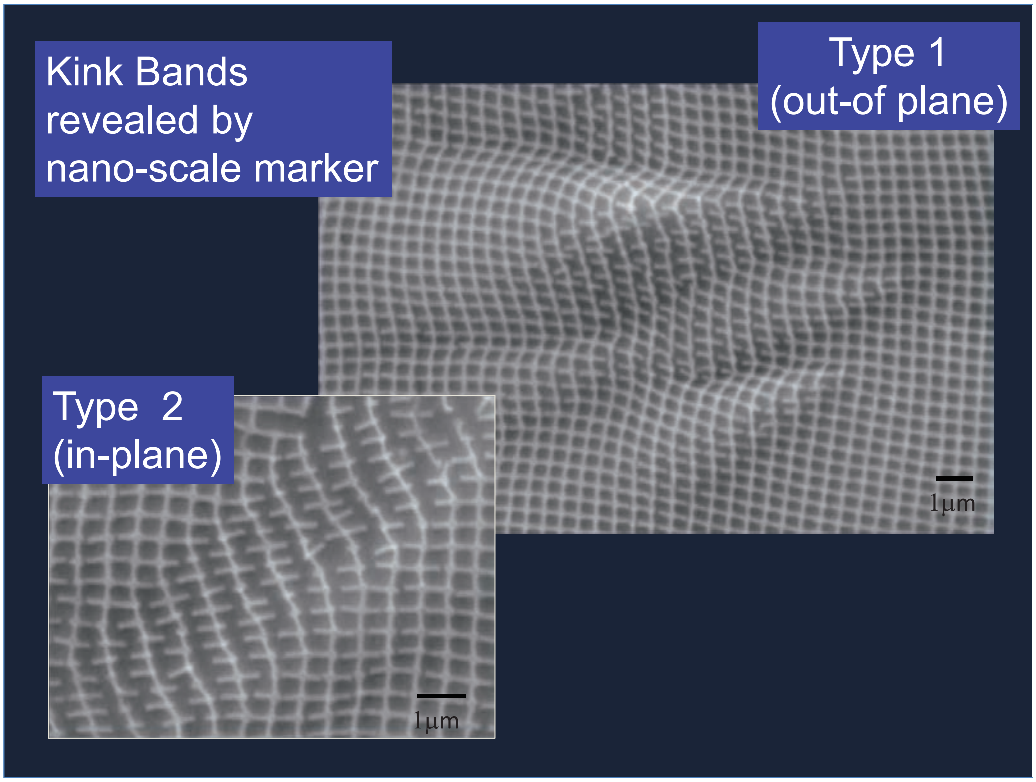
Kink Bands
revealed by
nano-scale marker
Type 1
(out-of plane)
1μm
Type 2
(in-plane)
1μm

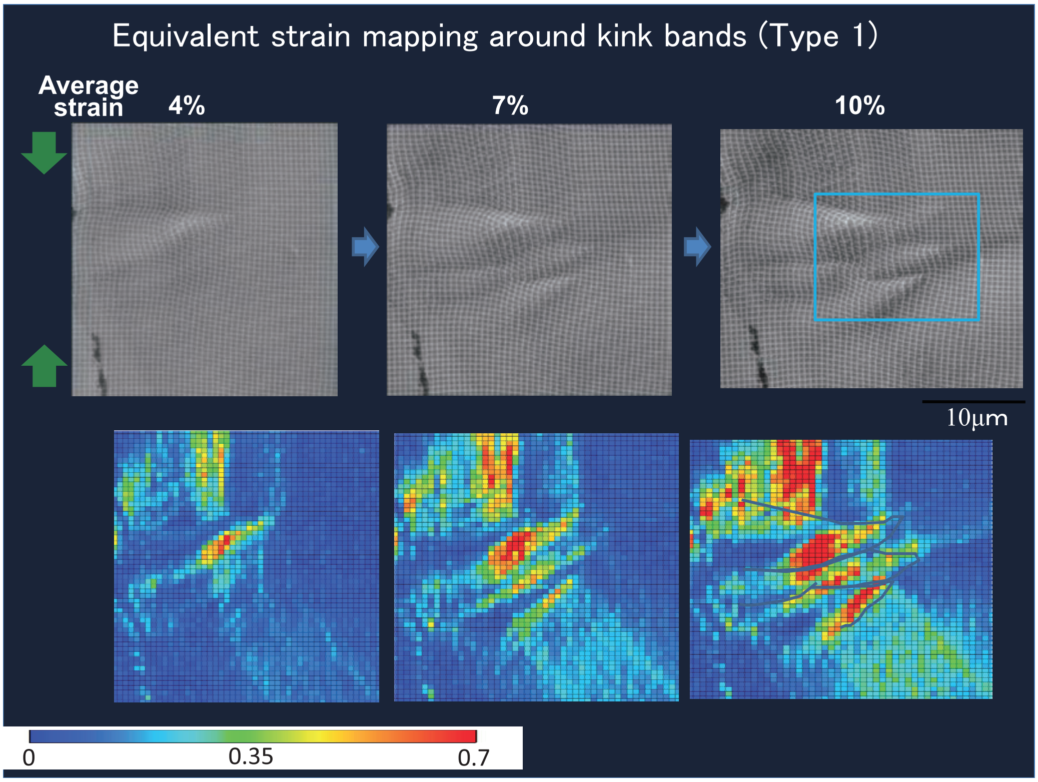

Motion of a Kink Boundary in Mg-Y-Zn LPSO crystal

The same area observation

Compressive strain 6%,

Compressive Strain 9%,

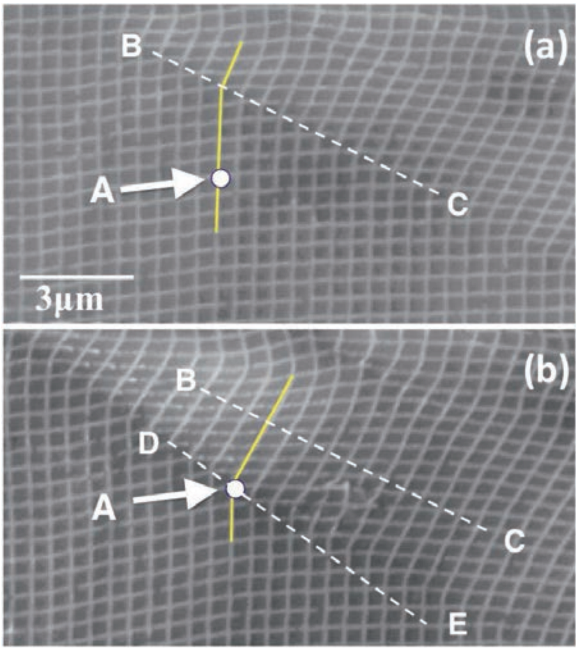

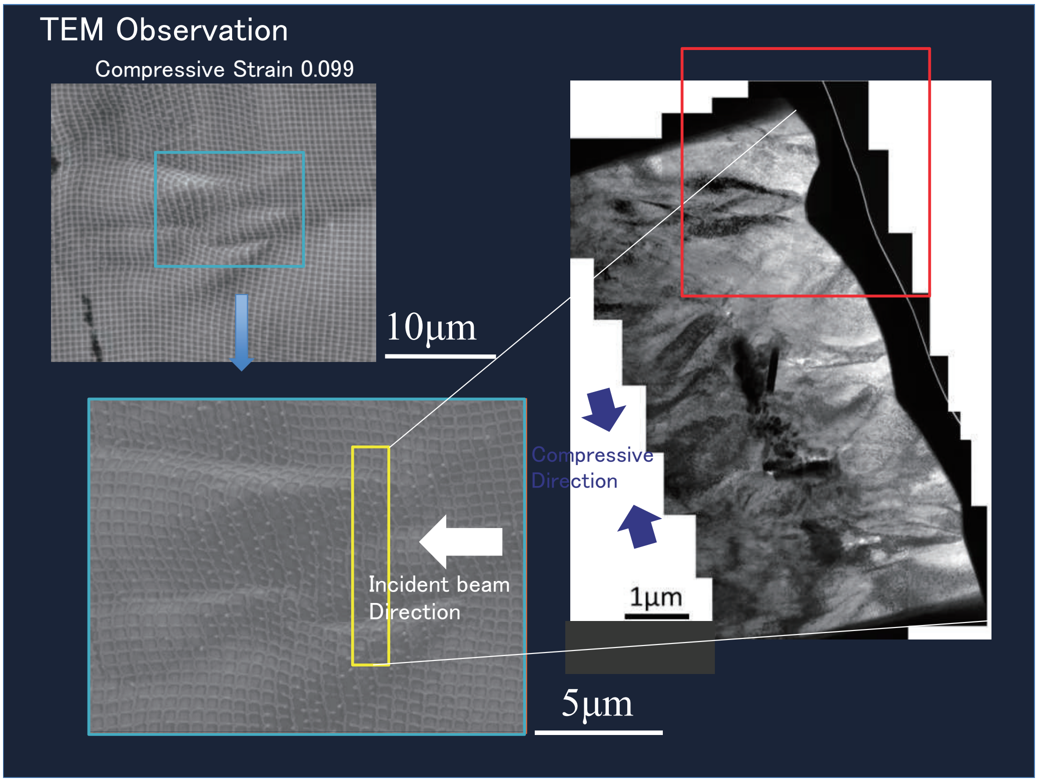
TEM Observation
Compressive Strain 0.099
10μm
Compressive
Direction
Incident beam
Direction
1μm
5μm

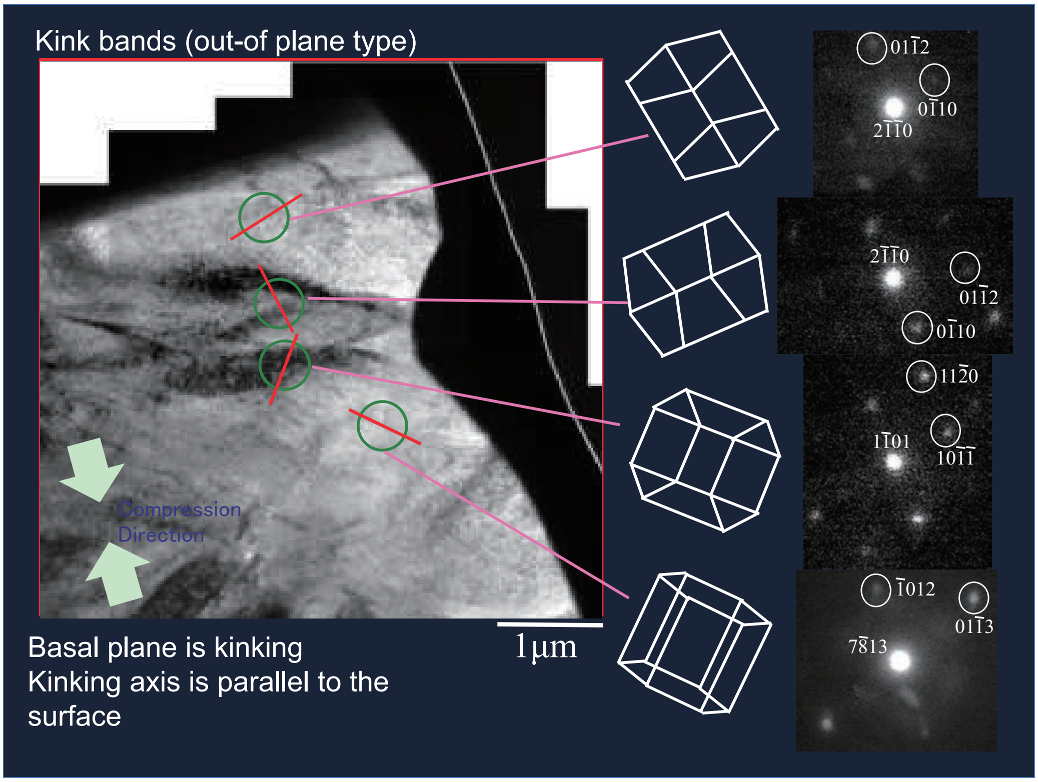
Kink bands (out-of plane type)
Compression
Direction
Basal plane is kinking
Kinking axis is parallel to the
surface
1μm
01$\bar{1}$2
0$\bar{1}$10
2$\bar{1}\bar{1}$0
2$\bar{1}\bar{1}$0
01$\bar{1}$2
0$\bar{1}$10
11$\bar{2}$0
1$\bar{1}$01
10$\bar{1}\bar{1}$
$\bar{1}$012
01$\bar{1}$3
7$\bar{8}$13

Development of kink bands (in-plane shear type)

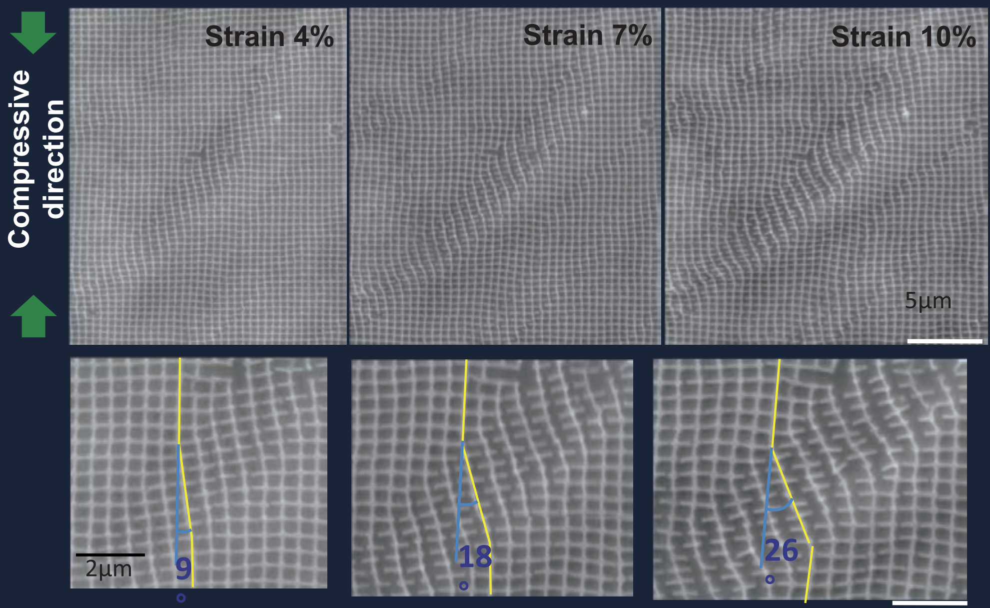

No displacement perpendicular to the surface
No surface undulation

Kink bands (in-plane shear type)

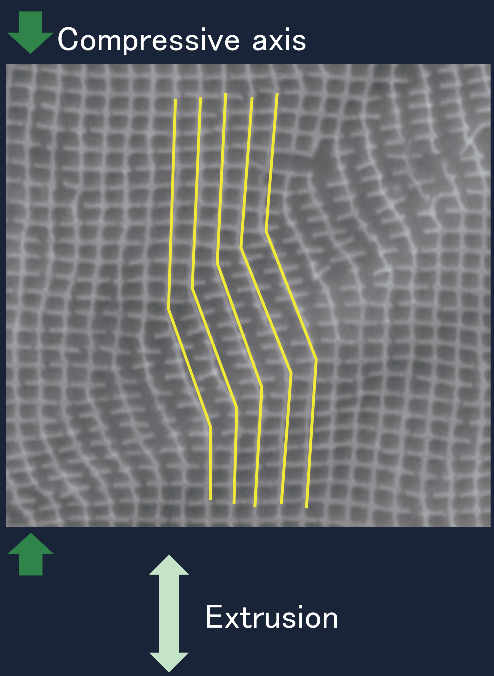

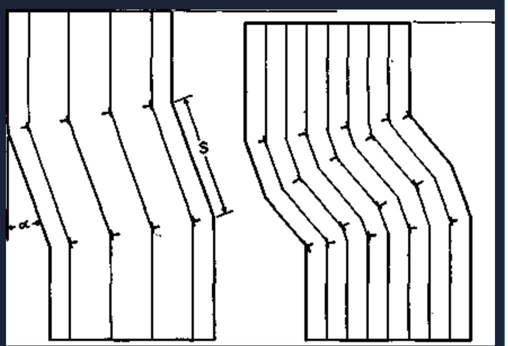

Hess and Barrett:
Metals Transactions(1949)

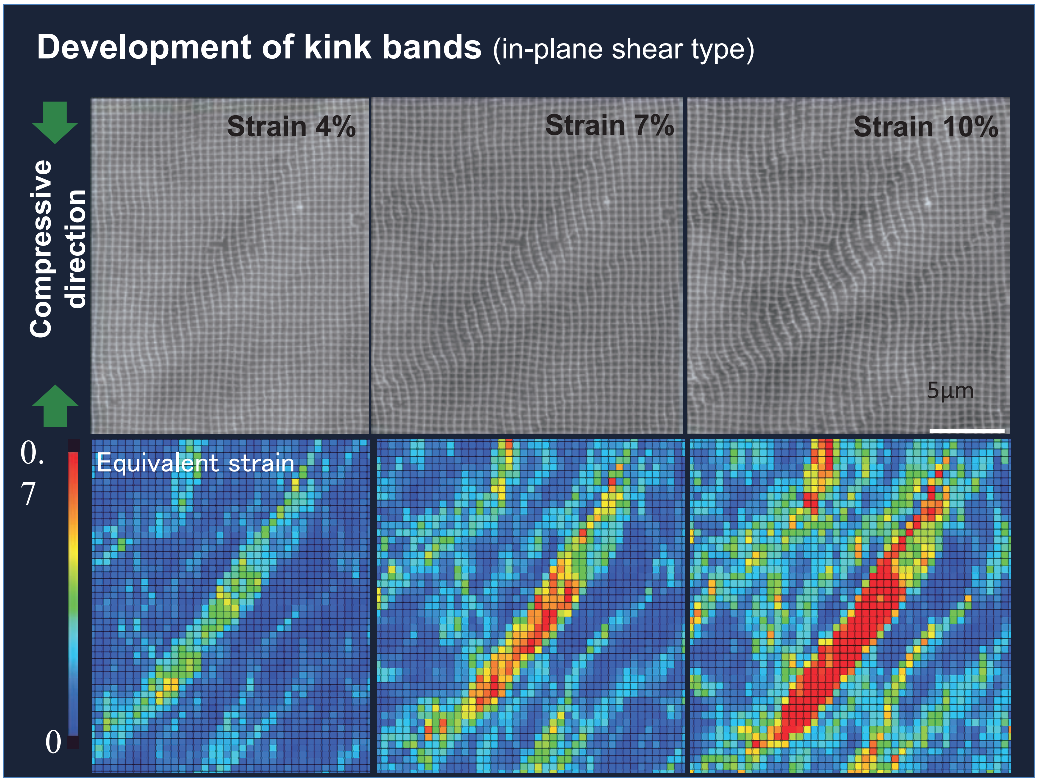

E.Orowan, Nature, Vol.149 (1942)

"A type of plastic deformation new in metals"

Fig. 1.
PHOTOGRAPHS OF KINKS IN ORIGINALLY CYLINDRICAL CADMIUM SINGLE-CRYSTAL WIRES OF 1 MM. DIAMETER.

Kink Bands in Cd

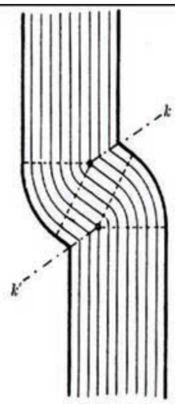

Fig. 2.
STRUCTURE OF THE KINK IN FIG. 1 a.
Thin parallel lines, glide planes. Broken lines, boundaries of the wedge-shaped regions of flexural glide. Dash-dotted lines k and k' : planes of kinking.

A kind of Buckling

Kink Bands in Ti_3SiC_2

M.W. BARSOUM, L. FARBER, and T. El-RAGHY
METAL. MATER. TRANSACTIONS A(1999)

Fig. 7—(*a*) Bright-field image of and (*b*) schematic of a region containing two adjacent kink bands denoted as i and ii. The crystal is close to the edge-on position for the basal planes. The numbers show the measured rotation angles between the blocks of the crystal around [11 00] directions provided, mostly, by the kink boundaries.

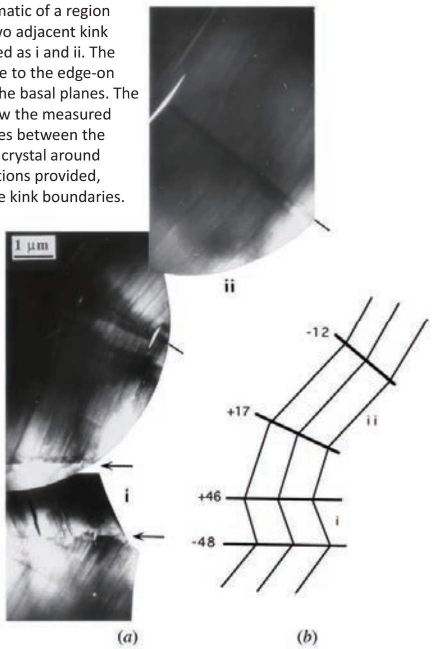

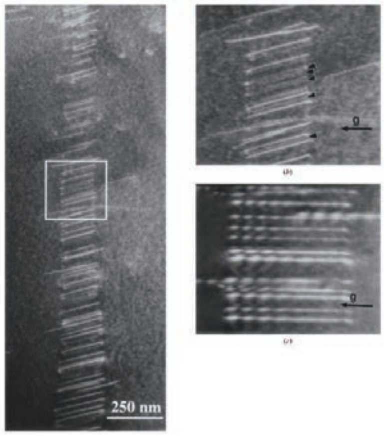

ig. 4—(*a*) Dislocation wall; dislocations are parallel and positioned in different basal planes one under another. (*b*) Same area as white square in (a), but at higher magnification (imaged in *g* □336 0□). (*c*) Weak beam image of the same area as in (b), but tilted and imaged in *g* of □33 00□. Dislocations that become invisible in (c) are perfect edge dislocation; those that remain visible are mixed dislocations.

Outline

1. Characteristic behaviors in plastic deformation of HCP crystals.

2. Origin of high strength and good ductility in Mg–Zn–Y alloy with a synchronized LPSO structure

Kink bands contribute not only to plastic deformation but also to an essential strengthening mechanism.

Strengthening by formation of kink bands　　K. Takashima et al.

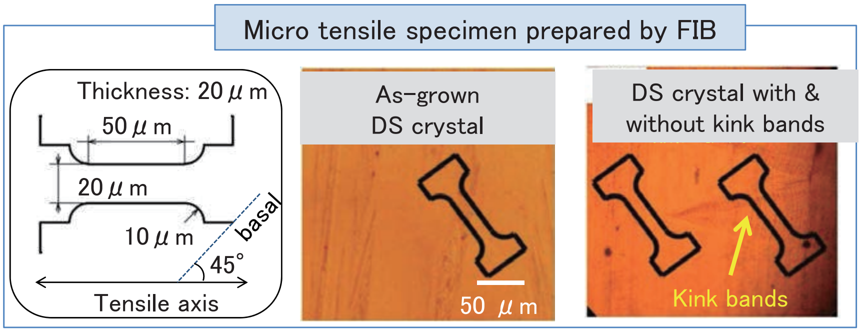

Micro tensile specimen

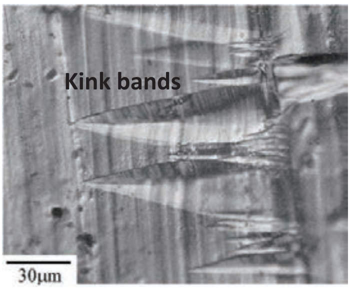

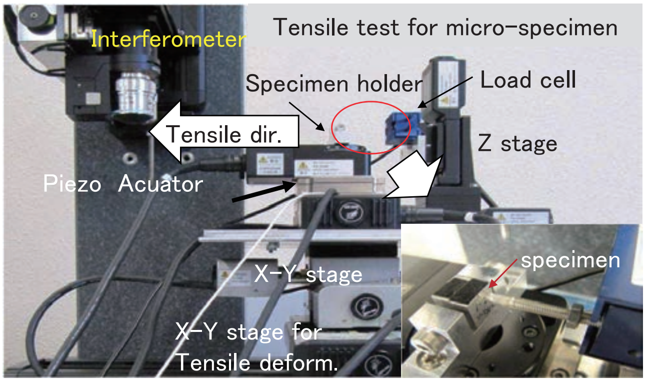

Strengthening by formation of kink

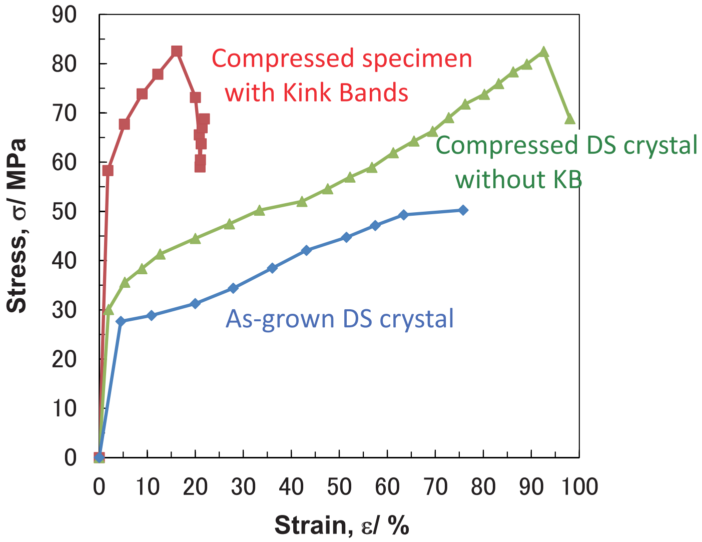

Kink bands

⇩

Remarkable increase in yield strength and work-hardening rate.

	YS MPa	TS MPa	WHR MPa	Fracure str. %
As−grown DS	28	51	41 (ε:11-57%)	76
Compressed DS	35	82	53 (ε:20-93%)	98
DS with KB	65	84	167 (ε:5-14%)	22

Relation between hardness and kink bands spacing (Mg-Zn-Y)

M. Fujiwara et al.

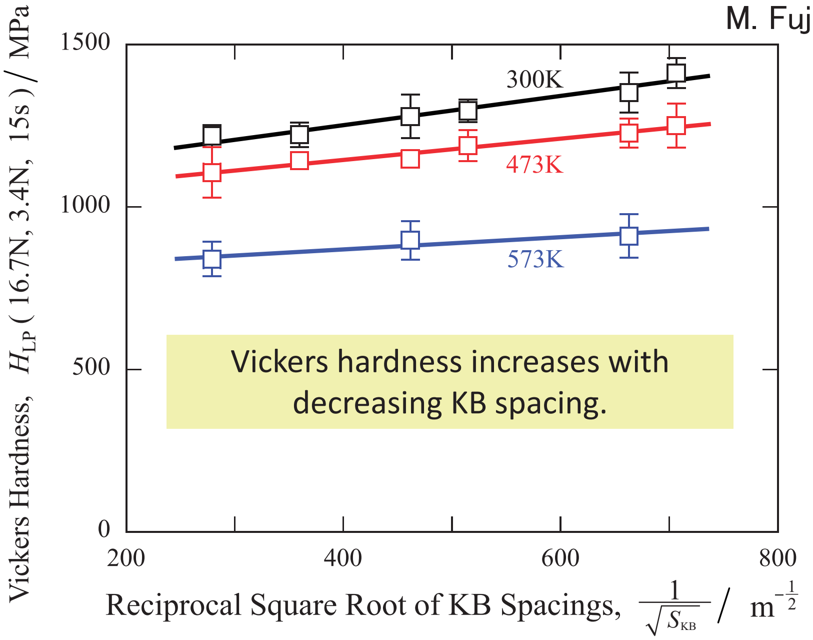

Hv

Summary

1. 転位と塑性変形
   Dislocations and plastic deformation

2. 種々の転位観察
   Observations of various dislocation configurations

3. キンク変形について
   Observations of Kink Deformation

個々の転位の記述と
同時に集団運動の記述
の重要性

液晶における転位と準周期性
(Quasi-periodicity and dislocation in liquid crystals)

時弘哲治, Tetsuji Tokihiro
東京大学・大学院数理科学研究科
Graduate School of Mathematical Sciences, The University of Tokyo

By the analogy between liquid crystals and super conductors in statistical physics, a screw dislocation in a liquid crystal corresponds to a magnetic vortex in a super conductor. According to this analogy, there exists the twisted grain boundary (TGB) phase in liquid crystals that is an analogue of the Abrikosov phase in super conductors. In this talk, we wish to explain relations of the quasi-periodicity of TGB phase to the classification of quasi-crystals in terms of class numbers in number theory.

References

[1] N. D. Mermin, "The topological theory of defects in ordered media", Rev. Mod. Phys., **51**, pp. 591-648 (1979).
[2] P. M. Chaikin and T. C. Lubensky, *Principles of condensed matter physics*, Cambridge University Press, (1995).
[3] S. R. Renn and T. C. Lubensky, "Abrikosov dislocation lattice in a model of the cholesteric-to-smectic-A transition", Phys. Rev. A, **38**, pp.2132-2147 (1988).
[4] J. Goodby et al., "Characterization of a new helical smectic liquid crystal", Nature (London), **337**, 449-452 (1989).
[5] N. D. Mermin, D. S. Rokhsar and D. C. Wright, "Beware of 46-fold symmetry: The classification of two-dimensional quasicrystallographic lattices", Phys. Rev. Lett. **58**, pp.2099-2102 (1987).
[6] T. C. Lubensky, T. Tokihiro and S. Renn, "Quasicristallinity in a model of stacked polymers", Phys. Rev. Lett., **67**, pp.89-92 (1991).
[7] T. Tokihiro, "Liquid crystals and topological defects", Forma, **8**, pp. 83-97 (1993).

液晶における転位と準周期性

時弘哲治(東京大学・数理科学)

お話したいこと

- 液晶におけるトポロジカル欠陥
  - ✓欠陥は秩序変数の空間のホモトピー群によって表現できる.
- TGB相(smectic-A*相)
  - ✓第2種超伝導体との類似から, Smectic-Cholesteric 転移点近傍で screw dislocation が規則的にならぶ液晶の相が存在する.
- 準結晶-quasicristallography-
  - ✓2次元準結晶は円分体のイデアル類群で分類できる
- TGB相における準結晶的構造
  - ✓TGB相では, screw dislocation 間の相互作用によって, 高い回転対称性をもつ準結晶的パターンが生じる.

参考文献

- N. D. Mermin, “The topological theory of defects in ordered media”, Rev. Mod. Phys., **51**, pp. 591-648 (1979).
- P. M. Chaikin and T. C. Lubensky, *Principles of condensed matter physics*, Cambridge University Press, (1995).
- S. R. Renn and T. C. Lubensky, “Abrikosov dislocation lattice in a model of the cholesteric-to-smectic-A transition”, Phys. Rev. A, **38**, pp.2132-2147 (1988).
- J. Goodby et al., “Characterization of a new helical smectic liquid crystal”, Nature (London), **337**, 449-452 (1989).
- N. D. Mermin, D. S. Rokhsar and D. C. Wright, “Beware of 46-fold symmetry: The classification of two-dimensional quasicrystallographic lattices”, Phys. Rev. Lett. **58**, pp.2099-2102 (1987).
- T.C.Lubensky, TT and S.Renn, “Quasicristallinity in a model of stacked polymers”, Phys. Rev. Lett., **67**, pp.89-92 (1991).
- TT, “Liquid crystals and topological defects”, Forma, **8**, pp. 83-97 (1993).

液晶(Liquid Crystal)

- 力学特性や対称性が液体と固体の中間的な物質(相)
- 例)コレステロールエステル酸

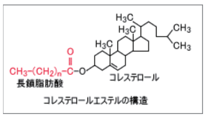

- 対称性)
  - 結晶: positional order, long-range orientational order
  - 液体: disorder

液晶の相

(1)Nematic 相
- Orientational order のみ

(2)Choresteric 相
- 2次元面内の orientational order が存在し，回転している．Chiral nematic ともいう．

(3)Smectic 相
- Orientational order と一方向の positional order
- Smectic A,C,A*,C*など様々に分類されている．

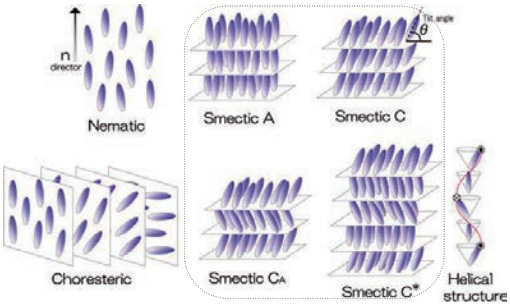

http://www.rs.noda.tus.ac.jp/~furuelab/introduction/phase2.html より

液晶における秩序変数 (order parameter)

- $\vec{n}(\vec{r})$: Frank director（unit vector parallel to local preferred axis at $\vec{r}$ ）
- $\Psi(\vec{r})$: density fluctuation
- Nemactic 相 : $\vec{n}(\vec{r})$ のみ
- Smectic 相 : $\vec{n}(\vec{r})$ と $\Psi(\vec{r})$
  - $\rho(\vec{r}) - \rho_0 = \Psi(\vec{r})$+c.c.
    ($\rho(\vec{r})$: density, $\rho_0 = \langle\rho(\vec{r})\rangle$)
  - Perfect smectic → $\Psi(\vec{r}) \propto e^{iq_0 z}$ $\left(q_0 = \frac{2\pi}{d}\right)$

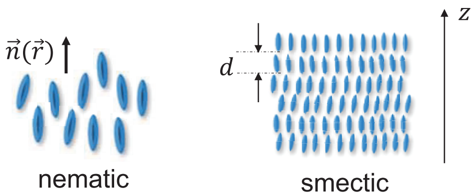

トポロジカル欠陥 (topological defect)

--- (古典)2次元XYスピン模型を例に ---

- 2次元格子上に，大きさ S の古典的なスピンが並ぶ系を考える.
- 秩序変数 $\theta(\vec{x})$:

  $\vec{s}(\vec{x}) = S(\cos\theta(\vec{x}), \sin\theta(\vec{x}))$ ⋯ spin at $\vec{x} = (x, y)$

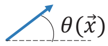

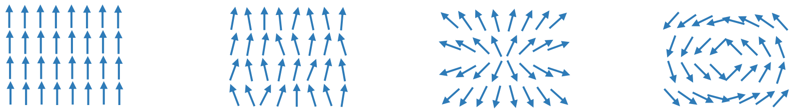

(a) homogeneous （基底状態）　(b) distorted　(c) topological defects

✓(b) は連続的に (a) に変形できるが，(c) はできない.

Winding number

- 経路 Γ に沿うspinの変化
  - (a) : ↑ → ↑ → ↑ → ⋯ → ↑
  - (b) : ↖ → ↖ → ↗ → ↗ → ↖ → ↖
  - (c) : ↘ → → → ↗ → ↖ → ↙ → ↘
  - (c’) : ↗ → ↑ → ↖ → ↙ → ↘ → ↗

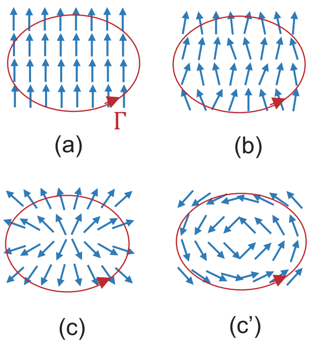

- (a),(b) は回転しない ⋯ winding number $n = 0$
- (c), (c’) は正の方向に1回転 ⋯ $n = 1$

ホモトピー群の要素としてのwinding number

- Winding number のとりうる値？

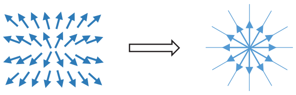

1. 格子系を粗視化→Spin系は連続的なベクトル場
2. 秩序変数: $\theta(\vec{x}) \equiv \theta(\vec{x})+2\pi$
   ∴ θ は実空間 $D \subseteq \mathbb{R}^2$から秩序変数の空間 $X = \mathbb{R}/2\pi\mathbb{Z} \cong S^1$ への連続写像.
   ∴ Γ は閉曲線→基点を定めれば $[\theta(\Gamma)] \in \pi_1(X)$.　($\pi_1(X)$: Xの基本群)
3. $\pi_1(X) \cong \pi_1(S^1) \cong \mathbb{Z}$　である.
4. Winding number は 連続変形で不変.
   ∴ winding number を $\pi_1(X)$ の要素と同一視
5. 3. の同値関係から winding number は任意の整数値を取りうる.

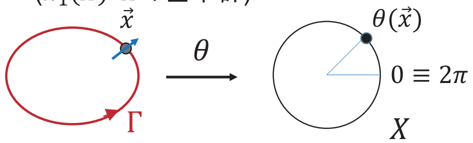

$\pi_1(S^1) \cong \mathbb{Z}$ による2次元XY-spin系の点欠陥の分類例

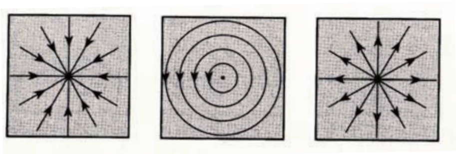

(a)　$n = 1$

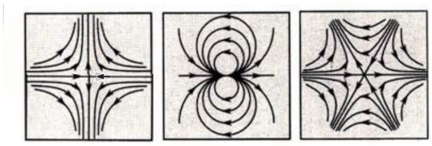

(b) 左から $n = -1, +2, -2$

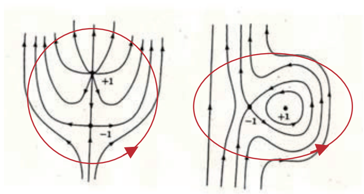

(c) 点欠陥のペア

局所的には点欠陥が存在しているが，図に示した経路に沿っては winding number は 0 になる.

液晶におけるトポロジカル欠陥 1 (nematic相)

- 秩序変数$(\vec{n}(\vec{r}))$： $\|\vec{n}(\vec{r})\| = 1, \quad \vec{n}(\vec{r}) \equiv -\vec{n}(\vec{r})$
  $\therefore \vec{n}(\vec{r}) \in \mathbb{P}^2(\mathbb{R}) = S^2/\mathbb{Z}_2$

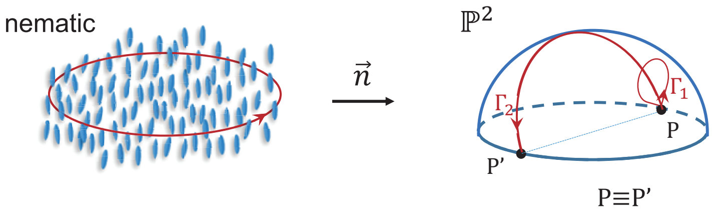

Nematic相の回位（線欠陥，disclination）1

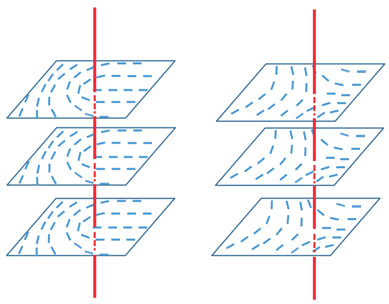

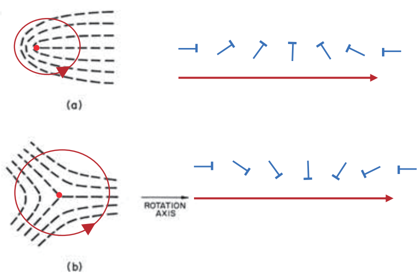

✓ $\pi_1(\mathbb{P}^2) \cong \mathbb{Z}_2$ なので基本群の要素としては，disclination は1種類

◆ 図に鉛直な方向への3次元的な連続変形を考えると，(a) から (b) へ連続的に移りうる．

Nematic相の回位 2

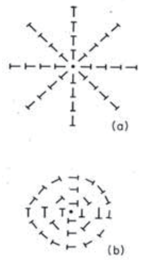

$n = 1$
disclination ?

画面鉛直方向
に連続的に起
こしてゆく

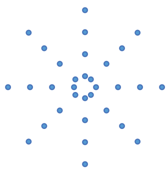

disclination
は解消する

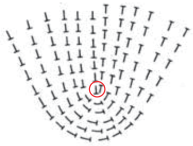

$n = +\frac{1}{2}$ では3次元方向への変形でも連続的にdislocationは解消しない.

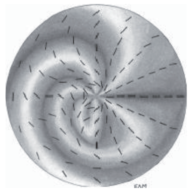

少し複雑な$+\frac{1}{2}$
disclination

Nematic相の点欠陥(hedgehog)

- 実空間の閉曲面($\cong S^2$)上の Frank director $\vec{n}(\vec{r})$の変化を見る.
- $\pi_2(\mathbb{P}^2) \cong \mathbb{Z}$ なので $n \in \mathbb{Z}$ で記述される欠陥がある.

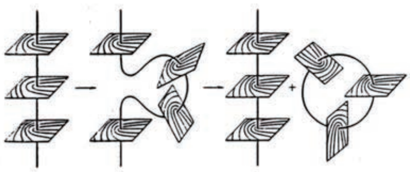

Line disclination からの
ring disclination の生成

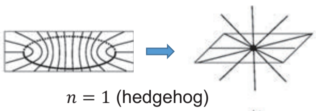

$n = 1$ (hedgehog)

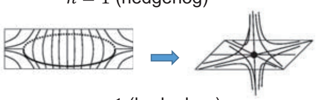

$n = -1$ (hedgehog)

Photo:
Lindsay Bosslett

液晶におけるトポロジカル欠陥 2 （smectic A 相）

- 秩序変数：$(\vec{n}(\vec{r}), \Psi(\vec{r}))$
  - $\vec{n}(\vec{r})$ は nematic と同様.
  - $\rho(\vec{r}) - \rho_0 = \Psi(\vec{r})$+c.c., $\Psi(\vec{r}) \sim |\Psi| e^{iq_0(z-u(\vec{r}))}$
    $q_0 = \frac{2\pi}{d}$,　$u(\vec{r})$: 平衡位置からのずれ

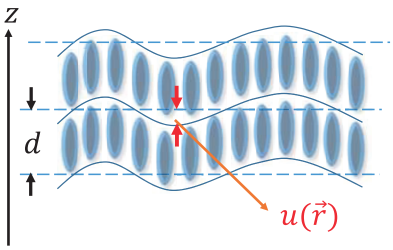

- $u(\vec{r})$ を $\Psi(\vec{r})$ の代わりに秩序変数とみる.
  - $u(\vec{r}) \to u(\vec{r}) + md$,　$\Psi(\vec{r}) \to \Psi(\vec{r})$,　　$\therefore u(\vec{r}) \equiv u(\vec{r}) + md$
  - したがって，秩序変数$u(\vec{r})$の空間はS^1と同相.
  - $\pi_1(S^1) \equiv \mathbb{Z}$ なので，トポロジカル欠陥は整数値によって分類される.

Smectic A　のトポロジカル欠陥

- $u(\vec{r})$に伴う欠陥 (dislocation)
  a. edge dislocation（刃状転位）
  b. screw dislocation（らせん転位）

- $\vec{n}\,(\vec{r})$ に伴う欠陥 (disclination)
  - 2次元的であるので，$\pi_1(\mathbb{P}^1) \cong \frac{1}{2}\mathbb{Z}$
  - c:$+\frac{1}{2}$，d: $-\frac{1}{2}$，e: -1，f: $+1$

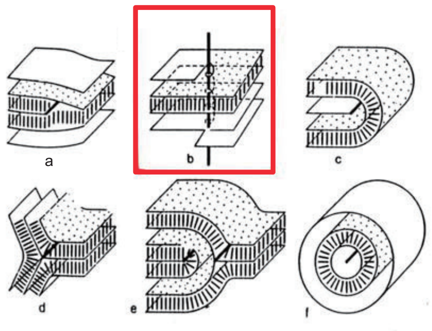

✓smectic相のトポロジカル欠陥は非常に複雑であり，knot理論などに基づく分類など現在でも研究が盛んなようである.

cf. H. Aharoni, T. Machon, and R. D. Kamien, “Composite Dislocations in Smectic Liquid Crystals”, Phys. Rev. Lett. **118**, 257801 (2017)

Twisted Grain Boundary 相 (TGB相)

- TGB相（smectic A*相）

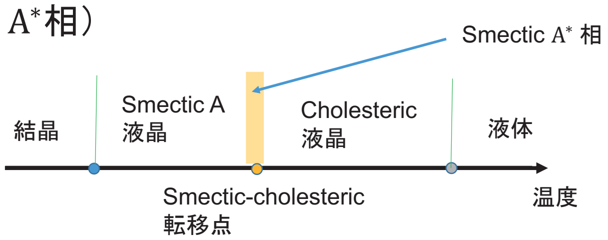

- de Gennes (1972) : Smectic-cholesteric 転移点近傍で，第2種超伝導体の Abrikosov 相に対応する新しい相（後のTGB相）の存在を予言．（1991年，液晶理論等の功績でノーベル物理学賞受賞）
- S.Renn-T.C.Lubensky (1988): 理論的にTGB相の構造，性質を提案
- Goodby et al. (1989): Smectic A^* 相を報告．（後にTGB相とわかる）

秩序変数による自由エネルギーの表現

- nematic(cholesteric)-smectic 転移近傍の自由エネルギー（de Gennes (1972)）

- $F_{dG} = F_L + G_F$
- $F_L := \int d^3r \left\{ a|\Psi(\vec{r})|^2 + c\left|\left(\vec{\nabla} - iq_0\,\vec{n}(\vec{r})\right)\Psi(\vec{r})\right|^2 + \frac{g}{2}|\Psi(\vec{r})|^4 \right\}$
- $G_F := \int d^3r \left\{ K_1\left(\vec{\nabla}\cdot\vec{n}(\vec{r})\right)^2 + K_2\left(\vec{n}(\vec{r})\cdot\vec{\nabla}\times\vec{n}(\vec{r})\right)^2 + K_3\left|\vec{n}(\vec{r})\times\left(\vec{\nabla}\times\vec{n}(\vec{r})\right)\right|^2 \right\}$
  $- \int d^3r\, K_2 q_0 \left(\vec{n}(\vec{r})\cdot\vec{\nabla}\times\vec{n}(\vec{r})\right)$

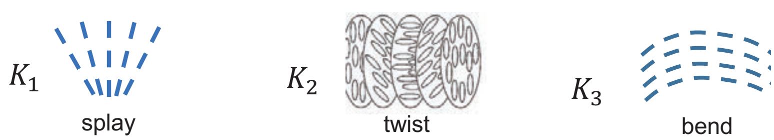

超伝導体の Landau-Ginzburg 自由エネルギー

- 超伝導相の秩序変数:
  （$\vec{A}(\vec{r})$: vector potential, $\Phi(\vec{r})$: cooper 対の波動関数）
  - $F_{LG} = F_c + G_v$
  - $F_c := \int d^3r \left\{ a|\Phi(\vec{r})|^2 + \frac{\hbar^2}{2m}\left|\left(\vec{\nabla} - \frac{2ie}{\hbar c}\vec{A}(\vec{r})\right)\Phi(\vec{r})\right|^2 + \frac{g}{2}|\Phi(\vec{r})|^4 \right\}$
  - $G_v := \int d^3r\, \frac{1}{8\pi\mu_0}\left|\vec{\nabla}\times\vec{A}(\vec{r})\right|^2 - \int d^3r\, \frac{H_0}{4\pi}\left|\vec{\nabla}\times\vec{A}(\vec{r})\right|$

✓F_{LG} は F_{dG} に“とてもよく似ている”.（de Gennes 1972）

F_{dG} と F_{LG} との比較

- $F_{dG} = F_L + G_F$
- $F_L := \int d^3r \left\{ a|\Psi(\vec{r})|^2 + c\left|\left(\vec{\nabla} - iq_0\,\vec{n}(\vec{r})\right)\Psi(\vec{r})\right|^2 + \frac{g}{2}|\Psi(\vec{r})|^4 \right\}$
- $G_F := \int d^3r \left\{ K_1\left(\vec{\nabla}\cdot\vec{n}(\vec{r})\right)^2 + K_2\left(\vec{n}(\vec{r})\cdot\vec{\nabla}\times\vec{n}(\vec{r})\right)^2 + K_3\left|\vec{n}(\vec{r})\times\left(\vec{\nabla}\times\vec{n}(\vec{r})\right)\right|^2 \right\}$
  $- \int d^3r\, K_2 q_0 \left(\vec{n}(\vec{r})\cdot\vec{\nabla}\times\vec{n}(\vec{r})\right)$

- $F_{LG} = F_c + G_v$
- $F_c := \int d^3r \left\{ a|\Phi(\vec{r})|^2 + \frac{\hbar^2}{2m}\left|\left(\vec{\nabla} - \frac{2ie}{\hbar c}\vec{A}(\vec{r})\right)\Phi(\vec{r})\right|^2 + \frac{g}{2}|\Phi(\vec{r})|^4 \right\}$
- $G_v := \int d^3r\, \frac{1}{8\pi\mu_0}\left|\vec{\nabla}\times\vec{A}(\vec{r})\right|^2 - \int d^3r\, \frac{H_0}{4\pi}\left|\vec{\nabla}\times\vec{A}(\vec{r})\right|$

超伝導体と液晶との対応関係

超伝導体	液晶
常伝導相	nematic (cholesteric) 相
超伝導相	smectic 相
$\vec{A}(\vec{r})$: vector potential	$\vec{n}(\vec{r})$: Frank derector
$\Phi(\vec{r})$: wave function of Cooper pairs	$\Psi(\vec{r})$: density fluctuation
$\frac{1}{8\pi\mu_0}$ (μ_0 : 透磁率)	K_2, K_3 (elastic constants)
$H = \lvert\vec{\nabla}\times\vec{A}\rvert$: magnetic field strength	$H = K_2 q_0$: chirality
$\vec{\nabla}\times\vec{A} = \vec{0}$: Meissner effect	$\vec{\nabla}\times\vec{n} = \vec{0}$: no twist, no bend
flux quantization ($\Phi(\vec{r}) = \lvert\Phi(\vec{r})\rvert e^{i\theta(\vec{r})}$) $\oint d\vec{l}\cdot\vec{\nabla}\,\theta(\vec{r}) = 2m\pi$	topological index ($\Psi(\vec{r}) = \lvert\Psi(\vec{r})\rvert e^{iq_0 u(\vec{r})}$) $q_0\oint d\vec{l}\cdot\vec{\nabla}\,u(\vec{r}) = 2m\pi$

超伝導体と液晶との対応関係（続き）

超伝導体	液晶
magnetic vortex (磁束)	screw dislocation
λ_L: London penetration depth	λ_t: twist penetration depth
ξ_c : coherence length	ξ_s : radius of screw dislocation
$\kappa := \lambda_L/\xi_c$: Ginzburg parameter	$\kappa := \lambda_t/\xi_s$: Ginzburg parameter
Abrikosov 相	TGB 相

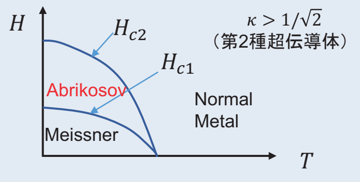

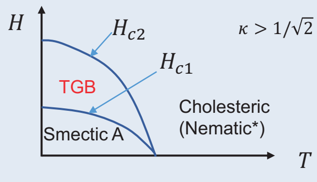

第2種超伝導体のAbricosov 相

- Abrikosov 相（vortex lattice phase）:
  量子化された磁束が浸入し，磁束の渦糸が3角格子を形成する.

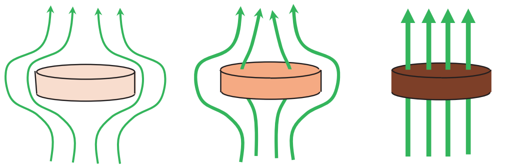

(a) $H < H_{c1}$
Meisner 状態
磁場は侵入できない

(b) $H_{c1} < H < H_{c2}$
Abrikosov 相
磁場は渦糸（量子化された磁束）として部分的に浸入する.

(c) $H_{c2} < H$
Normal metal
磁場は完全に浸入する

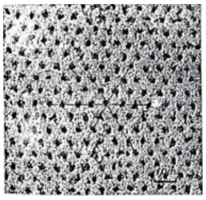

アブリコソフ相にある金属の電子顕微鏡写真.
黒く見える場所が渦糸

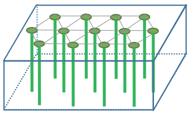

磁束（渦糸）は3角格子を構成している

Screw dislocation の3角格子？

- Screw dislocation が平行に3角格子を組むことはできない.

∵ screw dislocation の回りを1周すると，内部にある screw dislocation の数に比例して（図のz方向に）分子の位置がずれる.（smectic A の層がその数だけずれる.）
半径Rの円を1周すると，内部にある screw dislocation　の数は R^2 に比例する.
従って，分子位置はR^2のオーダーで移動するので，図で各層の傾き $\tan\gamma$ は $\tan\gamma\ \to +\infty\ (R\ \to\ +\infty)$.
従って，screw dislocation と層が平行になるが，このようなことは起きえない.

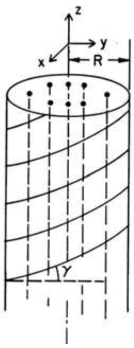

TGB相 (Renn-Lubensky, Phys. Rev. A **38**, 2132 (1988))

等間隔に並んだ
screw dislocation
のシート

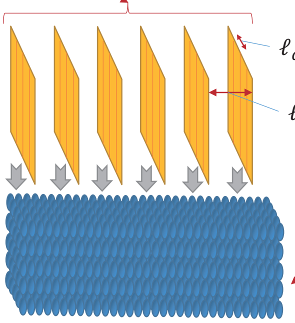

SmA

Smectic A に2次元平面上に等間隔に並んだ screw dislocation のシートを差し込む.

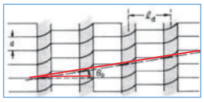

screw dislocation によって同位相の層が傾く

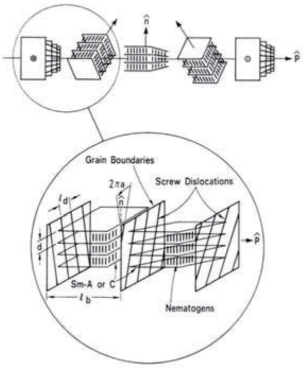

Fig. 4. The twist-grain-boundary phase (TGB phase). In the inset, we see that, between pair of slabs, there exists a grid of parallel equispaced screw dislocations. These grids are known as grain boundaries and, like the smectic slabs, also form a twisted stack.

TT, Forma **8**, 83 (1993)

TGB相の発見を伝えるNature誌の論文

Characterization of a new helical smectic liquid crystal

J. W. Goodby, M. A. Waugh, S. M. Stein, E. Chin, R. Pindak & J. S. Patel*

AT&T Bell Laboratories, Murray Hill, New Jersey 07974, USA
* Bell Communications Research, Redbank, New Jersey 07001, USA

The discovery of the first liquid-crystalline material in 1888[1,2] also heralded an age of fascination with chirality and optical activity in ordered fluids. The cholesteric mesophase, which was the first liquid crystal to be found, exhibits form optical activity by virtue of a helical arrangement of its constituent molecules. One hundred years after the discovery of this first liquid crystal, we report the discovery of a new helical smectic liquid crystal, the smectic-A* phase. In this phase the lath-like molecules are arranged in layers with their long axes on average normal to the layer planes. Parallel to the layers there is a helical ordering of the molecules (Fig. 1). We suggest that this phase may be described by a model in which grain boundaries of screw dislocations rotate blocks of layers with respect to each other.

This novel phenomenon was found to occur in an homologous series of ferroelectric liquid crystals, the *R*- and *S*-1-methylheptyl 4'-[(4"-*n*-alkoxyphenyl)propionoyloxy]-biphenyl-4-carboxylates (*n*P1M7). These materials were prepared by the esterification of a variety of 4-*n*-alkoxyphenylpropiolic acids with *R*- or *S*-1-methylheptyl 4'-hydroxybiphenyl-4-carboxylate (ref. 3, and M.A.W. and S.M.S., to be published). The helical A* phase was found in the *n*-tridecyloxy, *n*-tetradecyloxy and *n*-pentadecyloxy homologues, which have the general chemical formula:

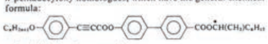

and exhibit the phase transitions:

Isotropic liquid ↔ A* ↔ C* ↔ S3 ↔ S4

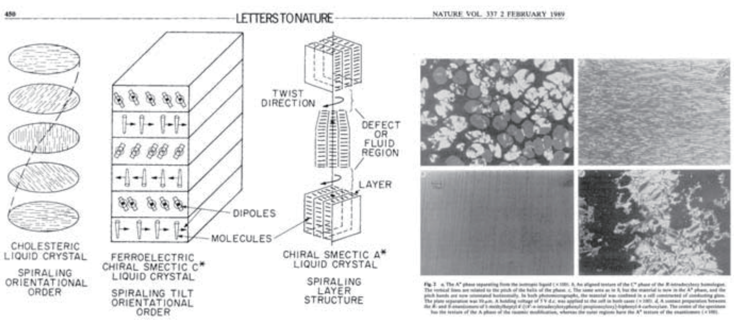

J.R.Goodby et al.
"Characterization of a new helical smectic liquid crystal",
Nature 337, 449 (1989)

準結晶(quasicrystal)

Dan Schechtman

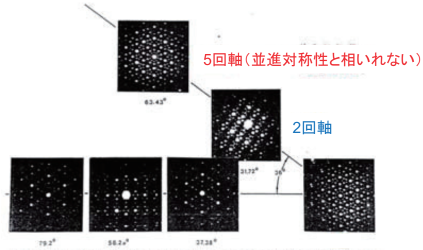

FIG. 2. Selected-area electron diffraction patterns taken from a single grain of the icosahedral phase. Rotations match those in Fig. 1.

D.Schechtman et al. Phys. Rev. Lett. **53**, 1951 (1984)

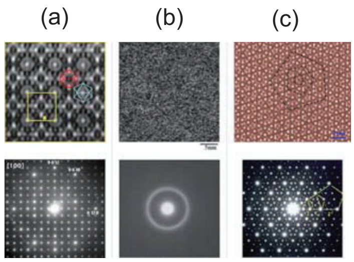

(a) 結晶，(b) アモルファス，© 準結晶の電子顕微鏡パターンとX線回折パターン (東北大　蔡安邦 研究室）

1984年，Schechtmanらによって AlMn合金系で，結晶ともアモルファスとも異なる対称性（正20面体の対称性）を持つ固体が発見され，Steinhardtによって準結晶(quasicrystal)と名付けられた.
Schechtman はその功績によって2011年にノーベル化学賞を受賞.

準結晶の色々

Cr-Ni-Si 合金のX線回折パターン：
8回対称軸を持つ

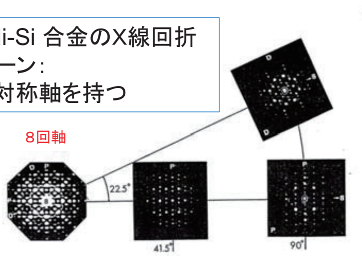

Zhang et al. (1986)

AL-Cu-Fe 合金の準結晶相の顕微鏡写真：正12面体構造が見られる.

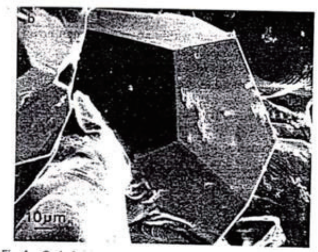

金材研　井上 et al.(1990?)

現在では非常に多くの，また，安定な準結晶が発見されている.
本質的に2次元（鉛直方向には周期的）の準結晶も多数存在する.
今年初めに名大のチームが超伝導を示す準結晶を発見している.

2次元準結晶のモデル（Penrose tiling）

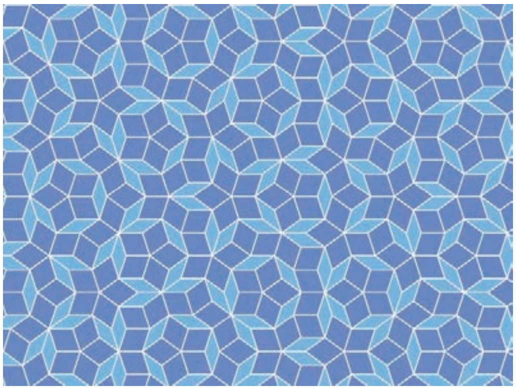

2種類のひし形の組み合わせで平面を埋めることが可能.
5回の回転対称性を持たせることができる.

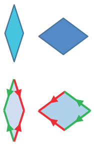

同じ色の矢印が，方向も含めて重なるように組み合わせてゆけば自然に構成できる.

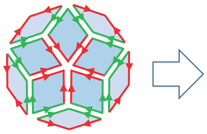

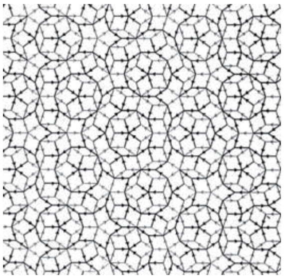

余談1）周期的Penrose格子

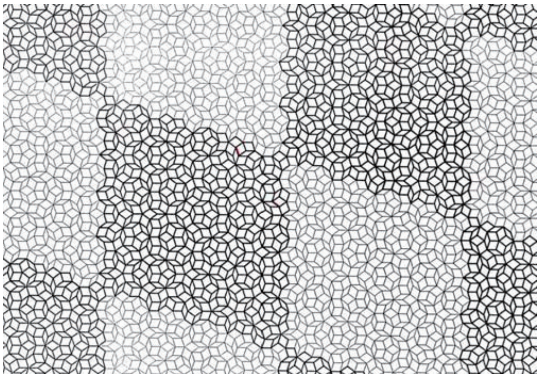

周期的Penrose格子

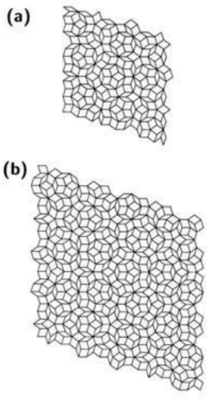

2つのフィボナッチ数のペアで指定できる周期的Penrose格子の単位胞.
(a) (3,5) (b) (5,8)

Tsunetsugu-Fujiwara-Ueda-T (1986)

余談2)Penrose格子上の tight-binding model の厳密解

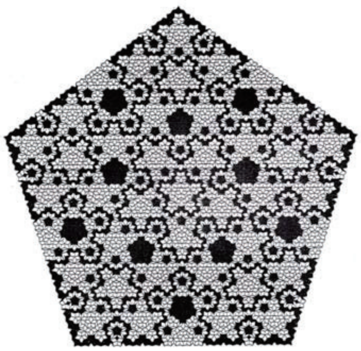

Confined state:
黒い菱形では波動関数の値は0になる.
Fujiwara-Arai-T-Kohmoto (1988)

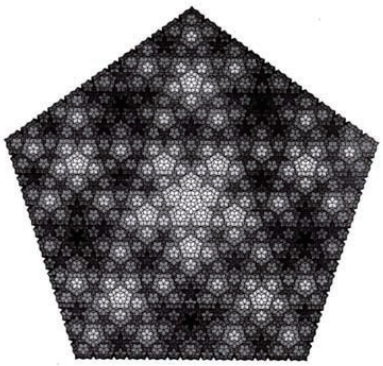

Self-similar state:
自己相似性があり(multi-)fractal次元が定まる.
T-Fujiwara-Arai (1988)

2次元準結晶の分類理論(逆格子空間による分類)

(N. D. Mermin et al., Phys. Rev. Lett. 58, 2099 (1987))

Penrose 格子の逆格子ベクトル空間 (V_{10}):
(実空間の物質分布のFourier 変換, X線回折パターン, を表現する空間)

$$V_{10} := \left\{\vec{v}\,\middle|\,\vec{v} = \sum_{k=0}^{4} n_k \overrightarrow{e_k}\,,\ (n_k \in \mathbb{Z})\right\}, \text{ ただし } \overrightarrow{e_k} = {}^{t}\left(\cos\frac{k\pi}{5}, \sin\frac{k\pi}{5}\right)$$

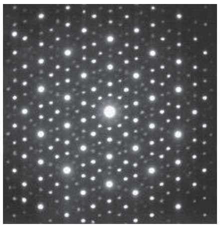

問:10回回転対称性を持つ逆格子ベクトル空間はすべてV_{10}と同型か?
答え: Yes

問:一般に$2n$回回転対称性を持つ逆格子ベクトル空間はただひとつのベクトル空間に同型となるか?
答え: No
$n = 2,3,4, \dots, 21,22,24,25,27,30,33,35,42,45$ の29個だけunique.

2次元準結晶の逆格子ベクトル空間

- 定義：　n を正整数とする．2次元の実ベクトルの集合 U_{2n} が $2n$回回転対称性を持つ逆格子ベクトル空間であるとは，以下の 1~3 が成り立つことである．
  1. $\vec{v}_1, \vec{v}_2 \in U_{2n}$ ならば $\vec{v}_1 \pm \vec{v}_2 \in U_{2n}$.
  2. $\vec{v} \in U_{2n}$ ならば $\hat{R}_n \vec{v} \in U_{2n}$. ただし，$\hat{R}_n$ は $\frac{\pi}{n}$ の回転を表す．
  3. あるベクトル $\vec{w}$ が存在して，任意の $\vec{v} \in U_{2n}$ は $\vec{v} = \sum_{k=0}^{n-1} m_k \vec{w}_k$ $(m_k \in \mathbb{Z})$ と表せる．ただし，$\vec{w}_k \coloneqq \left(\hat{R}_n\right)^k \vec{w}$.

✓ $\hat{T}$ を $\hat{R}_n$ と可換な任意の正則変換とする．$U'_{2n} = \hat{T}(U_{2n})$ が成り立つとき，U'_{2n}と U_{2n} は逆格子ベクトル空間として同型である．同型か否かを議論するときは，$\vec{w}$ は固定して考えて良い．

✓ $V_{2n} \coloneqq \left\{\vec{v} \,\middle|\, \vec{v} = \sum_{k=0}^{n-1} m_k \vec{w}_k, m_k \in \mathbb{Z}\right\}$ は1~3を満たす．V_{2n} と同型でないU_{2n}が存在するかどうかが問題．

円分体との関係

- ∘ $\vec{v} \in \mathbb{R}^2 \leftrightarrow z \in \mathbb{C}$,　∘ $\vec{w} \in \mathbb{R}^2 \leftrightarrow 1 \in \mathbb{C}$,　∘ $\hat{R}_n \vec{v} \leftrightarrow \zeta_n z$ $(\zeta_n \coloneqq e^{\frac{i\pi}{n}})$ と対応させる．
- $V_{2n} \to Z_{2n} \coloneqq \left\{z \,\middle|\, z = \sum_{k=0}^{n-1} m_k \zeta_n^k,\ m_k \in \mathbb{Z}\right\}$ であり，$U_{2n} \to Y_{2n}$として，1~3は次と等価．
  ① $z_1, z_2 \in Y_{2n} \to z_1 \pm z_2 \in Y_{2n}$
  ② $z \in Y_{2n} \to \zeta_n z \in Y_{2n}$
  ③ $z \in Y_{2n} \to {}^\exists m_k \in \mathbb{Z},\ z = \sum_{k=0}^{n-1} m_k \zeta_n^k$

④ 同型（同値）であること：$Y_{2n} \sim Y'_{2n} \leftrightarrow {}^\exists \xi \in \mathbb{C}^\times, Y_{2n} = \xi Y'_{2n} \to {}^\exists \alpha,\ \beta \in Z_{2n}\ \alpha Y_{2n} = \beta Y'_{2n}$

- 命題：円分体 $\mathbb{Q}(\zeta_n)\left(= \left\{z \in \mathbb{C} \,\middle|\, z = \sum_{k=0}^{n-1} a_k \zeta_n^k,\ a_k \in \mathbb{Q}\right\}\right)$ において，Z_{2n}はその整数環である．
- ①~③は Y_{2n} が Z_{2n} のイデアルであることを意味する．
- ④は ～ によって（mod 単項イデアルの）同値類（イデアル類）が定義されることを意味する．
- よって，逆格子ベクトル空間の分類は，Z_{2n}のイデアル類を決定することに帰着する．

2次元準結晶と円分体の類数

- 定義：上述のイデアル類（群をなす）の位数を $\mathbb{Q}(\zeta_n)$ の類数と呼び，h_{2n}と書く.
  ✓ $h_{2n}=1$ ならば，準結晶は1種類，$h_{2n}>1$ なら2種類以上存在する.

- 定理 (Masley-Montgomery 1976)：$h_{2n}=1$ となるのは，$n=2,3,4,\ldots,21,22,24,25,27,30,33,35,42,45$ の29個のみである.

- Cf.) $h_{46}=h_{52}=3, h_{56}=2, h_{58}=h_{62}=9, h_{64}=17, h_{68}=32, \ldots$
  $h_{94}=695, \ldots, h_{128}=359057, \ldots$

  ✓現実の準結晶が23回以上の回転対称性を持つことは考えにくく，実際上，逆格子空間での分類では2次元準結晶は1種類と考えてよい.

TGB相における準結晶的構造

✓23回以上の回転対称性の逆格子ベクトル空間を持つ系は存在しないか？
- TGB相における screw dislocation 間の相互作用：

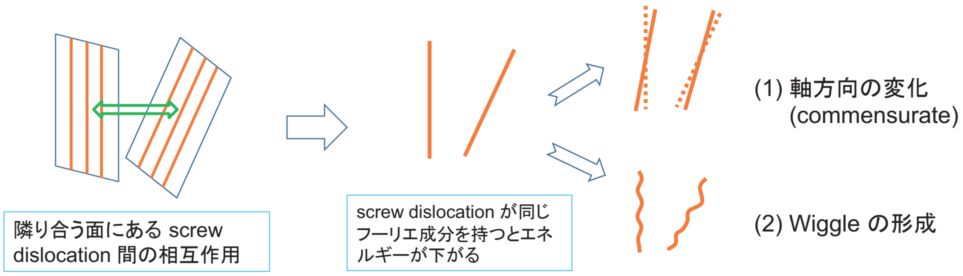

悪魔の階段構造

- $\alpha_0 \coloneqq \tan\theta_0$, θ_0: dislocation 間に相互作用のない場合の傾きの角度
- $\alpha \coloneqq \tan\theta$, θ: 相互作用がある場合の傾きの角度

- α は α_0 の関数になる → $\theta_0 = q\pi$ ($q \in \mathbb{Q}$) で必ず平坦な部分が生じる. (悪魔の階段)

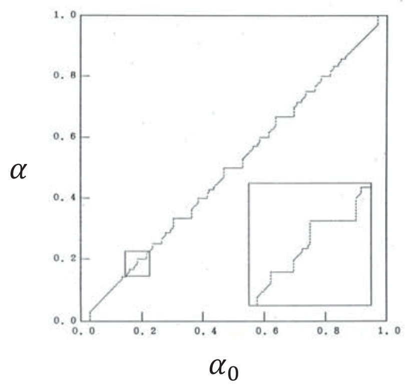

Screw dislocation の変形


(a)


(b)


(c)


(d)

7回回転対称性の逆格子空間をもつTGB相の screw dislocation.
(a)1シートと (b)7つのシートを重ねたもの

9回回転対称性の逆格子空間をもつTGB相の screw dislocation.
(c) 1シートと (d) 9つのシートを重ねたもの

Screw dislocation の形とそのX線回折パターン

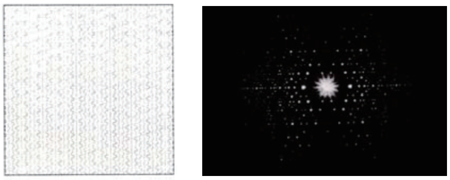

（a）

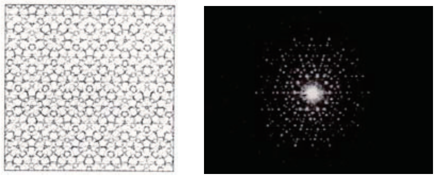

（b）

5回の回転対称性をもつ screw dislocation の X線回折パターン
(a) 1シートの回折像, (b) 全体の回折像

こうした構造を理論的に予言したが，残念ながら，30年たった今でも観測されたとは聞いていない…(´･ω･`)

ご清聴ありがとうございました

先進数理解析と結晶の転位問題
(Advanced mathematical investigation and dislocations in crystal lattice)

松谷茂樹, Shigeki Matsutani

佐世保工業高等専門学校
National Institute of Technology, Sasebo College

Crucial problems in industry, basically, cannot be solved in the framework of a single mathematical field or a single field in science. They are related to a variety of mathematical fields and wider scientific knowledge [1]. The study of Bernoulli-Euler's elastic curve (elastica) is a nice prototype [2,3]. I call such a study *advanced mathematical investigation* [1]. In this talk, after I give a short review of their study of elastica, I explain what is the advanced mathematical investigation. As examples of the investigation, I report the discrete geometry of screw dislocation [4] and recent study of kink phenomenon using the elastica [5].

REFERENCES

[1] 松谷茂樹 数学 Libre：先進数理解析とは，現代数学 2018 2 月号 86-87.
[2] 松谷茂樹エラスティカを巡る数理〜ベルヌイ、オイラーから現代まで〜, 応用数理 **13** (2003) 48-60.
[3] S. Matsutani, *Euler's Elastica and Beyond*, J. Geom. Symm. Phys **17** (2010) 45-86.
[4] H. Hamada, S. Matsutani, J. Nakagawa, O. Saeki, and M. Uesaka, *An algebraic description of screw dislocations in SC and BCC crystal lattices*, Pasific J. Math. for Industry, (2018) **10**:3.
[5] H. Hamada, K. Higashida, S. Matsutani, H. Nishiguchi, *in preparation.*

先進数理解析
と
結晶の転位問題

2018年9月10日

IMI Workshop II: 結晶転位の先進数理解析

九州大学マス・フォア・インダストリ研究所

松谷茂樹
佐世保工業高等専門学校

21世紀に入って，科学技術が大きく進歩し、従来の工業数学や物理数学では表現できない現象が増えてきている

純粋数学も含めた様々な数学を利用して、現象を表現する事が求められている
→　先進数理解析とよびたい

先進数理解析：
・先進数理解析の雛形は、ベルヌーイ・オイラーの弾性曲線の研究にある
・先進数理解析の事例は増えている

先進数理解析：
1. 先進数理解析の雛形である
ベルヌーイ・オイラーの弾性曲線研究

2. 先進数理解析の事例として
2. 1. らせん転位の代数的表現
2. 2. キンク現象の弾性曲線論の応用

フッサール（ワィエルシュトラスの弟子）
「幾何学は測量技術者の言葉を極限操作したもの」

弾性曲線(Elastica)問題

Elastica問題

Leonardo da Vinci (1452-1519)がスケッチを残し、Galileo Galilei (1564-1654)も研究をした梁のたわみの形状の決定問題が、この問題の起源である.

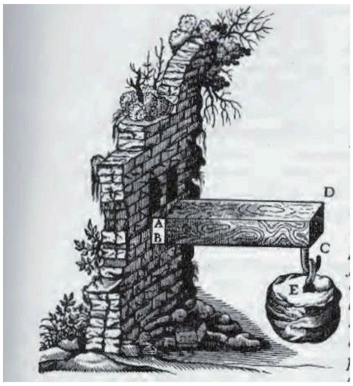

弾性曲線(Elastica)問題

Jacob Bernoulli はElastica問題を1691年に提示した：

「平面上の elastica（弾性曲線：太さゼロの極限の細い弾性棒）の形状を決定せよ！」

Jacob Bernoulli (1654-1705)

弾性曲線（Elastica）とは

$Z : N \to C$:解析的等長はめ込み

$(|\partial_s Z| = 1)$.

$N = S^1$ または $N = (0, 1)$

s : 弧長

$Z(s) = X(s) + iY(s)$,

$t = \partial_s Z = e^{i\phi}$,

$(\phi \in C^{\omega}(N, R))$

$= \cos\phi + i\sin\phi$

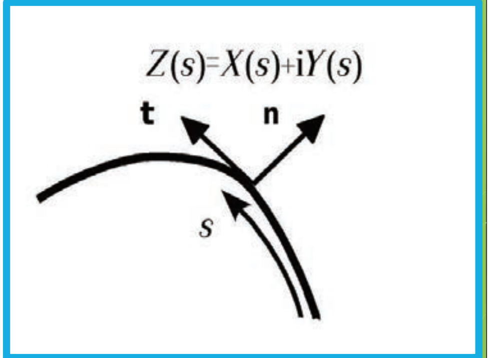

$k := \partial_s \phi$: 曲率; $k = 1/$[曲率半径].

Elastica問題

曲率 & Frenet-Serret 関係式

$t := \partial_s Z$, $\partial_s t = kn$, $\partial_s n = -kt$, $(\partial_s^2 Z = ik\partial_s Z)$

$k := \partial_s \phi$: 曲率; $k = 1/$[曲率半径].

Elastica 問題（Jacob Bernoulli（1691））

平面上に存在する弾性曲線（細い弾性棒）の形状を決定せよ

命題:(Jacob Bernoulli（1694)）
1. elastica に働く力は曲率に比例する.
2 1を実現する形状 $Z_R = X_R + iY_R$ は以下を満たす：

弧長：$s = \int_0^{X_R} \frac{dX_R}{\sqrt{1 - X_R^4}}$.　　Y軸：$Y_R = \int_0^{X_R} \frac{X_R^2 dX_R}{\sqrt{1 - X_R^4}}$

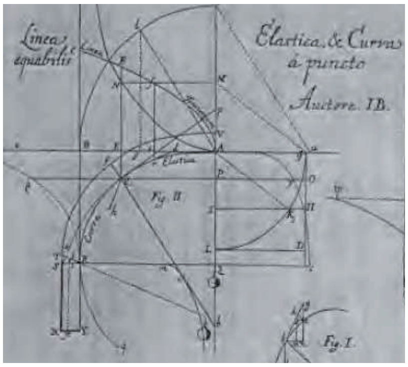

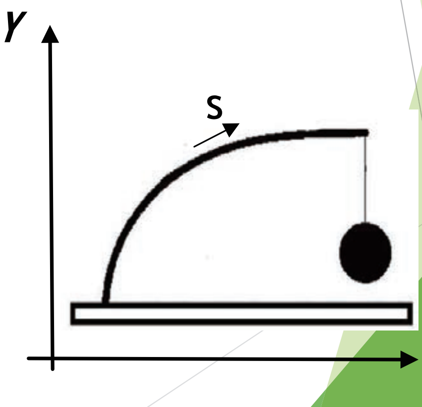

Lemniscate と Elastica

8の字のelastica形状を研究しながら、Jacobは8の字のLemniscate曲線を定義した

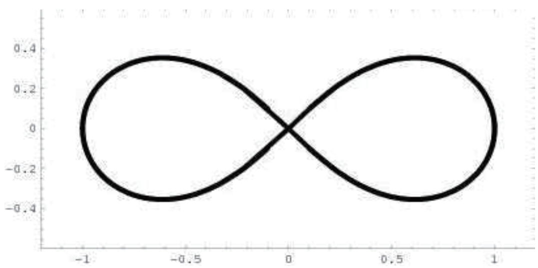

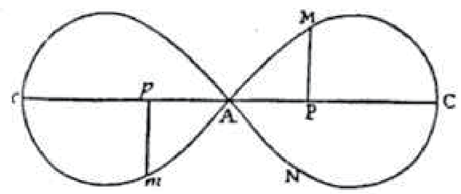

3c. Class 5

Lemniscate
$(x^2 + y^2)^2 = 2a^2(x^2 - y^2)$
φ_{lemni}**:tangential angle**

Elastica の8の字形状
φ_{elas}**:tangential angle**

Lemniscate と Elastica

8 の字の elastica 形状を研究しながら、Jacob は 8 の字の Lemniscate曲線を定義した

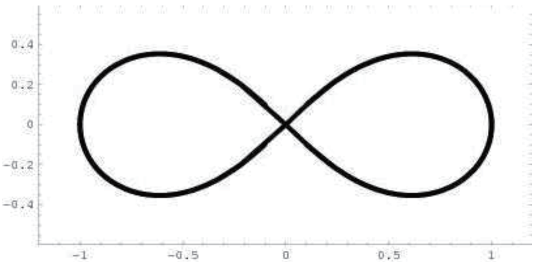

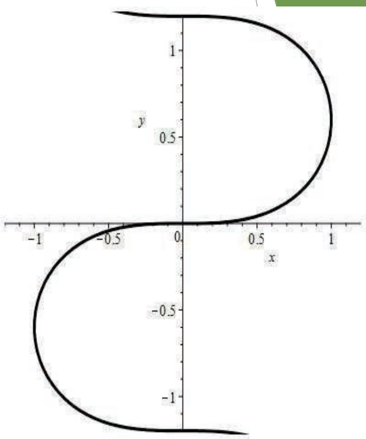

Lemniscate

$$(x^2 + y^2)^2 = 2a^2(x^2 - y^2)$$

φ_{lemni}**:tangential angle**

Jacobのelastica

Lemniscate と Elastica形状

elastica の形状 $Z_R = X_R + \mathrm{i}\, Y_R$ を固定：

次の写像で、新たなはめ込み $Z_\ell \in M_{(0,1)}$ を考える：

$$\partial_s Z_R = e^{\mathrm{i}\phi_R} \to \partial_s Z_\ell = e^{\mathrm{i}3\phi_\ell/2}$$

命題：（M,1995）Z_ℓ は *Lemniscate* 曲線となる。
弧長は *Lemniscate* 積分である

Lemniscate と Elastica形状

Lemniscate と Elastica：命題の証明

$Z_\ell(t) := \int_0^t \partial_s Z_\ell ds(X_R)$ は

$$\sqrt{-1}Z_\ell(t) = -\frac{t\sqrt{1+t^2}}{\sqrt{2}} + \sqrt{-1}\frac{t\sqrt{1-t^2}}{\sqrt{2}}$$

となる．$\sqrt{-1}Z_\ell(t) =: X_\ell(t) + \sqrt{-1}Y_\ell(t)$ とすると，X_ℓ, Y_ℓ は Lemniscate 曲線の方程式：

$$(X_\ell^2 - Y_\ell^2) = (X_\ell^2 + Y_\ell^2)^2 \qquad \text{符号は適当に定めることで}$$

を満たすことは簡単に判る．

楕円関数の故郷としてLemniscateが挙がるが、その背景にElasticaが存在する。

$$\sqrt{-1}\partial_s Z_R = e^{\sqrt{-1}\phi_R} \mapsto \sqrt{-1}\partial_s Z_\ell = e^{\sqrt{-1}3\phi_R/2}$$

Elastica → Lemniscate への変換

$$\sqrt{-1}\partial_s Z_R = e^{\sqrt{-1}\phi_R} \mapsto e^{\sqrt{-1}\phi_R/2}$$

Elastica → Dirac作用素に関連
（一般化W.R.のひな型）
Poincareの保型関数論の類似

Elastica問題は非常に深い

命題：Daniel Bernoulli(1738)
Elasticaの形状は以下のエネルギー汎関数を最小化するように定まる

$$
\begin{aligned}
\mathcal{E}[Z] &:= \int_{S^1} k^2(s)ds = \int_{S^1} (\partial_s \phi(s))^2\, ds \\
&= \int \{Z, s\}_{\mathrm{SD}} ds \\
&= \int_{S^1} g^{-1}dg * g^{-1}dg, \quad g \in \mathrm{U}(1)
\end{aligned}
$$

$\{Z, s\}_{\mathrm{SD}}$:Schwarz derivative

Euler(1744)
変分法を開発し、Danielの発見に従い、Elasticaの形状を完全に分類した

- 変分法
- 曲線論
- 楕円積分
- 楕円曲線のモデュライ
- 数値積分

$$\frac{\delta E}{\delta X} = 0$$

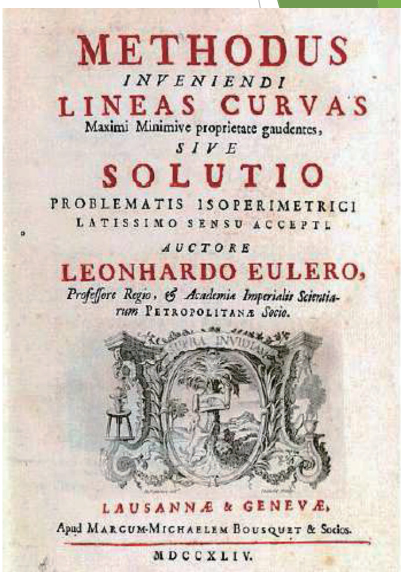
METHODUS
INVENIENDI
LINEAS CURVAS
Maximi Minimive proprietate gaudentes,
SIVE
SOLUTIO
PROBLEMATIS ISOPERIMETRICI
LATISSIMO SENSU ACCEPTI.
AUCTORE
LEONHARDO EULERO,
Professore Regio, & Academiae Imperialis Scientiarum PETROPOLITANAE Socio.
LAUSANNÆ & GENEVÆ,
Apud MARCUM-MICHAELEM BOUSQUET & Socios.
MDCCXLIV.

弾性曲線(Elastica)とは

Eulerの解

$$s = \int^X \frac{\lambda^2 dX}{\sqrt{\lambda^4 - (\alpha + \beta X + \gamma X^2)^2}},$$

$$Y = \int^X \frac{(\alpha + \beta X + \gamma X^2) dX}{\sqrt{\lambda^4 - (\alpha + \beta X + \gamma X^2)^2}}.$$

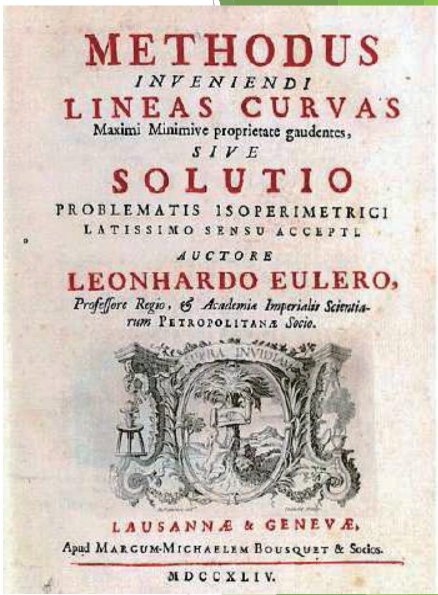

現代的には
静MKdV方程式の解

$$ak + \frac{1}{2}k^3 + \partial_s^2 k = 0.$$

非線形可積分方程式の原型でもある

弾性曲線(Elastica)とは

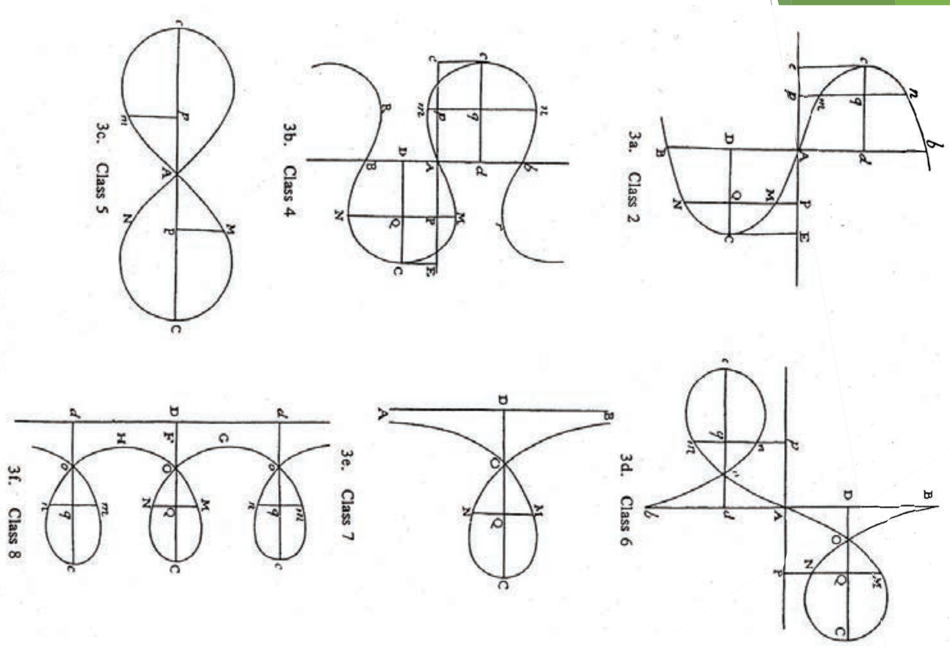

Eulerの数値解析(1744)

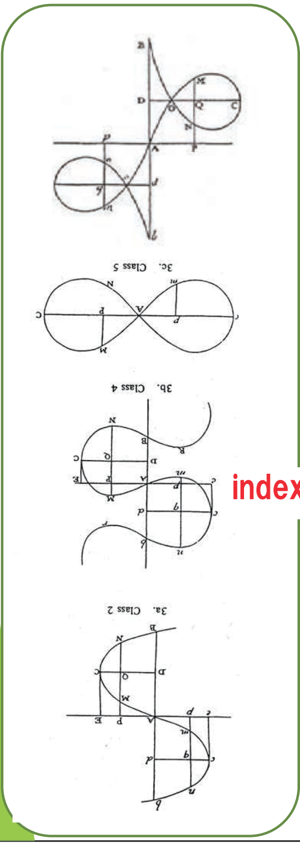

弾性曲線(Elastica)のモデュライ

index (Z)
$=(\Phi(L)-\Phi(0))/2\pi$

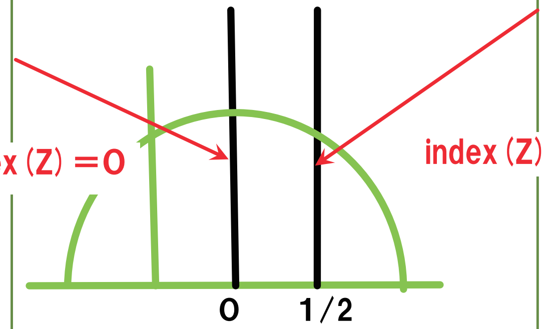

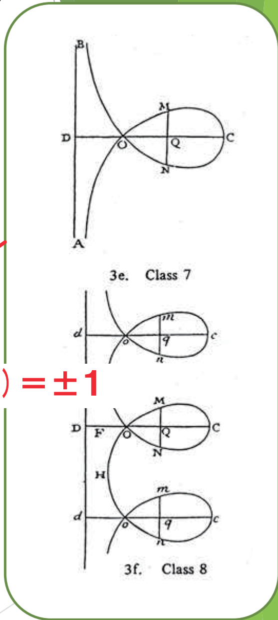

Eulerの数値解析(1744)

弾性曲線(Elastica)とは

弾性曲線（Elastica）問題は
- 変分法
- 楕円積分
- 楕円曲線のモデュライの幾何
- 数値計算

により分類・表示することで弾性曲線問題を**完全に解決**した。

微分幾何・代数幾何・解析の萌芽を開発・酷使し問題を解決

Elastica問題

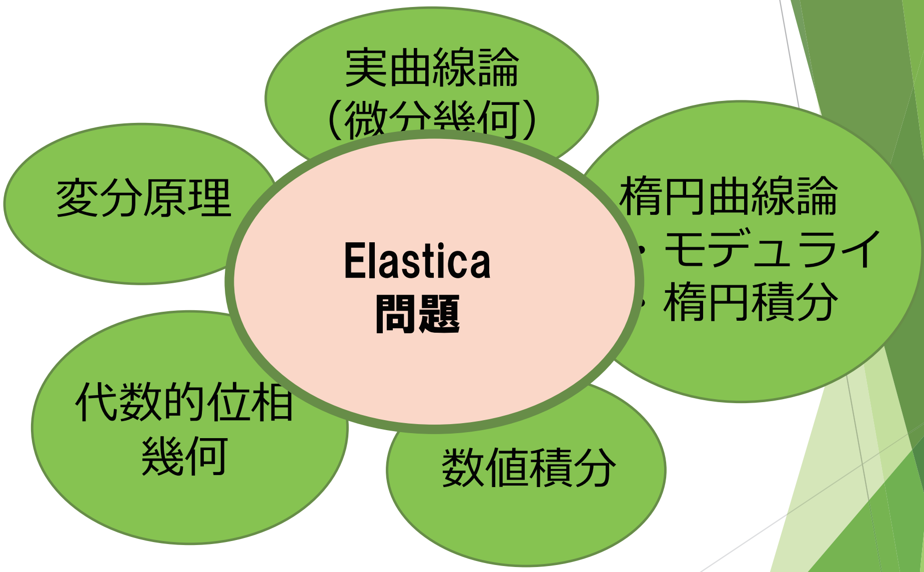

一つの数学分野の収まらない

オイラー・ベルヌーイの弾性曲線の研究からは

0. 対象の(物理的)本質を理解する.
1. 問題を解く際に手段を選んではならない,
言葉がなければ、作ってでも表現する
2. 繊細な数学的事実を決して蔑ろにしない

という精神が読み取れる

⇒ これが先進数理解析の方針である

弾性曲線(Elastica)問題の一般化

弾性曲線の統計力学

弾性曲線の統計力学とは

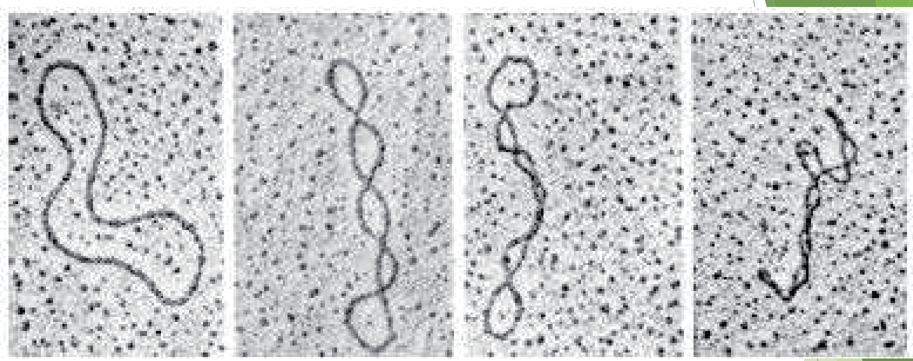

DNAの原子間力顕微鏡像：

http://www.udel.edu/chem/bahnson/chem645/websites/Sapra/Supercoiling.html

弾性曲線の統計力学とは

$$\mathcal{Z}[\beta] = \int_{\mathbb{M}} DZ \exp(-\beta \mathcal{E}[Z])$$

**形状のパラメータ空間(モデュライ)に適当な位相を入れ、
オイラー・ベルヌーイ エネルギー汎関数のボルツマン重みから定まる測度により、
上記積分を定式化し、積分を実行せよ**

弾性曲線の統計力学とは

形状のモデュライに適当な位相を入れ、オイラー・ベルヌーイ エネルギー汎関数のボルツマン重みから定まる測度により、上記積分を定式化し、積分を実行せよ

・MKdV階層
・超楕円ヤコビ多様体の「実部」
・「実」超楕円曲線のモデュライ
により幾何構造が定まる

M 1997, M-Onishi 2001, M-Previato 2015

弾性曲線の統計力学とは

形状のモデュライに適当な位相を入れ、オイラー・ベルヌーイ エネルギー汎関数のボルツマン重みから定まる測度により、上記積分を定式化し、積分を実行せよ

アーベル関数論が楕円関数論と同レベルの精緻性と具体性があれば、この問題は解決する！が、そのレベルにない

アーベル関数論を、楕円関数論と同レベルの精緻性と具体性を持つよう再構築する。

主たる研究は、アーベル関数論の再構築

オイラー・ベルヌーイの方針：

0. 対象の(物理的)本質を理解する.
1. 問題を解く際に手段を選んではならない, 言葉がなければ、作ってでも表現する
2. 繊細な数学的事実を決して蔑ろにしない

オイラー・ベルヌーイの方針に従った研究：

- インクジェットプリンターにおける計算流体力学の三相界面の取り扱い： 特異点論の階層性を利用
- 電子放出素子のメカニズム解明
- 計算流体力学での層理論の援用
- 確率論の点過程を利用した画像処理
- ロボットのCaging問題への合同変換群の枠内でのホモトピー論の適用
- グラフのζ関数とランダム行列理論による乱れたグラファイト系での電気伝導度予測
- 量子ウォーク理論による拡散色と構造色の数学モデルの構築
- パーコレーション理論とΓ収束による、ナノ微粒子系の物性予測
- らせん転位のメゾ領域での振る舞いの表現

先進数理解析：
1. 先進数理解析の雛形である
ベルヌーイ・オイラーの弾性曲線研究

2. 先進数理解析の事例として
2. 1. らせん転位の代数的表現
2. 2. キンク現象の弾性曲線論の応用

2. 1. らせん転位の代数的表現

中川・佐伯・上坂・濱田・松谷
2015-2018

Hamada-Matsutani-Nakagawa-Saeki-Uesaka
Pasfic J. Math. Industry 2018

Hamada *et al. Pacific Journal of Mathematics for Industry* (2018) 10:3
https://doi.org/10.1186/s40736-018-0037-8

Pacific Journal of
Mathematics for Industry

ORIGINAL ARTICLE Open Access

CrossMark

An algebraic description of screw dislocations in SC and BCC crystal lattices

Hiroyasu Hamada[1], Shigeki Matsutani[1*], Junichi Nakagawa[2], Osamu Saeki[3] and Masaaki Uesaka[4,5]

Abstract

We give an algebraic description of screw dislocations in a crystal, especially simple cubic (SC) and body centered cubic (BCC) crystals, using free abelian groups and fibering structures. We also show that the strain energy of a screw dislocation based on the spring model is expressed by the Epstein-Hurwitz zeta function approximately.

Keywords: Crystal lattice, Screw dislocation, Topological defect, Monodromy, Group ring of abelian group, Dislocation energy, Epstein-Hurwitz zeta function

らせん転位

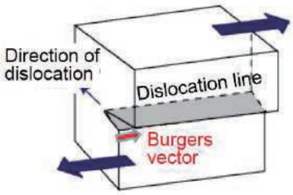

Burgers Vector: (ズレの方向) と転位の
軸の方向が並行となっている.

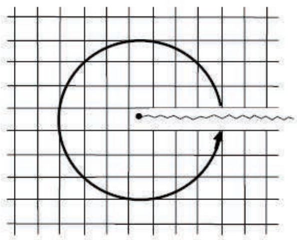

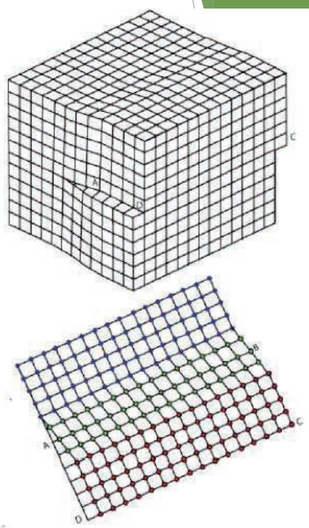

D. Hull and D. J. Bacon, Introduction to Dislocation,
Butterworth-Heinemann (2011)

転位の研究の状況（2015）

1980年代までに
連続に関しては構築可能な理論は
構築できていた

- 位相幾何的な特徴
- 微分幾何的な解析（最小化問題）

Mermin Rev.Mod.Phys 1979
Nabarro 1967 (Amari,Kondo)

2015年のSGW (Study Group Workshop) の課題

BBC格子でのらせん転位を数学的に表現しそれをエネルギー論的に論ぜよ　by　中川氏

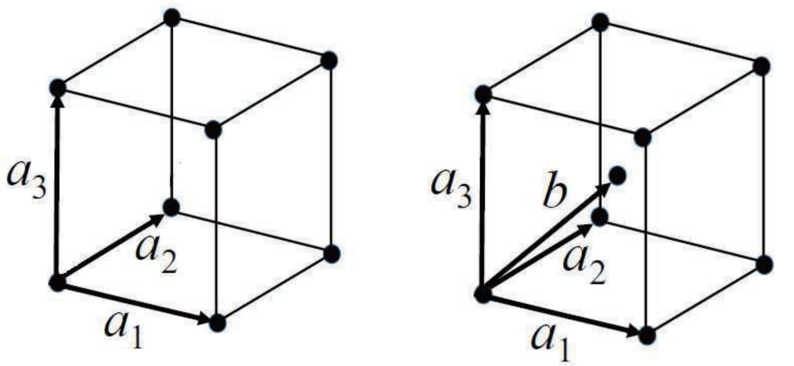

単純格子　　体心立方格子(BCC)

転位の研究の状況

2015年の状況：

離散的な考察（結晶の型）と位相的な考察、エネルギー（不変量）の考察の組み合わせは未検討課題

代数的な考察

数論的な考察

らせん転位の
結晶論的考察

最小化問題
（エネルギー論的）

代数的位相幾何
的な考察

微分幾何的
な考察

オイラー・ベルヌーイの方針：

0. 対象の（物理的）本質を理解する.
1. 問題を解く際に手段を選んではならない,
   言葉がなければ、作ってでも表現する
2. 繊細な数学的事実を決して蔑ろにしない

オイラー・ベルヌーイでないので、チームで対応

現場の課題

インター
プリター

数学専門家

離散の取り扱い

BBC格子でのらせん転位を数学的に表現しそれをエネルギー論的に論ぜよ　by　中川氏

方針：

1. ユークリッド空間の性質で原子配置を定め、空間内で実現

2. 結晶の対称性（並進対称性など）を幾つかは保存するように対称性を破る（群の作用を制限する）

3. トポロジカルな性質は連続空間で定め、離散系を埋め込む

4.　対称性に不変で、格子で定義されるエネルギー関数はζで書き下す（ζの知見を利用して、系を理解する）

5. 結晶系の違いは(初等)代数的に表現すべき

離散の取り扱い

BBC格子でのらせん転位を数学的に表現しそれをエネルギー論的に論ぜよ　by　中川氏

方針：

1. ユー（分子力学）MM計算、第一原理計算や、弾性体の数値計算、固体物理の基礎、対称性の破れなどの知見　実現

2. 結晶　　　　　　　　　　　　　　　　　　　　　　ように対称性を破る（群の作用を制限する）

3. トポロジ　代数的位相幾何の物理への応用の知見　指数定理でのHurwitzζの計算　埋め込む

4.　対称性に不変で、格子で定義されるエネルギー関数はζ

で書き下す　アーベル関数論の知見、ファイバー射の知見

5. 結晶系の違いは(初等)代数的に表現すべき

Deligne列（Brylinski）

完全列

$$\begin{tikzcd}
& & \mathbb{E} \arrow[r, "\psi"] & S^1 & \\
0 \arrow[r] & \mathbb{Z} \arrow[ur, "\varphi_\delta"] \arrow[r, "\iota"] & \mathbb{R} \arrow[u, "\tilde{\iota}_\delta"] \arrow[r, "\exp 2\pi\sqrt{-1}"] & \mathrm{U}(1) \arrow[u, "\iota_\delta"] \arrow[r] & 1,
\end{tikzcd}$$

$$\mathbb{Z} \times \mathbb{E}^2 = \mathbb{Z}_{\mathbb{E}^2} \xrightarrow{\widehat{\varphi}_\delta} \mathbb{E}_{\mathbb{E}^2} \xrightarrow{\widehat{\psi}} S^1_{\mathbb{E}^2} ,$$

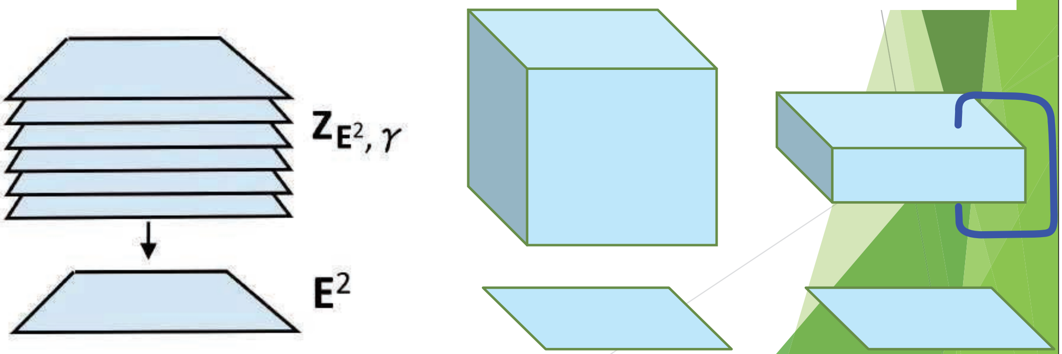

らせん構造をファイバー構造として システマティックに構成する

$$\mathbb{Z}_{\mathbb{E}^2 \setminus \{z_0\}} \xrightarrow{\widehat{\varphi}_\delta} \mathbb{E}_{\mathbb{E}^2 \setminus \{z_0\}} \xrightarrow{\widehat{\psi}} S^1_{\mathbb{E}^2 \setminus \{z_0\}} ,$$

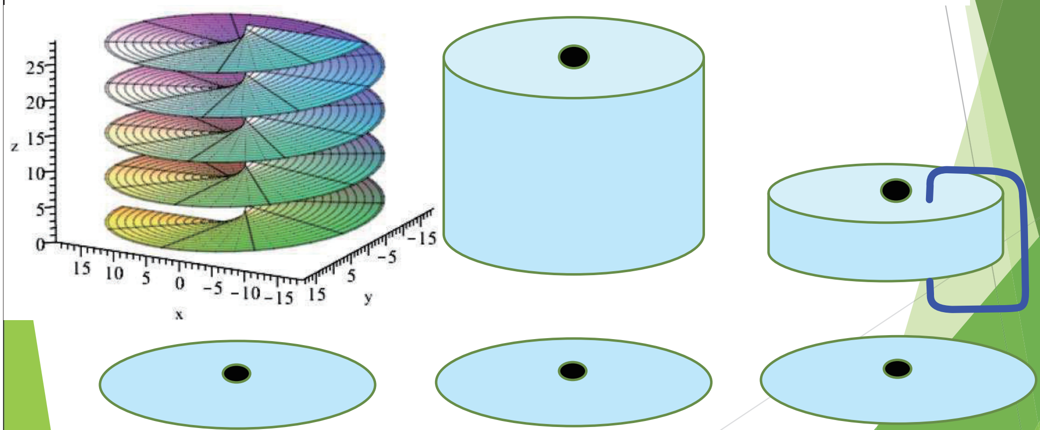

らせん構造に格子を埋め込む

らせん型の立体駐車場に
各階の同じ位置に格子点
のマークをペンキで記す

数学的にはファイバー射を考えること

$$
\begin{tikzcd}
\mathbb{Z}_{\mathbb{E}^2\backslash\mathcal{S}} \arrow[r, "\widehat{\phi}_\delta"] & \mathbb{E}_{\mathbb{E}^2\backslash\mathcal{S}} \arrow[r, "\widehat{\psi}"] & S^1_{\mathbb{E}^2\backslash\mathcal{S}} \\
\mathbb{Z}_{\mathcal{A}_p} \arrow[u, "\widehat{\iota}^{\mathrm{SC}}_{\bar{\delta}}"] \arrow[r, "\widehat{\phi}_\delta"] & \mathbb{E}_{\mathcal{A}_p} \arrow[u, "\widehat{\iota}^{\mathrm{SC}}_{\bar{\delta}}"] \arrow[r, "\widehat{\psi}"] & S^1_{\mathcal{A}_p} \arrow[u, "\widehat{\iota}^{\mathrm{SC}}_{\bar{\delta}}"]
\end{tikzcd}
$$

$$\mathcal{A}_p \approx \mathbb{Z}^2 \subset \mathbb{E}^2$$

らせん構造に格子を埋め込む

ほぼユークリッド空間

数学的にはファイバー射を考えること

$$
\begin{tikzcd}
\mathbb{Z}_{\mathbb{E}^2\backslash\mathcal{S}} \arrow[r, "\widehat{\phi}_\delta"] & \boxed{\mathbb{E}_{\mathbb{E}^2\backslash\mathcal{S}}} \arrow[r, "\widehat{\psi}"] & S^1_{\mathbb{E}^2\backslash\mathcal{S}} \\
\boxed{\mathbb{Z}_{\mathcal{A}_p}} \arrow[u, "\widehat{\iota}^{\mathrm{SC}}_{\bar{\delta}}"] \arrow[r, "\widehat{\phi}_\delta"] & \mathbb{E}_{\mathcal{A}_p} \arrow[u, "\widehat{\iota}^{\mathrm{SC}}_{\bar{\delta}}"] &
\end{tikzcd}
$$

ユークリッド空間内に
らせん格子が

$\mathcal{A}_p \approx$

結晶科学者が発見・伝承して
きたものが明確な言葉（数学）
になった

らせん結晶格子

BCCのらせん転位の構造の表記

$$\mathbb{B}^a := \langle a_1, a_2, a_3, b\rangle_{\mathbb{Z}} / \langle 2b - a_1 - a_2 - a_3\rangle_{\mathbb{Z}},$$

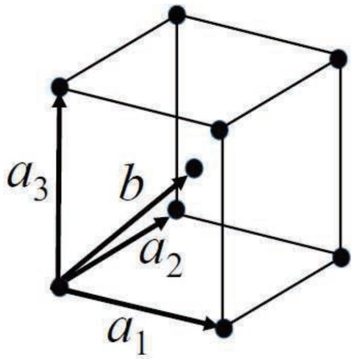

体心立方格子(BCC)を代数的に理解し、構造まではたどり着けた

⇒ BCCのらせん転位の結晶構造をシステマティックに構築できた

単純格子でのらせん転位のエネルギー

単純格子においては、バネモデルに従ってらせん転位によるエネルギーの増加分を評価できる

$$E_\rho(x_0, y_0) = \frac{1}{8\pi^2} k_d a^2 \sum_{(\ell_1,\ell_2)\in D_\rho} \frac{a^2}{(\ell_1 a - x_0)^2 + (\ell_2 a - y_0)^2}$$

$+$ その他の項

Epstein-Hurwitz ζ関数と関連する

BBC格子でのらせん転位を数学的に表現しそれをエネルギー論的に論ぜよ　by　中川氏

達成できた事

- 単純格子・BCC格子でのらせん転位の離散幾何学構造を、代数学的(システマティック)に表現できた
- 単純格子でのメゾスコピックレベルでの転位のエネルギーが計算できるようになった

これからの課題

- FCCなどでのらせん転位の離散幾何構造の表現
- BCC、FCCなどでの転位のエネルギーの表記
- パイエルス障壁の結晶格子依存性

先進数理解析：

1. 先進数理解析の雛形である
　ベルヌーイ・オイラーの弾性曲線研究

2. 先進数理解析の事例として
　2. 1. らせん転位の代数的表現
　2. 2. キンク現象の弾性曲線論の応用

2. 2. キンク現象の弾性曲線論の応用

東田・濱田・西口・松谷
2017-2018

キンク現象

異方性のある圧力によって、金属結晶が転位を生じさせることで格子レベルで不可逆的に形状の変化が起きること

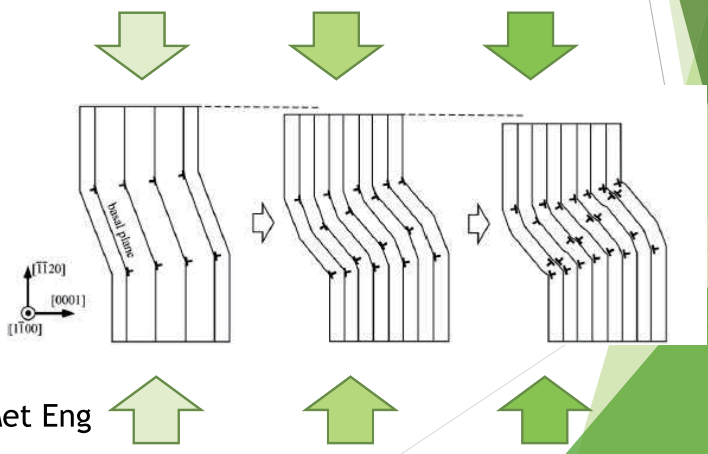

Hess-Barrett,
Trans Am Inst Min Met Eng
1949;185:599-606.

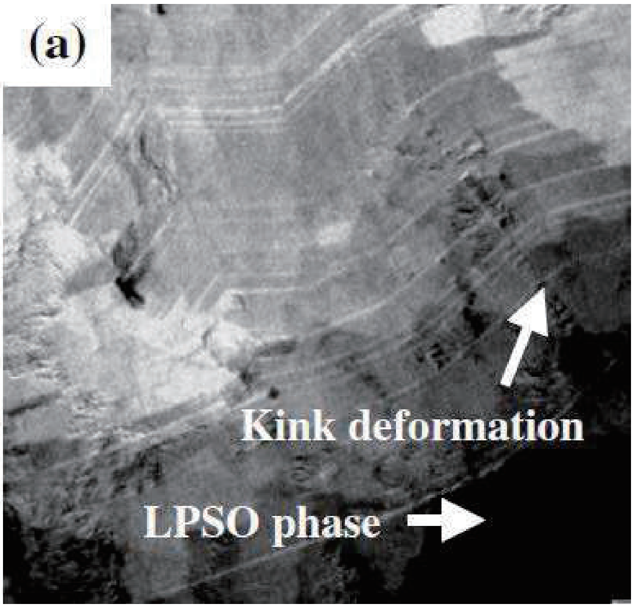

Evolution of Mechanical Properties and Microstructure in Extruded Mg96Zn2Y2 Alloys by Annealing
Masafumi Noda1, Tsuyoshi Mayama2 and Yoshihito Kawamura2
Materials Transactions, Vol. 50, No. 11 (2009) pp. 2526 to 2531

キンク現象に現れる様々形状を数学的に分類しその性質を述べよ
by 中谷彰宏先生（大阪大学）

Analysis of stress field of kink boundary based on lattice defect theory

“Mathematics in Interface, Dislocation and Structure of Crystals” (2017.9)

キンク現象の普遍性

キンク現象は、金属の格子の問題だけではなく、地層の歪み（断層）などとも関わる数理的に普遍性のある現象である

長い歴史と、様々な議論が繰り広げられている. e.g., Phil. Trans. R. Soc. Aで2012年に特集号が組まれた

硬い紙の束（層）の場合

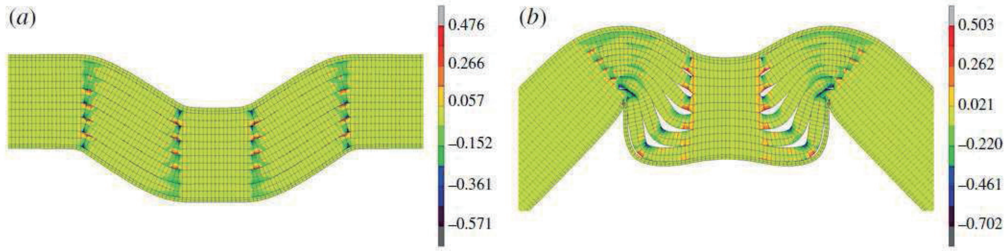

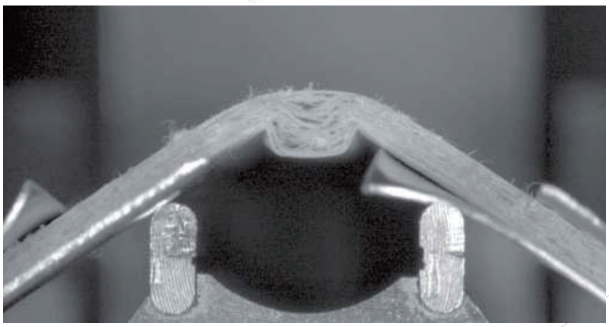

On the influence of delamination on laminated paperboard creasing and folding
BY LARS A. A. BEEX AND RON H. J. PEERLINGS
Phil. Trans. R. Soc. A (2012) **370**, 1912-1924

布の束（層）の場合

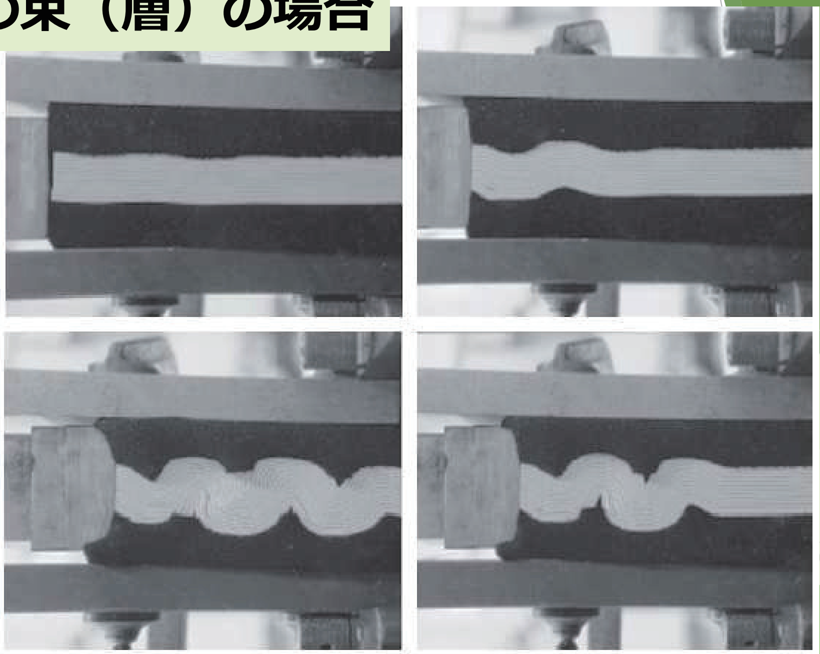

Multi-layered folding with voids
T. J. DODWELL, G. W. HUNT, M. A. PELETIER AND C. J. BUDD
Phil. Trans. R. Soc. A (2012) **370**, 1740–1758

布の束（層）の場合

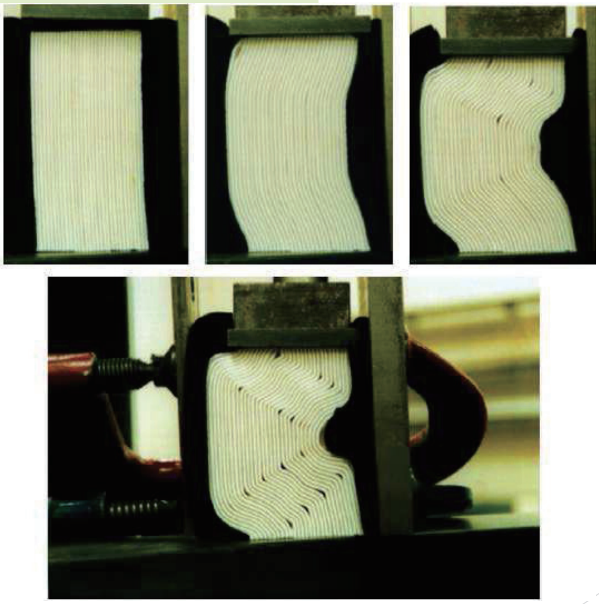

Multi-layered folding with voids
T. J. DODWELL, G. W. HUNT, M. A. PELETIER AND C. J. BUDD
Phil. Trans. R. Soc. A (2012) **370**, 1740–1758

布の束（層）の場合（と同質の形状）

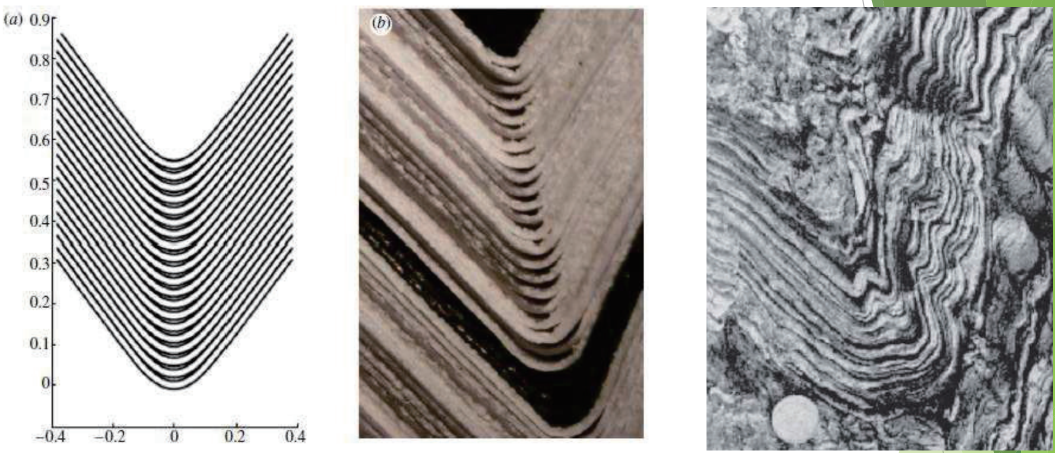

Multi-layered folding with voids
T. J. DODWELL, G. W. HUNT, M. A. PELETIER AND C. J. BUDD
Phil. Trans. R. Soc. A (2012) **370**, 1740–1758

粘性液体の層の場合

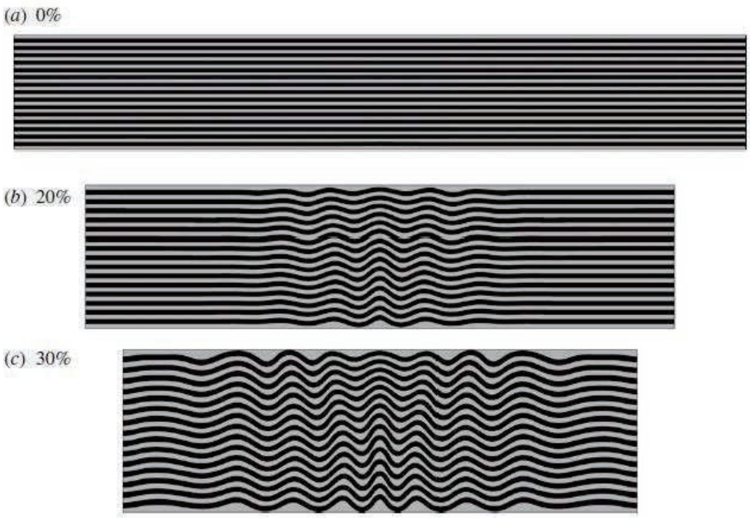

Folding in power-law viscous multi-layers
BY STEFAN M. SCHMALHOLZ, AND DANIEL W. SCHMID
Phil. Trans. R. Soc. A (2012) **370**, 1798–1826

粘性液体の層の場合（と同質の形状）

Folding in power-law viscous multi-layers
BY STEFAN M. SCHMALHOLZ, AND DANIEL W. SCHMID
Phil. Trans. R. Soc. A (2012) **370**, 1798-1826

2017年「結晶の界面、転位、構造の数理」において、見られた形状

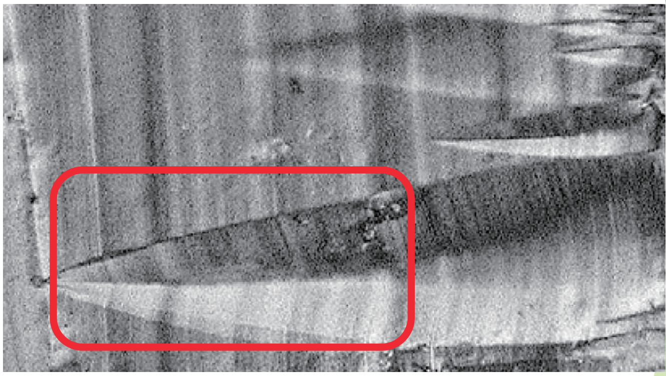

Hagihara-Yokotani-Umakoshi
Intermetallics 18 (2010) 267-276

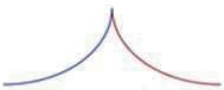

問題：なぜ尖がった形状が現れるのか？

問題：なぜ尖がった形状が現れるのか？

kink現象でも弾性力がドミナントとなる現象が存在するのでは？

弾性変形　vs　塑性変形

塑性変形：元の形状（計量）をどんどん忘れてゆく（変形後のユークリッド空間から誘導された計量に変化する）

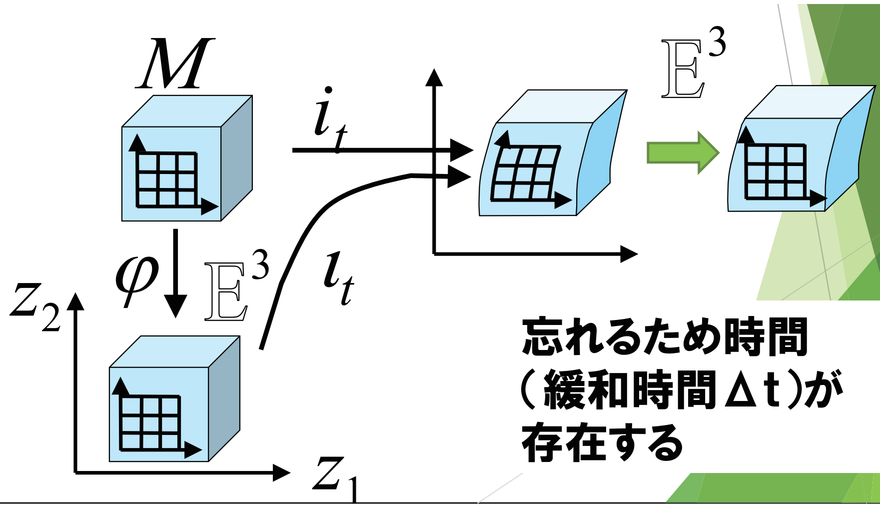

忘れるため時間（緩和時間Δt）が存在する

問題：なぜ尖がった形状が現れるのか？

kink現象でも弾性力がドミナントとなる現象が存在するのでは？

δt:Kinkの形状が作られるに要する時間
Δt:塑性変形となる時間

δt ≪ Δt であればどのようになるか？

Elasticaの屈曲

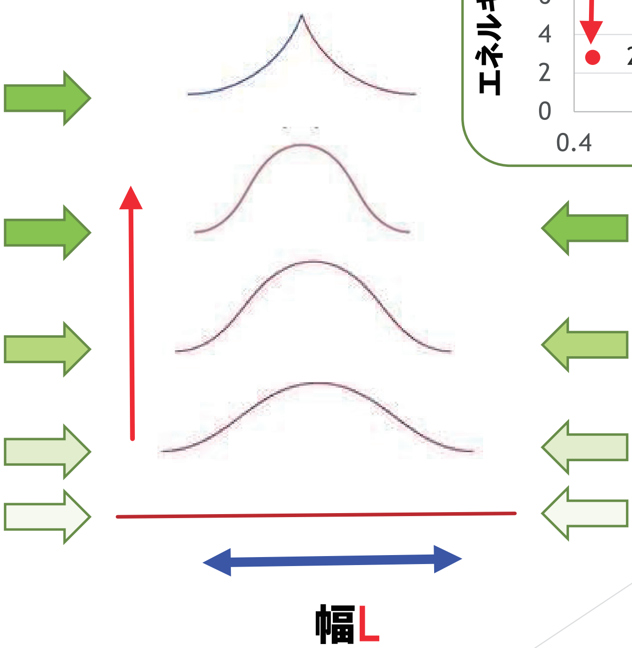

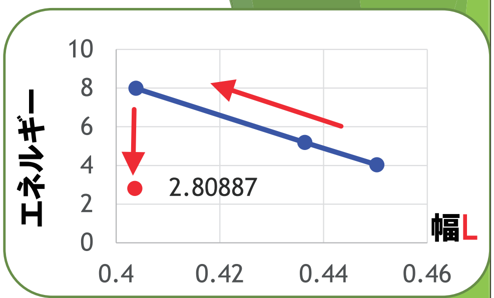

屈曲Elasticaの条件

- 弧長が屈曲前と同じ
- 幅Lが屈曲前と同じ
- 接合角Θがパラメータ

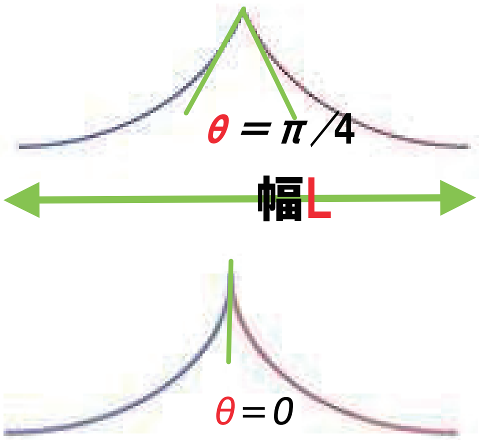

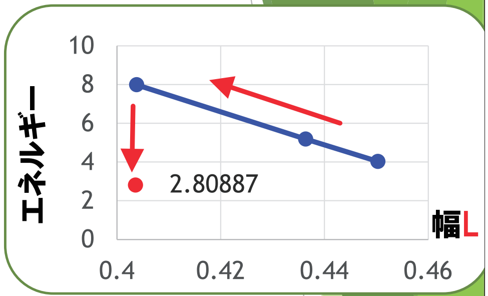

Elasticaの屈曲

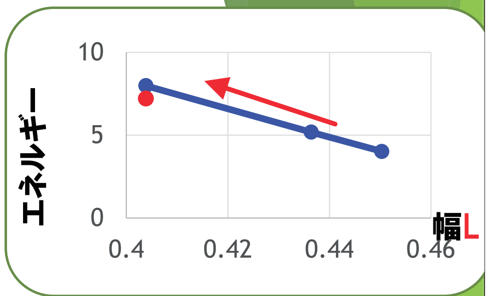

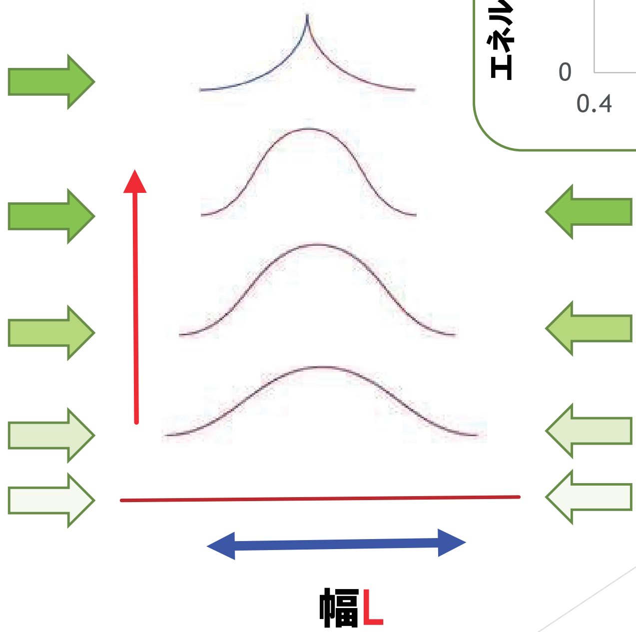

Elasticaの屈曲

数学的には
1. 最小化問題としては、探索する関数空間を連続かつ区分的解析な関数の空間に拡張

2. 楕円曲線のモデュライの視点では、指数の異なる非連結の部分空間をジャンプする現象

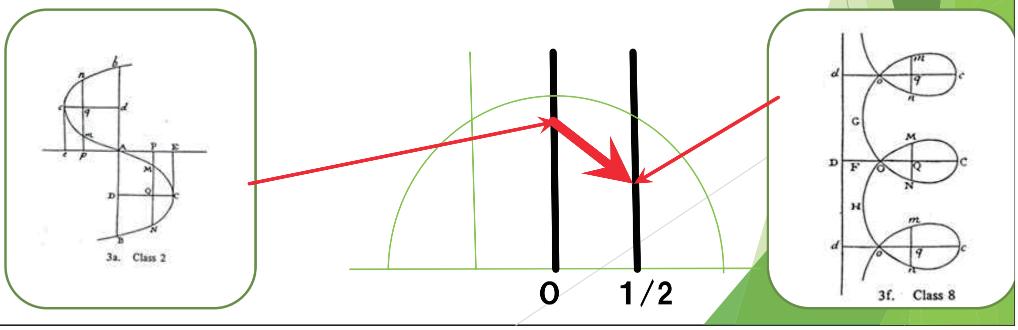

δt:Kinkの形状が作られるに要する時間
Δt:塑性変形となる時間

δt ≪ Δt で、弾性変形によって変形後、塑性変形したとする仮定すると

弾性体としての形状がキンク形状を決める場合がある.

厚さにより弾性エネルギーが比例

q 離れた場所の微小長さ

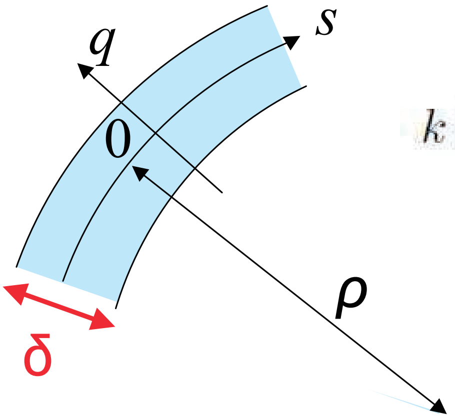

$$ds_q = (1 + k(s)q)ds$$

k は曲率　$k = 1/\rho$

$$\mathcal{F} = \frac{1}{2}\kappa\left(\frac{\partial e_q}{\partial q}\right)^2 (1 + kq)$$

$$e_q = 1 + k(s)q$$

$$\int_{-\delta/2}^{\delta/2} \mathcal{F} dq \sim \frac{1}{2}\delta\left(\kappa k^2 + \frac{1}{2}\delta k^3\right) \Rightarrow \boxed{\delta \int k^2(s)ds}$$

厚さによる破断直前の形状の違い

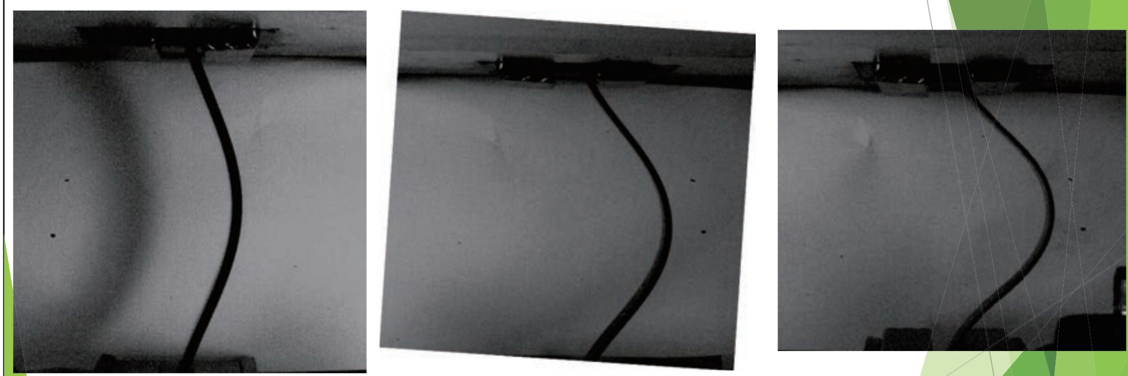

t = 5 mm　　t = 3 mm　　t =2mm

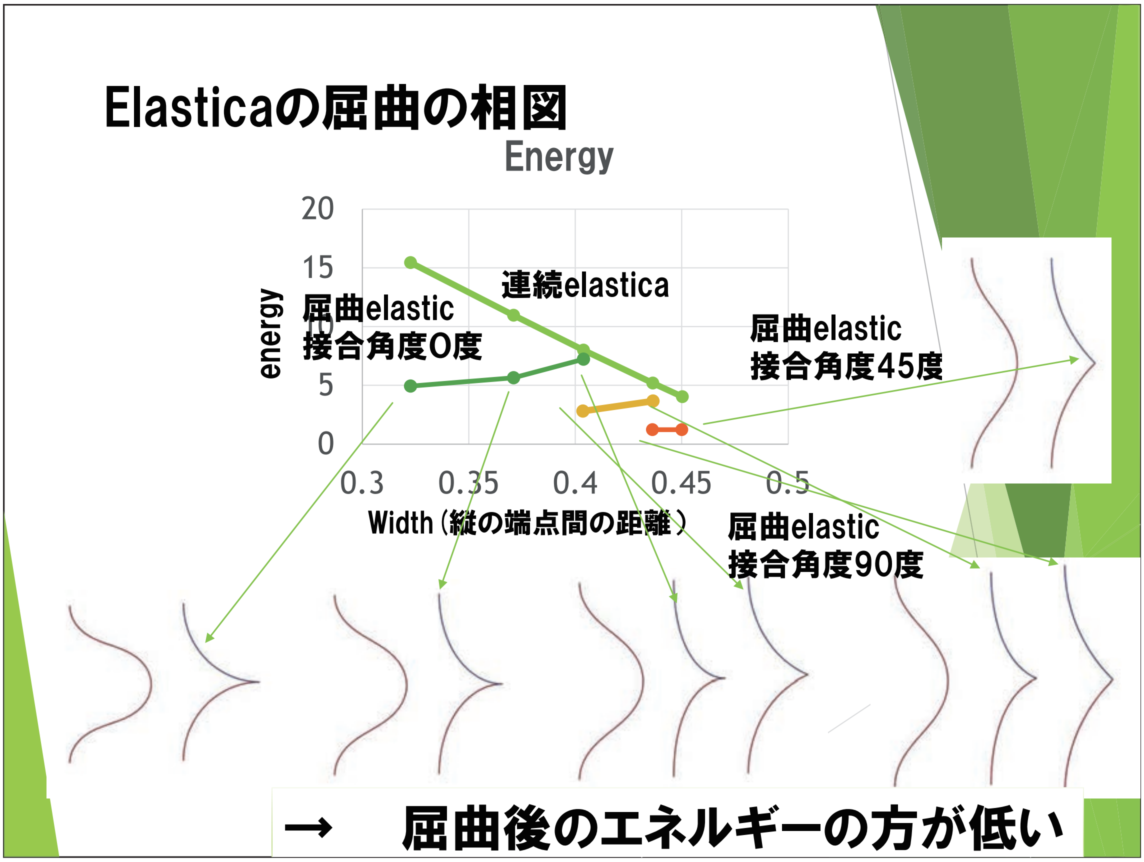
Elasticaの屈曲の相図
Energy
energy
20
15
10
5
0
0.3
0.35
0.4
0.45
0.5
Width（縦の端点間の距離）
連続elastica
屈曲elastic
接合角度0度
屈曲elastic
接合角度45度
屈曲elastic
接合角度90度
→　屈曲後のエネルギーの方が低い

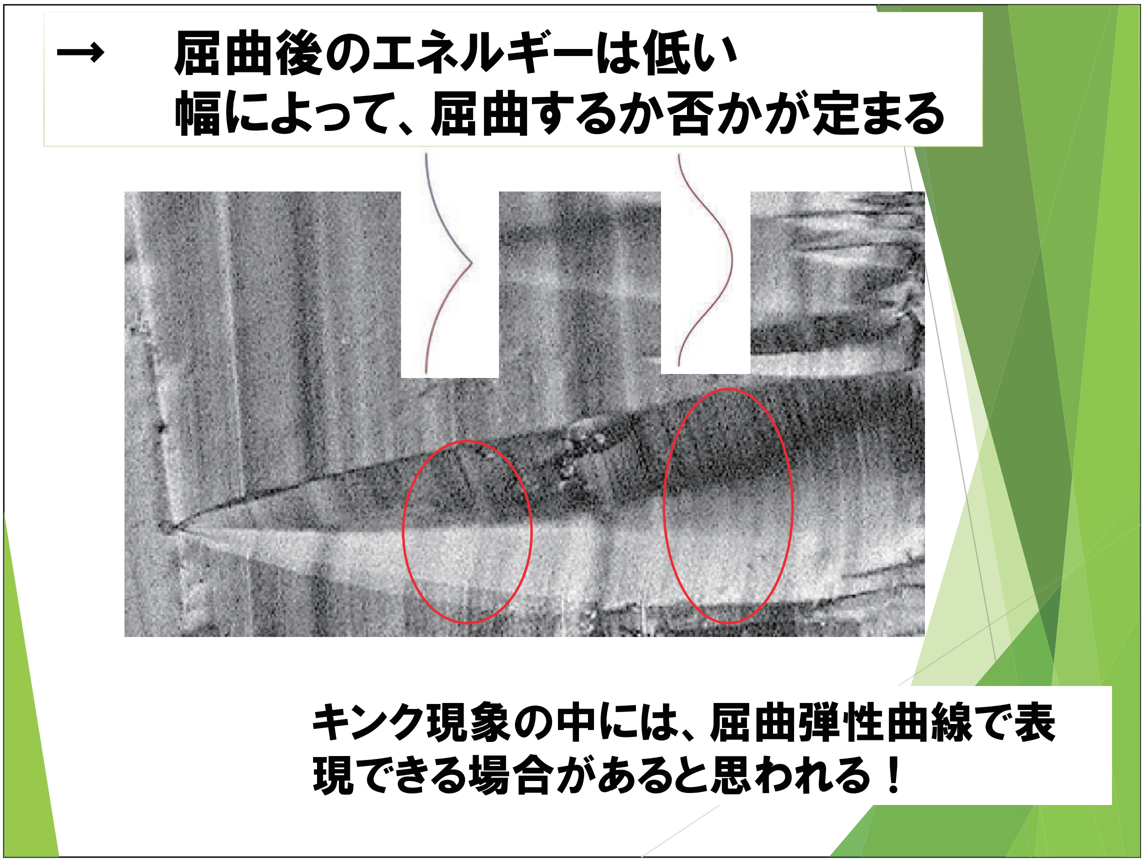
→　屈曲後のエネルギーは低い
幅によって、屈曲するか否かが定まる
キンク現象の中には、屈曲弾性曲線で表現できる場合があると思われる！

地層でもそうのようなものが存在する

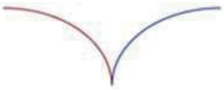

南西諸島　中之島

http://www8.plala.or.jp/Geo/OutcropSw.html

但し，本南西諸島　中之島の地層の写真は、未固結の地層（火山灰，火砕サージなど）が引張応力場でクリープを伴う正断層の露頭と言われている.

キンク現象に現れる様々形状を数学的に分類しその性質を述べよ
by　中谷彰宏先生(2017.9)

達成した事

・キンクの発生において、弾性力が支配的な場合が想定され、その場合を屈曲弾性曲線で形状を提示した

・屈曲弾性曲線の形状とエネルギーを決定した

（屈曲elasticaの考察は調査した範囲ではしられていない）

今後の課題

・物理的な視点：界面生成との関係をエネルギー論的に考察する

・屈曲弾性曲線の最小化問題としての定式化

先進数理解析の発展に
ご協力をお願いいたします。

ご清聴ありがとうございました

結晶構造の数学的記述 Growth
(Mathematical Description of Crystal Lattice Structure, Growth)

中川淳一, Junichi Nakagawa
新日鐵住金（株） Nippon Steel & Sumitomo Metal Co.
社会数理実践研究 (東大数理)
FMSP mathematical research on real world problems of the University of Tokyo

The mathematical research on real world problems is an educational program for doctorate course students in FMSP (Leading Graduate Course Frontiers of Mathematical Science and Physics) of the University of Tokyo. Nippon Steel & Sumitomo Metal Corporation proposes themes for the program, and has provided several themes for students who major in geometry or algebra. In this presentation, the growth is highlighted as a theme that is of interest in mathematics and important in materials. The growth is defined as a sequential representation of the graphical structure of a crystal lattice. The 1st growth corresponds to the coordination number of crystals, which is used as a numerical index to describe the crystalline structure in material science. The number of the nth growth was counted step by step and the numerical sequences at $n \to \infty$ are a quasi-polynomial, i.e. the coefficients are periodic functions with an integral period. The generating functions can be derived from the quasi-polynomial and showed symmetrical properties. We are studying the mathematical conditions such that the growth becomes a quasi-polynomial and the relationship between the growth of a crystal lattice and the growth of the crystal group.

IMI Workshop：結晶転位の先進数理解析

東大数理科学FMSPの社会数理実践研究
- 結晶構造の数学的記述Growth -

FMSP mathematical research on real world problems of the University of Tokyo

- Mathematical Description of Crystal Lattice Structure, **Growth** -

2018.9.10-21
Institute of Mathematics for Industry
Kyushu University

Nippon Steel & Sumitomo Metal Corporation
Advanced Technology Research Laboratories
Mathematical Science & Technical Research Lab.

Junichi Nakagawa

1

新日鐵住金 NIPPON STEEL & SUMITOMO METAL

FMSP社会数理実践研究

- ✓ 東大数理科学FMSPのコース生教育プログラムのひとつ（2016年度から開始）
- ✓ D1コース生は必須であり、複数の企業・国立研究所から提示された現実問題の課題に対し、1年間に亘り数学の実践研究を行う。
- ✓ コース生は自身の専門性と興味に基づき、上記課題提示機関課題のひとつ課題を選択する。
- ✓ 新日鐵住金㈱は、3年間継続して、「結晶と数学」に関するテーマを提示、幾何学と代数学を専攻するコース生が主体となっている。

2

新日鐵住金 NIPPON STEEL & SUMITOMO METAL

新日鐵住金㈱の課題

結晶とは、原子，分子が規則正しく配列している固体であり、離散的な空間並進対称性をもつ理想的な物質のことです。結晶材料において、格子欠陥、析出物、転位等の結晶格子の乱れが材料の諸性質（強度や延性等）を決定する重要因子となっていることが知られています。

本研究会では、過去のスタディグループで数年以上に亘り議論してきました内容と昨年度の社会数理実践研究の内容を当面の題材にして、「①結晶の対称性」、「②対称性の乱れ」と「③ミクロ（離散）からマクロ（連続）への階層構造」に起因し発現する材料の諸性質を数学でゼロから考えるための議論の場とします。

> 今後重要性を増してゆく異分野連携の視点から、**自分の数学の専門性をフルに発揮できるような「数学の問題設定」を如何におこなうか**を一緒に考えませんか！

新日鐵住金
NIPPON STEEL & SUMITOMO METAL

2016Fy実践研究成果と現実世界との接点

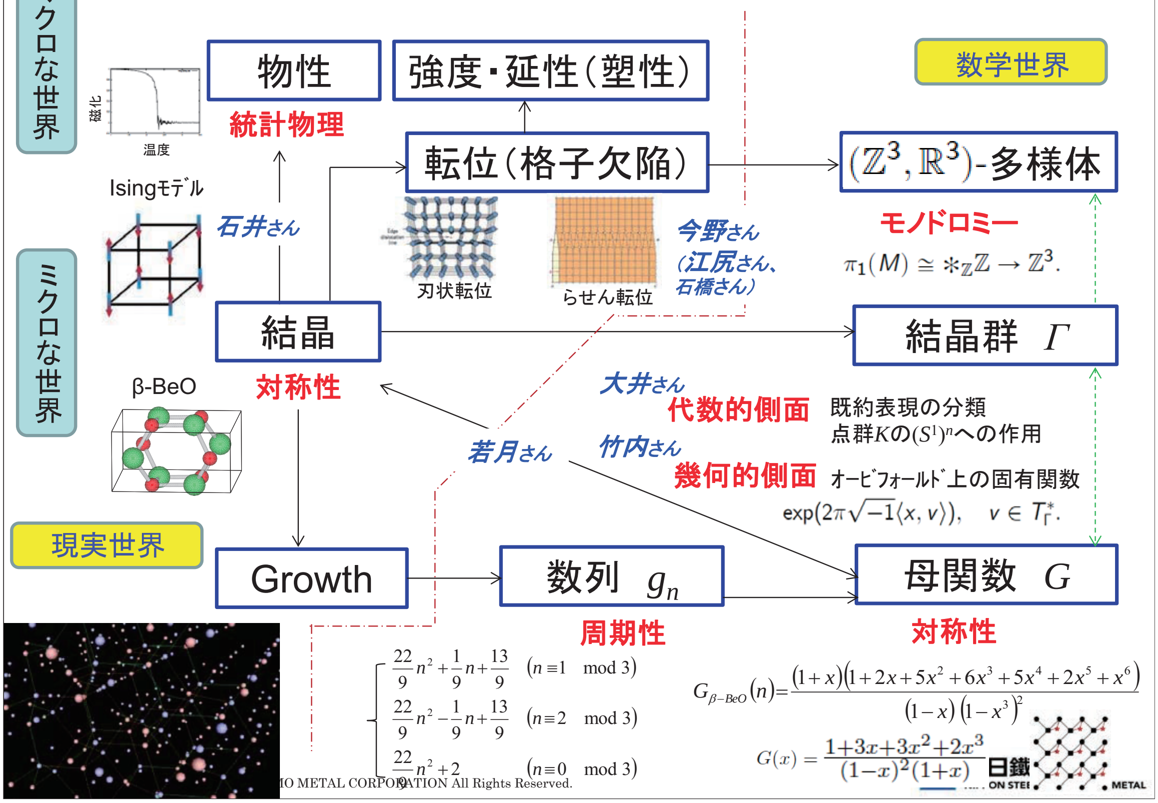

Crystal Group G

A discrete subgroup of the isometry group $Isom(\mathbb{R}^3)$ included 3 linearly independent translations.

- ✓ The lattice group H : = normal subgroup of G generated by these translations
- ✓ $K := G/H$ is a finite group called as the point group.

The 7 Lattice System and The 14 Bravais Lattice

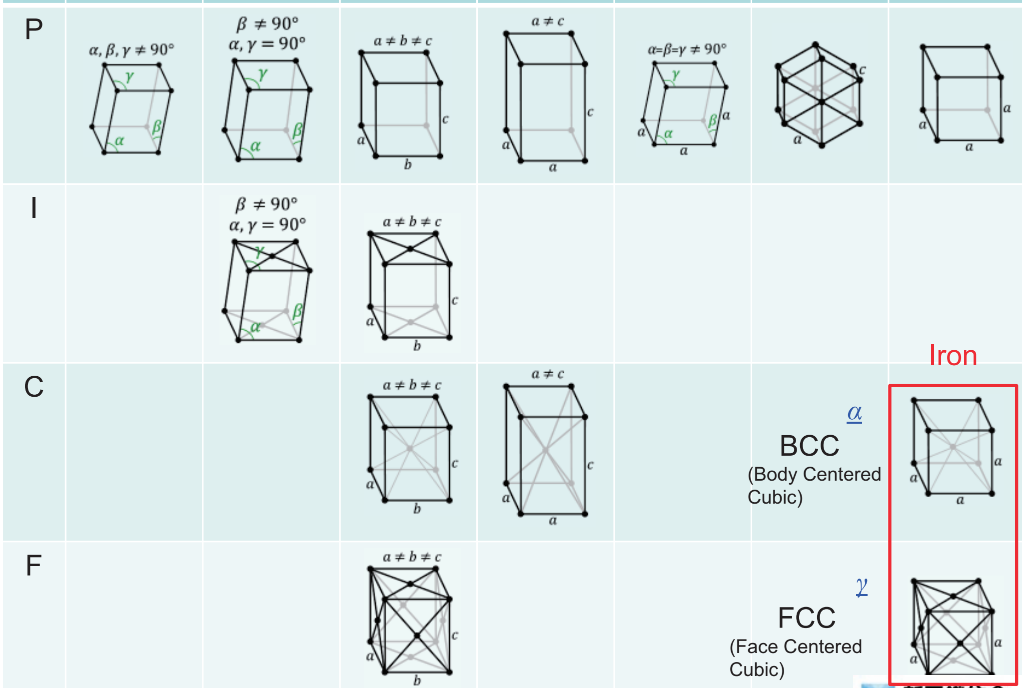

	Triclinic 三斜晶	Monoclinic 単斜晶	Orthorhombic 直方晶	Tetragonal 正方晶	Trigonal 三方晶	Hexagonal 六方晶	Cubic 立方晶
P	$\alpha,\beta,\gamma \neq 90°$	$\beta \neq 90°$ $\alpha,\gamma = 90°$	$a \neq b \neq c$	$a \neq c$	$\alpha=\beta=\gamma \neq 90°$		
I		$\beta \neq 90°$ $\alpha,\gamma = 90°$	$a \neq b \neq c$				
C			$a \neq b \neq c$	$a \neq c$		α BCC (Body Centered Cubic)	Iron
F			$a \neq b \neq c$			γ FCC (Face Centered Cubic)	

Problem in Materials Informatics

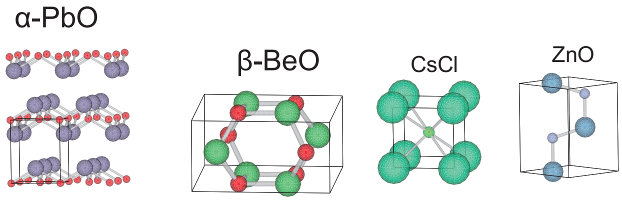

- different crystal lattice
- different configuration of atoms etc.

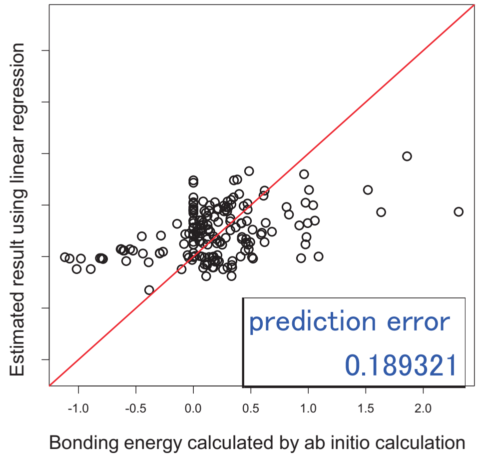

How do we describe the crystal geometry numerically?

京大 材料工学・田中教授、瀬古准教授からデータご提供

Regression Model

- This problem can be viewed as a regression problem
  - Predictors: information of atoms and crystal structure
  - Response variable: energy of compound

regression model: $\boldsymbol{y} = \beta_1 \boldsymbol{x}_1 + \beta_2 \boldsymbol{x}_2 + \cdots + \beta_p \boldsymbol{x}_p + \boldsymbol{\varepsilon}$

Descriptors x_i

Atomic number	**Position of periodic table**
Electron affinity	**Electronegativity**
Ionization Energy	**Number of electrons**
Atomic mass	**Coordination number**
Radius	**Growth**

Descriptors regarding crystal geometry

Response variable y

Bonding energy of compound

東大 Study Group 2014

Mathematical Description of Crystals

NaCl

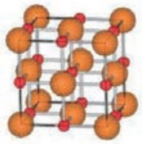

CsCl

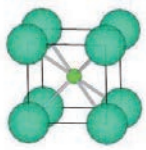

β-BeO

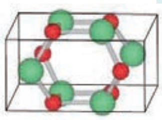

Chemical compounds	Lattice	Symmetry (order of point group)	Growth			
			1st	2nd	3rd	4th
NaCl	cubic	48	6	18	38	66
CsCl	cubic	48	8	26	56	98
β-BeO	tetragonal	16	4	11	18	41
ZnS	cubic	24	4	12	24	42
ZnO	hexagonal	12	4	12	25	44
α-PbO	tetragonal	16	4	8	12	16
TlI	orthogonal	8	7	22	47	82
NiAs	hexagonal	24	6	20	42	74

We focus on the coordination number in material science, and the growth generates it mathematically.

ZnS

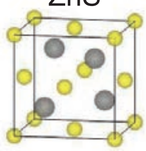

ZnO

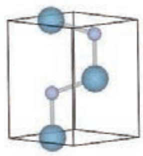

α-PbO

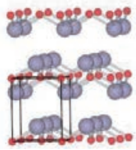

TlI

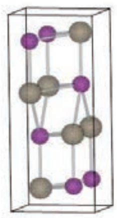

NiAs

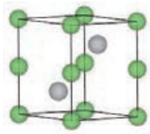

9

新日鐵住金 NIPPON STEEL & SUMITOMO METAL

東大 Study Group 2014

ZnO the 1st growth=4 (corresponding to coordination number)

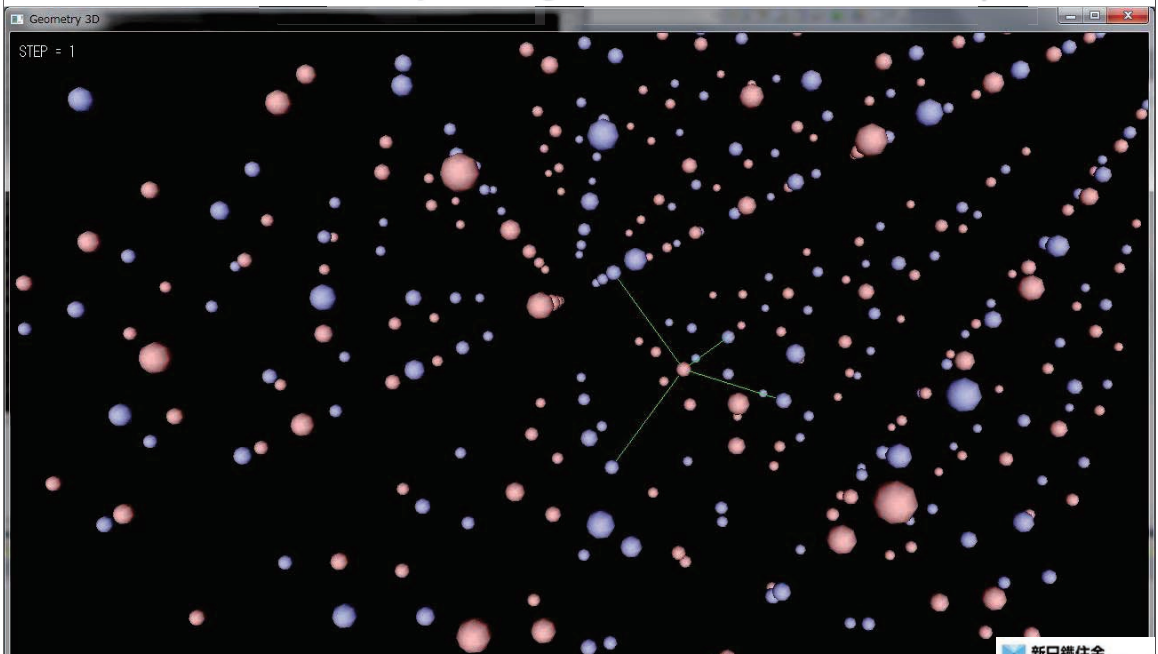

東大 Study Group 2014

ZnO
the 2nd growth=12

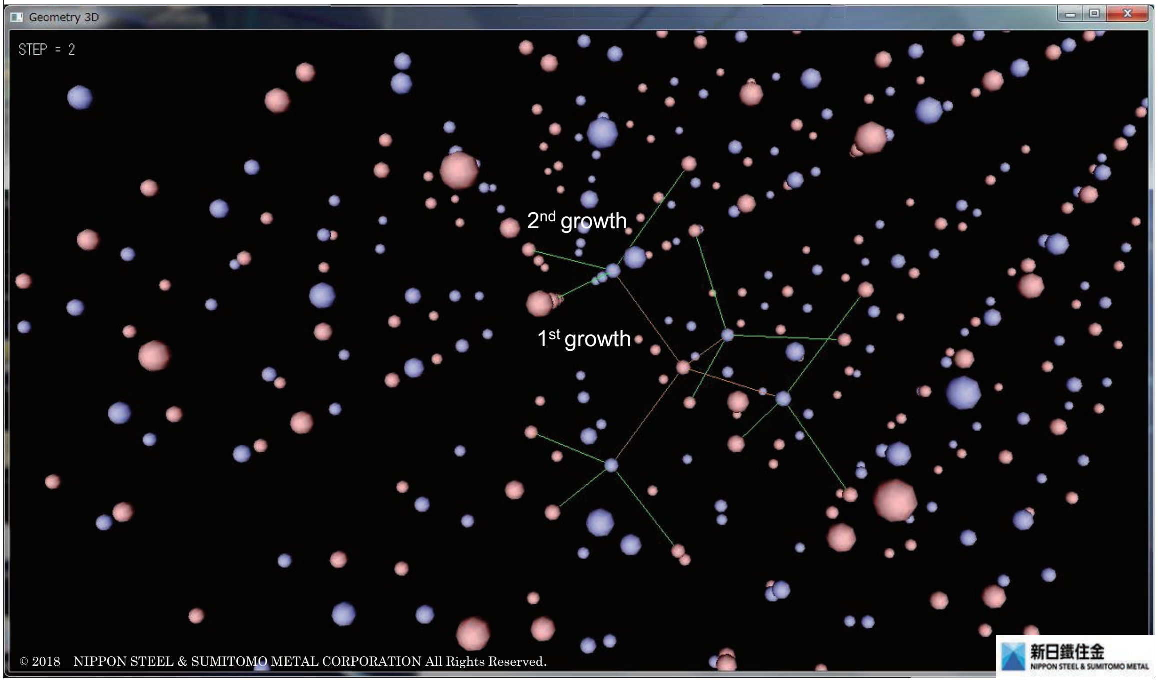

東大 Study Group 2014

ZnO
the 3rd growth=25

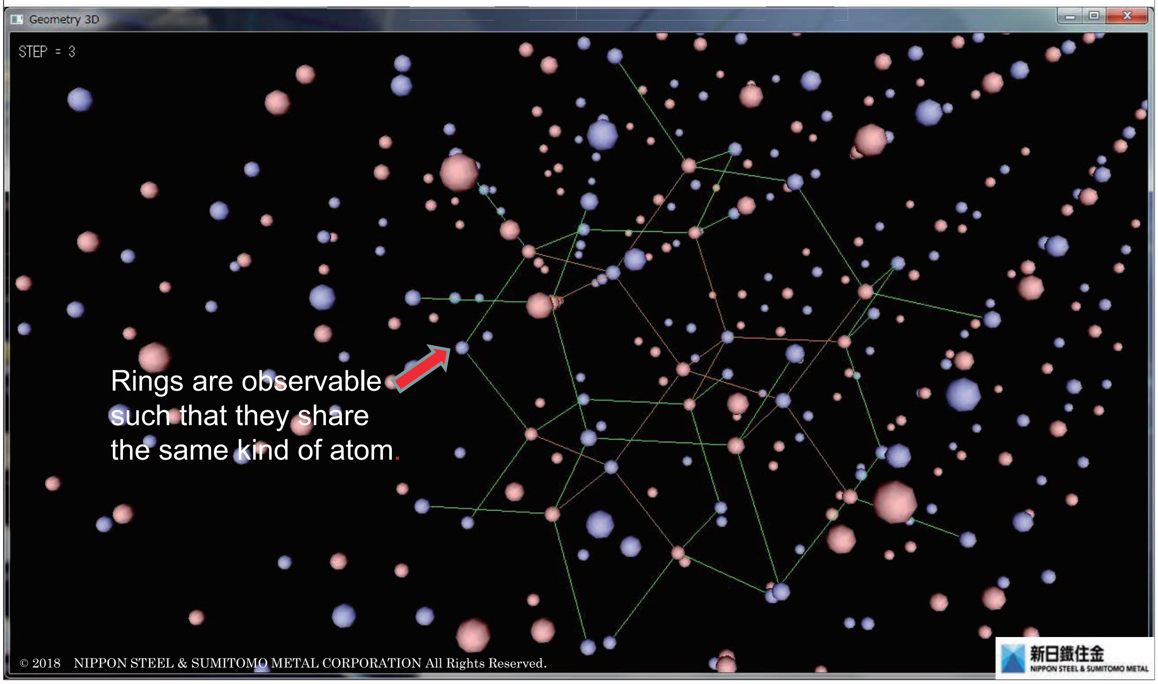

東大　Study Group 2014

ZnO
the 4th growth=44

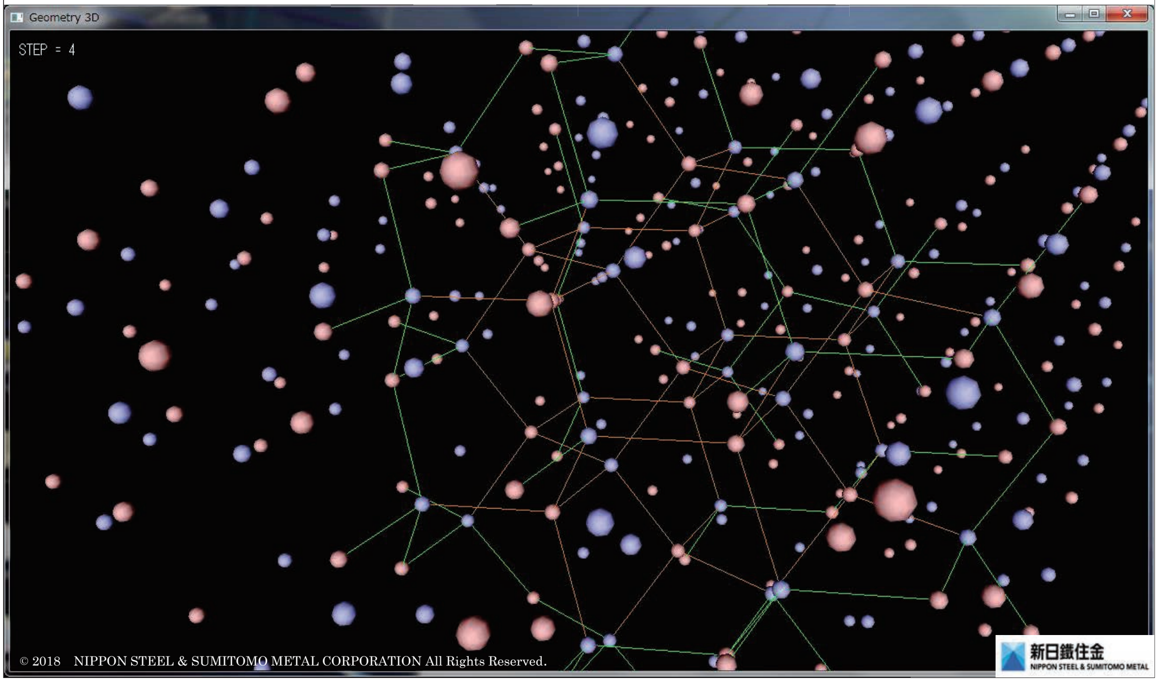

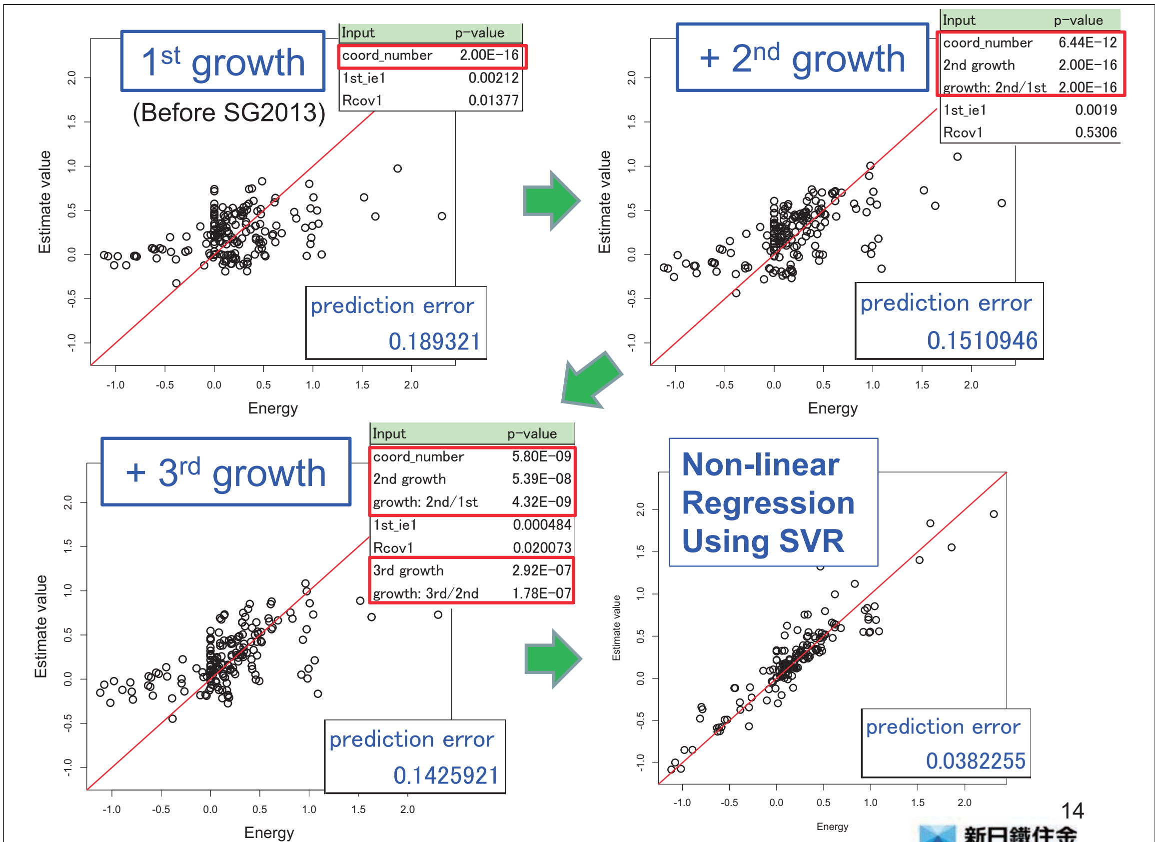

14

新日鐵住金
NIPPON STEEL & SUMITOMO METAL

SGW2014

Counting Out of # of Growth Using Computer

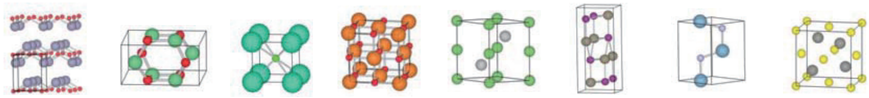

Growth	Crystals							
	α −PbO	β −BeO	CsCl	NaCl	NiAs	TlI	ZnO	ZnS
g1	4	4	8	6	6	7	4	4
g2	8	11	26	18	20	22	12	12
g3	12	24	56	38	42	47	25	24
g4	16	41	98	66	74	82	44	42
g5	20	62	152	102	114	127	67	64
g6	24	90	218	146	164	182	96	92
g7	28	122	296	198	222	247	130	124
g8	32	157	386	258	290	322	170	162
g0	36	200	488	326	366	407	214	204
g10	40	247	602	402	452	502	264	252
g11	44	296	728	486	546	607	319	304
g12	48	354	866	578	650	722	380	362
g13	52	416	1016	678	762	847	445	424
g14	56	479	1178	786	884	982	516	492
g15	60	552	1352	902	1014	1127	592	564
g16	64	629	1538	1026	1154	1282	674	642
g17	68	706	1736	1158	1302	1447	760	724
g18	72	794	1946	1298	1460	1622	852	812
g19	76	886	2168	1446	1626	1807	949	904
g20	80	977	2402	1602	1802	2002	1052	1002

Our interesting in mathematics is the g_∞.

SGW2014

Sequential Representation of # of Growth

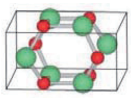

$$g_{\beta-BeO}(n)=\begin{cases}\frac{22}{9}n^2+\frac{1}{9}n+\frac{13}{9} & (n\equiv 1 \mod 3)\\ \frac{22}{9}n^2-\frac{1}{9}n+\frac{13}{9} & (n\equiv 2 \mod 3)\\ \frac{22}{9}n^2+2 & (n\equiv 0 \mod 3)\end{cases}$$

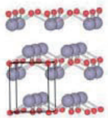

$$g_{\alpha-PbO}(n)=4n$$

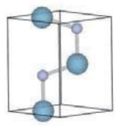

$$g_{ZnO}(n)=\begin{cases}\frac{21}{8}n^2+\frac{11}{8} & (n\equiv 1,3 \mod 4)\\ \frac{21}{8}n^2+\frac{3}{2} & (n\equiv 2 \mod 4)\\ \frac{21}{8}n^2+2 & (n\equiv 0 \mod 4)\end{cases}$$

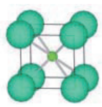

$$g_{CsCl}(n)=6n^2+2$$

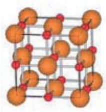

$$g_{NaCl}(n)=4n^2+2$$

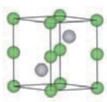

$$g_{NiAs}(n)=\begin{cases}\frac{9}{2}n^2+\frac{3}{2} & (n\equiv 1 \mod 2)\\ \frac{9}{2}n^2+2 & (n\equiv 0 \mod 2)\end{cases}$$

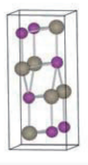

$$g_{TlI}(n)=5n^2+2$$

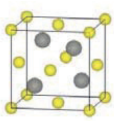

$$g_{ZnS}(n)=\begin{cases}\frac{5}{2}n^2+\frac{3}{2} & (n\equiv 1 \mod 2)\\ \frac{5}{2}n^2+2 & (n\equiv 0 \mod 2)\end{cases}$$

The family of the growth sequences is a quasi-polynomial, i.e. the coefficients are periodic functions with integral period.

Generating Function of Growth

$$\boxed{G(x):=1+\sum_{n=1}^{\infty} g_n\, x^n}$$

H. Ochiai ※1
(2016.9.30)
※1 : Kyusyu University, IMI

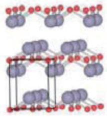

$$G_{\alpha-PbO}(x)=\frac{(1+x)^2}{(1-x)^2}$$

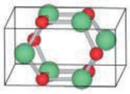

$$G_{\beta-BeO}(n)=\frac{(1+x)(1+2x+5x^2+6x^3+5x^4+2x^5+x^6)}{(1-x)(1-x^3)^2}$$

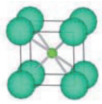

$$G_{CsCl}(x)=\frac{(1+x)(1+4x+x^2)}{(1-x)^3}$$

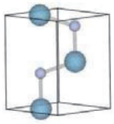

$$G_{ZnO}(x)=\frac{(1-x^3)(1+x+3x^2+x^3+x^4)}{(1-x)^3(1-x^4)}$$

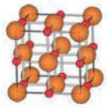

$$G_{NaCl}(n)=\frac{(1+x)^3}{(1-x)^3}$$

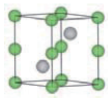

$$G_{NiAs}(x)=\frac{1+4x+8x^2+4x^3+x^4}{(1-x)^2(1-x^2)}$$

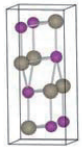

$$G_{TlI}(x)=\frac{(1+x)(1+3x+x^2)}{(1-x)^3}$$

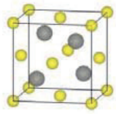

$$G_{ZnS}(x)=\frac{1+2x+4x^2+2x^3+x^4}{(1-x)^2(1-x^2)}$$

The family of the generating functions of growth looks symmetric.

Symmetrical Properties of Generating Function

Definition of the component of generating function :

for $k, N, n_0 \in \mathbb{N}$, $N>0,\ 0\le n_0 \le N$

Quasi-polynomial of growth

$$\left(g_k^{N,n_0}\right)_n = n^k \quad (n \equiv n_0 \bmod N)$$

$$\left(g_0^{N,n_0}\right)_0 = 1,\ \left(g_0^{N,N}\right)_0 = 0$$

generating function's component

$$G_k^{N,n_0}(x):=\sum_{n=0}^{\infty}\left(g_k^{N,n_0}\right)_n x^n$$

Proposition 1 (S. Wakatsuki)

(1) $G_{k+1}^{N,n_0}(x)=\left(x\dfrac{d}{dx}\right)G_k^{N,n_0}(x)$

(2) $G_k^{N,n_0}(x)=\dfrac{x^{n_0}}{(1-x^N)^{k+1}}\times(\text{polynomial of degree } N_k)$

(3) $G_0^{N,0}(x)=G_0^{N,N}(x)+1,\quad G_k^{N,N}(x)=G_k^{N,N} \quad \text{for } k>0$

Wakatsuki-san who is a doctor course student in the 3rd grade. He had studied this subject for one year as a curriculum of FMSP(Leading Graduate Course Frontiers of Mathematical Science and Physics).

Proposition 2 (S. Wakatsuki)

$$G_k^{N,n_0}\left(\frac{1}{x}\right)=(-1)^{k+1}G_k^{N,N-n_0}(x)$$

Example

For example, in the case of the quasi-polynomial of β-BeO

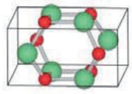

$$g_{\beta\text{-BeO}}(n)=\begin{cases}\frac{22}{9}n^2+\frac{1}{9}n+\frac{13}{9} & (n\equiv 1 \mod 3)\\ \frac{22}{9}n^2-\frac{1}{9}n+\frac{13}{9} & (n\equiv 2 \mod 3)\\ \frac{22}{9}n^2+2 & (n\equiv 0 \mod 3)\end{cases}$$

$$\left(g_k^{N,n_0}\right)_n = n^k \quad (n\equiv n_0 \mod N)$$

$$G_k^{N,n_0}(x):=\sum_{n=0}^{\infty}\left(g_k^{N,n_0}\right)_n x^n$$

$$G_{\beta\text{-BeO}}(x)=\frac{22}{9}G_2^{1,0}(x)+\frac{1}{9}G_1^{3,1}(x)-\frac{1}{9}G_1^{3,2}(x)+2G_0^{3,3}(x)+\frac{13}{9}G_0^{3,1}(x)+\frac{13}{9}G_0^{3,2}(x)+1$$

$$\begin{aligned}G_{\beta\text{-BeO}}\left(\frac{1}{x}\right)&=\frac{22}{9}G_2^{1,0}\left(\frac{1}{x}\right)+\frac{1}{9}G_1^{3,1}\left(\frac{1}{x}\right)-\frac{1}{9}G_1^{3,2}\left(\frac{1}{x}\right)+2G_0^{3,3}\left(\frac{1}{x}\right)+\frac{13}{9}G_0^{3,1}\left(\frac{1}{x}\right)+\frac{13}{9}G_0^{3,2}\left(\frac{1}{x}\right)+1\\&=-\frac{22}{9}G_2^{1,1}(x)+\frac{1}{9}G_1^{3,2}(x)-\frac{1}{9}G_1^{3,1}(x)-2G_0^{3,0}(x)-\frac{13}{9}G_0^{3,2}(x)-\frac{13}{9}G_0^{3,1}(x)+1\\&=-\frac{22}{9}G_2^{1,0}(x)+\frac{1}{9}G_1^{3,2}(x)-\frac{1}{9}G_1^{3,1}(x)-2\left(G_0^{3,3}(x)+1\right)-\frac{13}{9}G_0^{3,2}+1\\&=-G_{\beta\text{-BeO}}(x)\end{aligned}$$

Generating function has another symmetry.

Generating Function in the Case of Break of Symmetry

S. Wakatsuki

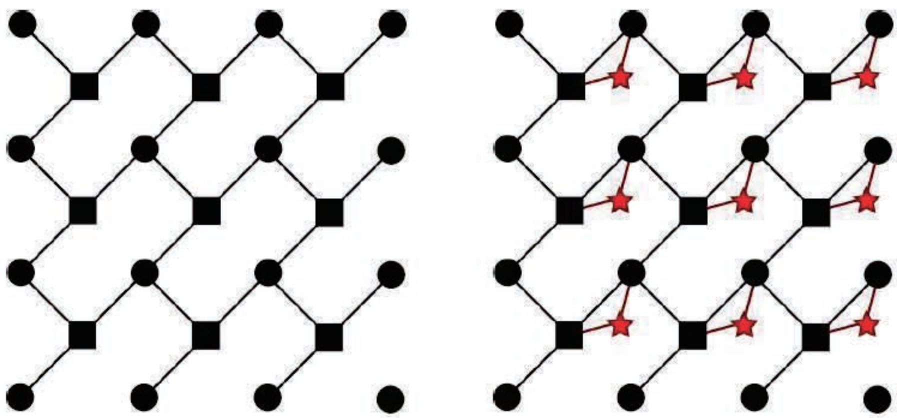

$$G(x)=1+3G_1^{1,0}=\frac{1+x+x^2}{(1-x)^2}$$

$$G(x)=1-G_0^{2,2}-\frac{1}{2}G_0^{2,1}+\frac{9}{2}G_1^{1,0}$$

$$=\frac{1+3x+3x^2+2x^3}{(1-x)^2(1+x)}$$

東京大学 数理科学研究科 中村勇哉 助教のアイデア（新日鐵住金チーム　主担当教員）

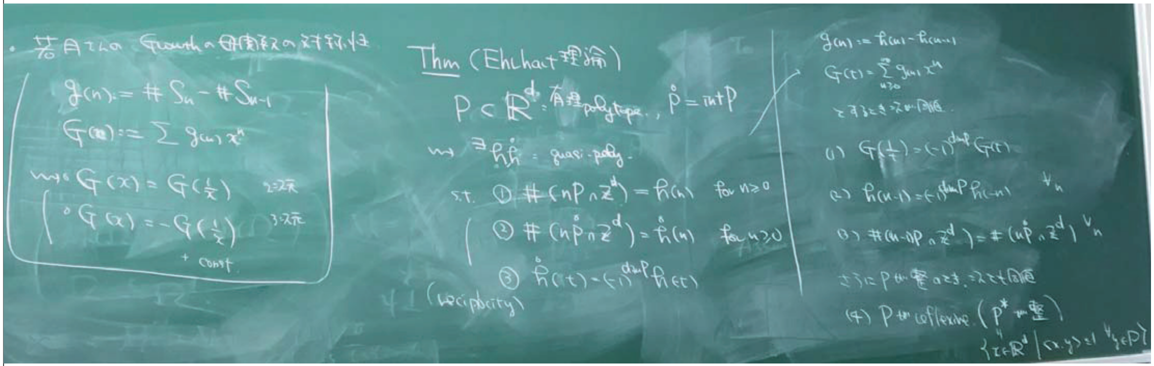

命題 5.3 (4 節参照)．結晶の growth は quasi polynomial type になる．

予想 5.4 (若月)．結晶の growth$g(n)$ の母関数 $G(t) = \sum_{n \geq 0}^{\infty} g(n)t^n$ は $G(t) = (-1)^{\dim C} G(1/t)$ を みたす．

命題 5.5 (1 節参照.)．上の予想は $h(n-1) = (-1)^{\dim C} h(-n)$ をみたすことと同値．

問題 5.8. 数学的な問題：

(1) 命題 5.3 において，quasi-polynomial (type でなく) となる数学的条件を調べる．命題 5.3 は translation が作用するグラフという設定であるが，さらにどんな条件を加えればよいだろうか．

(2) 命題 5.3 において存在が示されている quasi-polynomial $h(n)$ が $h(n-1) = (-1)^{\dim C} h(-n)$ をみたすような数学的条件を調べる．

(3) (1), (2) が対称性からみた結晶の特徴づけといえるだろうか??

(4) 結晶の growth と，結晶群の growth との関連を調べる．

Summary and Points under Discussion

1. Clarifying mathematically the relationship between the growth and the crystal lattice
2. Considering the relationship between the growth and the crystal group

Crystal lattice → Crystal group

e.g. β-BeO

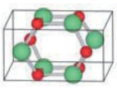

Eight crystals composed of two kinds of atoms

Growth $\xrightarrow{n \to \infty}$ quasi-Polynomial (Numerical sequence) → Generating function ?

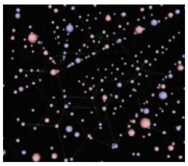

Cyclical property

e.g.

$$g_{\beta\text{-BeO}}(n) = \begin{cases} \frac{22}{9}n^2 + \frac{1}{9}n + \frac{13}{9} & (n \equiv 1 \mod 3) \\ \frac{22}{9}n^2 - \frac{1}{9}n + \frac{13}{9} & (n \equiv 2 \mod 3) \\ \frac{22}{9}n^2 + 2 & (n \equiv 0 \mod 3) \end{cases}$$

Symmetrical properties

$$G_{\beta\text{-BeO}}(n) = \frac{(1+x)(1+2x+5x^2+6x^3+5x^4+2x^5+x^6)}{(1-x)(1-x^3)^2}$$

$$G(x) = \pm G\left(\frac{1}{x}\right)$$

22

新日鐵住金 NIPPON STEEL & SUMITOMO METAL

Thank you for your attention!

23

新日鐵住金
NIPPON STEEL & SUMITOMO METAL

転位の連続体の動的理論：微分幾何によるアプローチ
(Space-Time Theory of Continuously Distributed Dislocations: Differential-Geometrical Approach)

甘利俊一, Shun-ichi Amari
理化学研究所 RIKEN

Metals have crystal structures and defects of such structures are responsible for their strength. Defects are typically dislocations and disclinations from the microscopic point of view, but they are continuously distributed from the macroscopic point of view. Riemannian and non-Riemannian theories had been developed in Japan and Europe in 1950-1970 for elucidating these aspects [1-3].

However, it looks mostly forgotten in the present days. We review these theories again. We recapitulate the four-dimensional continuum theory of moving dislocations in which motion, creation and annihilation of dislocations are described as torsions and curvatures of a four-dimensional material space-time.

References

[1] S. Amari, *On some primary structures of non-Riemannian plasticity theory*, RAAG Memoirs **3** (1962), 163–172.
[2] S. Amari, *A geometrical theory of moving dislocations and anelasticity*, RAAG Memoirs **4** (1968), 284–294.
[3] I. Kondo, *On the analytical and physical foundations of the theory of dislocations and yielding by the differential geometry of continua*, Int. J. Engng. Sci. **2** (1964) 219–251.

結晶転位の先進数理解析ー九大

転位の連続体の動的理論：
微分幾何によるアプローチ

理化学研究所　　　甘利俊一

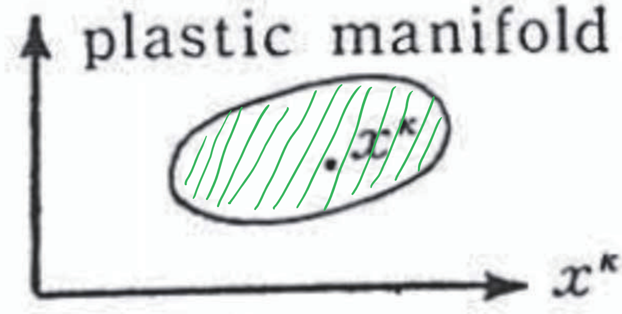

FIG. 1

弾性変形

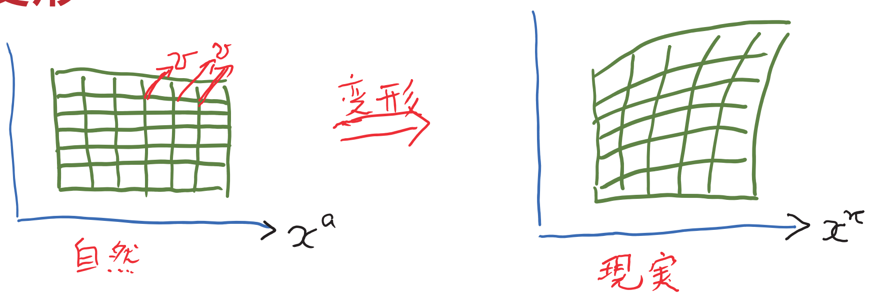

$$x^\kappa = f(x^a) = \delta^\kappa_a x^a + v^\kappa(x)$$

弾性論 : 変位 $v = (v^\kappa(x))$ 　　欠陥なし v, B

$$dx^\kappa = \sum_a \frac{\partial f^\kappa}{\partial x^a} dx^a = B^\kappa_a dx^a$$

$$B^\kappa_a = \delta^\kappa_a + \frac{\partial v^\kappa}{\partial x^a} \quad ; \ B^a_\kappa$$

$$\beta_{\lambda\kappa} = \frac{\partial v^\kappa}{\partial x^\lambda} = e_{\kappa\lambda} + \omega_{\kappa\lambda}$$

歪　回転

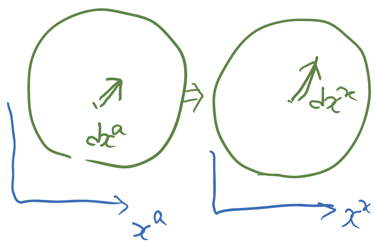

対称部分と反対称部分

転位（刃状）

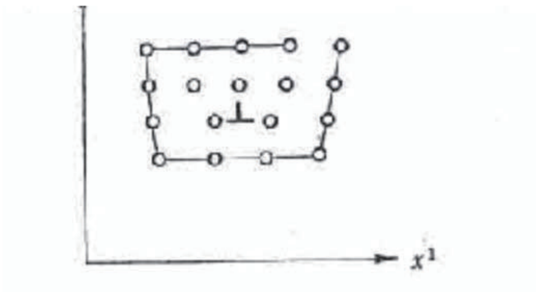

Fig. 5

線素の自然状態

$$dx^a = B^a_\varkappa \, dx^\varkappa$$

$$(B^a_\varkappa):$$

$$dx^\varkappa = \bar{B}^\varkappa_a dx^a$$

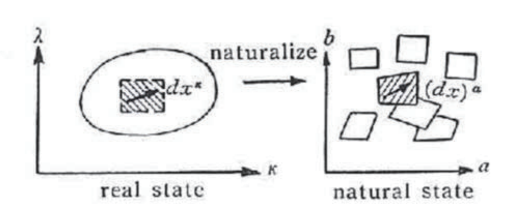

Fig. 2

自然計量：　実計量と違う

$$ds^2 = \sum (dx^a)^2 = \delta_{ab} B^a_\kappa B^b_\lambda dx^\kappa dx^\lambda$$

$$g_{\kappa\lambda} = \delta_{ab} B^a_\kappa B^b_\lambda \qquad (g_{\kappa\lambda} \neq \delta_{\kappa\lambda})$$

歪 strain　$e_{\kappa\lambda} = \dfrac{1}{2}(\delta_{\kappa\lambda} - g_{\kappa\lambda})$

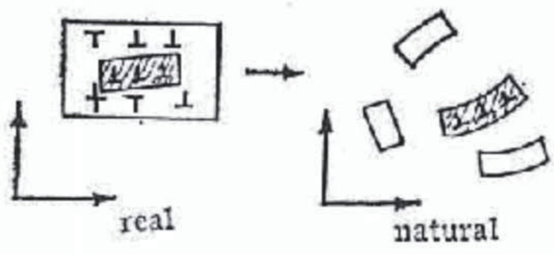

FIG. 4

アファイン接続：　平行性の定義

$$dX^{\lambda} = \Gamma^{\kappa}_{\mu\lambda} X^{\lambda} dx^{\mu}$$

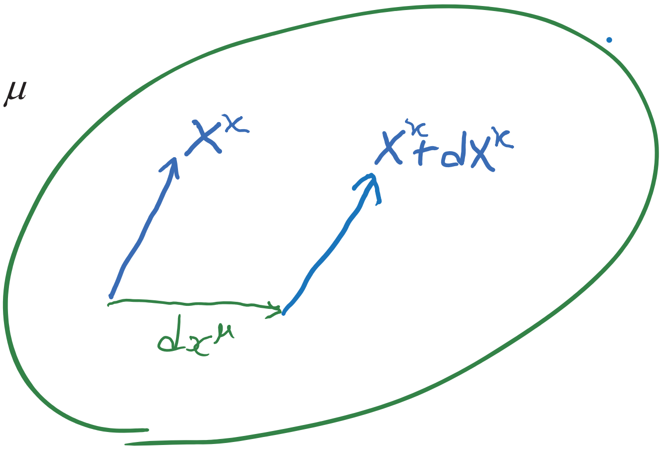

線素連の自然状態：平行性とアファイン接続

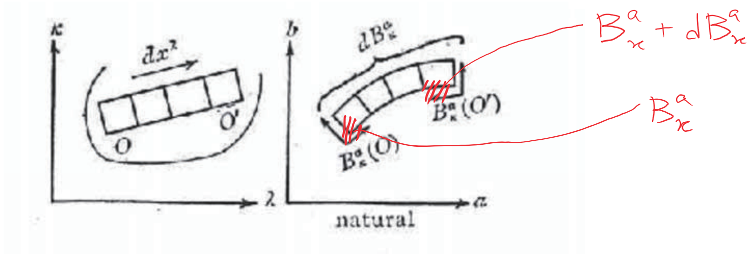

Fig. 3

$$B_\kappa{}^a X^\kappa = (B^a_\kappa + dB^a_\kappa)(X^\kappa + dX^\kappa) \qquad dX^\kappa = -B_\kappa^a\, dB^a_\mu X^\mu$$

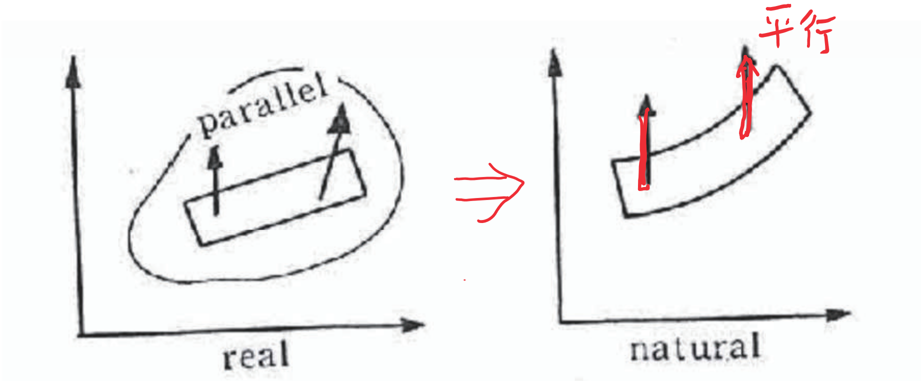

FIG. 5

$$\boxed{\Gamma^\kappa_{\mu\lambda} = -B^\kappa_a \frac{\partial}{\partial x^\mu} B^a_\lambda}$$

非リーマン空間：　アファイン接続を持つリーマン空間
Einstein 統一理論

$$\{M, g_{\nu\lambda}, \Gamma^\kappa_{\mu\lambda}\} \Rightarrow S^\kappa_{\mu\lambda}, R^\kappa_{\nu\mu\lambda}$$

捩率**(torsion)** $: S^\kappa_{\mu\lambda} = \Gamma^\kappa_{[\mu\lambda]}$

曲率 **(RC-curvature)** $: R^\kappa{}_{\nu\mu\lambda} = \partial_{[\nu}\Gamma^\kappa{}_{\mu]\lambda} - \Gamma\Gamma$

微小要素の平行移動

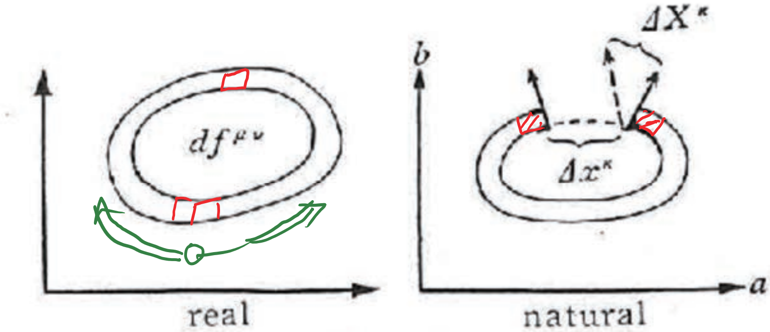

FIG. 6

Edge dislocation

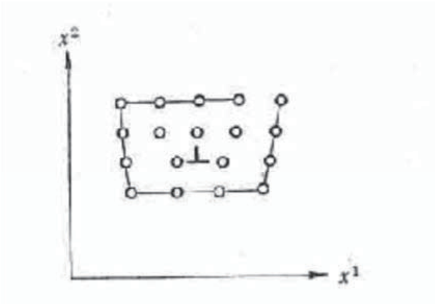

FIG. 5

screw dislocation

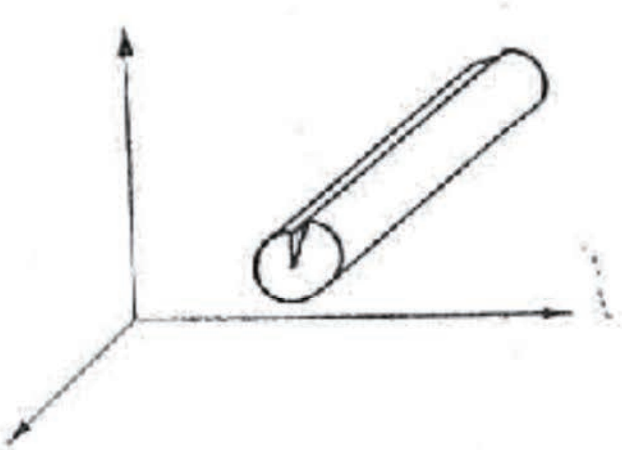

FIG. 6

捩率＝転位

遠隔平行性空間： R = 0

$$B^a_\kappa(x), B^\kappa_a(x)$$

$$\Gamma^\kappa_{\mu\lambda} = -B^\kappa_a \partial_\mu B^a_\lambda$$

$$\nabla S = 0$$

S=0: リーマン空間
K = R = 0 ：ユークリッド空間

適合条件：森口(積分可能条件)

$$e_{\kappa\lambda} = \frac{\partial v^{\kappa}}{\partial x^{\lambda}} + \frac{\partial v^{\lambda}}{\partial x^{\kappa}}$$

Cosserat連続体　　E.Cartan

rotational strain

$$\rho_{\mu\lambda\kappa} = \Gamma_{\mu[\lambda\kappa]} = \underbrace{\partial_{\mu}\omega_{\kappa\lambda}}_{R=0\ \text{なら}}$$

stress　$\sigma_{\lambda\kappa}$ は対称？

物質要素、
回転

転位の運動論

4次元物質時空

$x = (x^1, x^2, x^3, x^0 = t)$

遠隔平行性理論

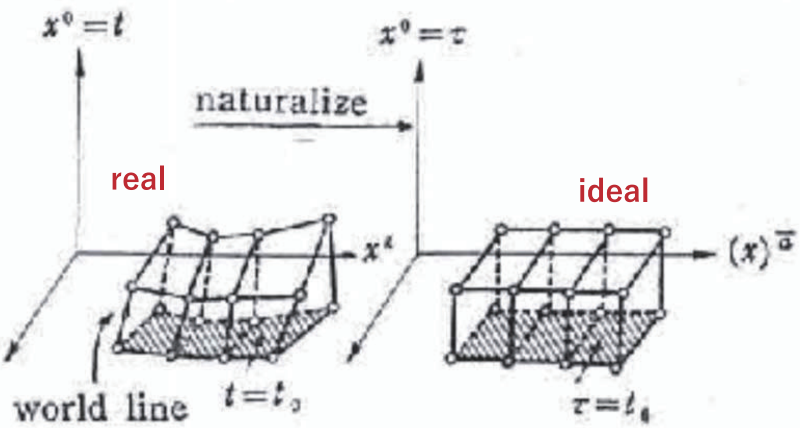

FIG. 1

自然状態

$$dx^{\bar\kappa} = B^{\bar\kappa}_{\bar a}\,dx^{\bar a}$$

$$dx^{\kappa} = B^{\kappa}_{a}\,dx^{a} + B^{\kappa}_{0}\,dt$$

$$dt = dt$$

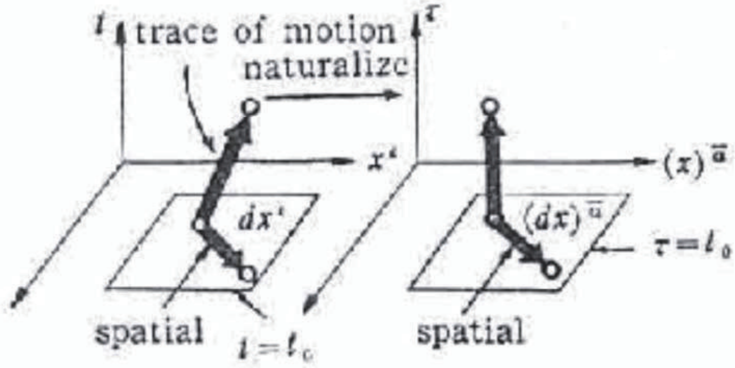

FIG. 2

$$B^{\kappa}_{\bar a} = \begin{array}{c|c:c|}
\kappa \backslash a & \overbrace{\qquad \bar a \qquad} & 0 \\
\hline
\bar\kappa & \delta^{\bar\kappa}_{\bar a} + \beta^{\bar\kappa}_{\bar a} & v^{\bar\kappa} \\
\hdashline
0 & 0 & 1 \\
\hline
\end{array},$$

計量

$$ds^2 = \sum (dx^a)^2 = \delta_{ab} B_\kappa^a B_\lambda^b dx^\kappa dx^\lambda$$

$$g_{\kappa\lambda} = \delta_{ab} B_\kappa^a B_\lambda^b$$

$$g_{\lambda\kappa} = \begin{array}{c|c|c} & \overbrace{\qquad\quad}^{\bar\kappa} & 0 \\ \hline \bar\lambda & \delta_{\bar\lambda\bar\kappa} - 2\beta_{(\bar\lambda\bar\kappa)} & -v^{\bar\lambda} \\ \hline 0 & -v^{\bar\kappa} & c \end{array}$$

歪

$$e_{\kappa\lambda} = \frac{1}{2}(\delta_{\kappa\lambda} - g_{\kappa\lambda})$$

$$\varepsilon_{\lambda\kappa} = \begin{array}{c|c|c} & \overbrace{\qquad\quad}^{\bar\kappa} & 0 \\ \hline \bar\lambda & \beta_{(\bar\lambda\bar\kappa)} & \frac{1}{2}v^{\bar\lambda} \\ \hline 0 & \frac{1}{2}v^{\bar\kappa} & 0 \end{array} ,$$

幾何学：遠隔平行性空間

$$g_{\kappa\lambda} = \delta_{ab} B^a_\kappa B^b_\lambda$$

$$\Gamma_{\mu\lambda}{}^{\kappa} = B^\kappa_a \partial_\mu B^a_\lambda$$

$$S_{\mu\lambda\kappa} = \Gamma_{[\mu\lambda]\kappa} = \sim \partial_{[\mu} B_{\lambda]\kappa}$$

$$R_{\nu\mu\lambda\kappa} = 0$$

転位：空間成分

$$S_{12}{}^{1}$$

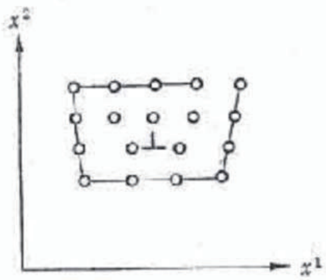

FIG. 5

転位：空間成分

$S_{12}{}^{3}$

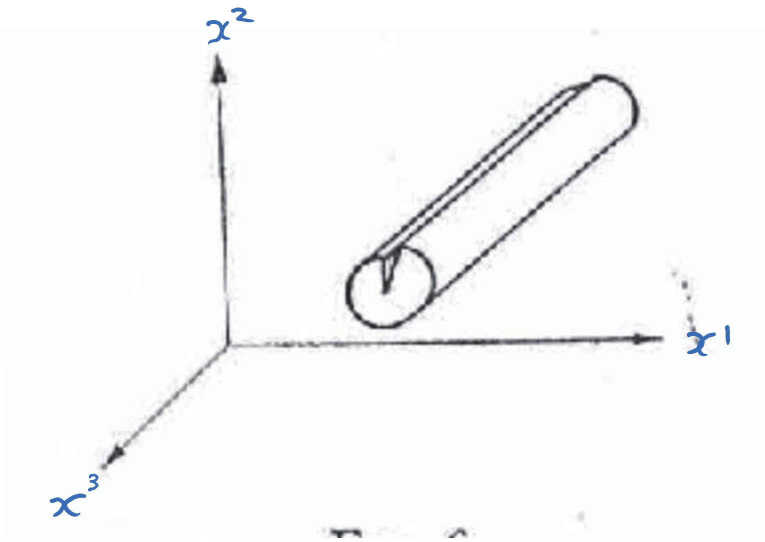

転位：時空間成分

$S_{01}{}^{1}$

$S_{01}{}^{2}$

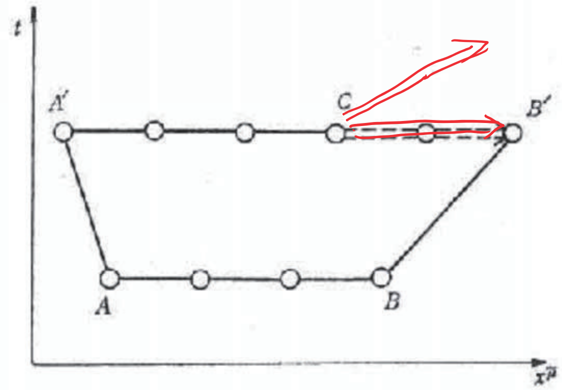

FIG. 7

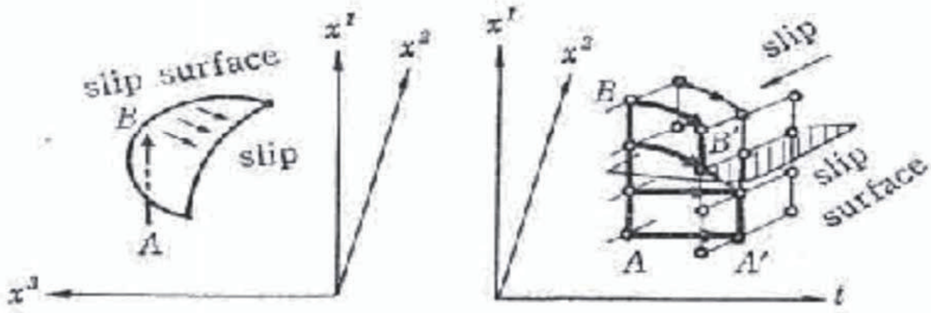

FIG. 8

運動転位；転位対の生成と消滅

u^ν

$S_{\mu\lambda}{}^{\kappa}(x^\nu - u^\nu t)$

$\perp$

$R=0$

$\partial_t S_{\mu\lambda}{}^{\kappa} = -u^\nu \partial_\nu S_{\mu\lambda}{}^{\kappa}$

$S_{01}{}^{2}$: $S_{31}{}^{2} \longrightarrow x_3$方向へ glide

$S_{21}{}^{2} \longrightarrow x_2$方向へ

$S_{01}{}^{1}$: $S_{21}{}^{1} \longrightarrow x_2$方向へ climb

運動の法則

$$S_{\mu\lambda\kappa} = -\partial_{[\mu}\beta_{\lambda]\kappa}$$

$$S_{0\lambda\kappa} = \frac{1}{2}(\partial_\lambda v_\kappa - \partial_t \beta_{\lambda\kappa})$$

$R=0$

$$\begin{cases} \operatorname{div} \mathbb{S} = 0 & \longleftrightarrow \quad \operatorname{div} \mathbb{H} = 0 \\ \dfrac{\partial}{\partial t}\mathbb{S} = \operatorname{rot} S_{0\lambda\kappa} & \longleftrightarrow \quad \operatorname{rot}\mathbb{E} = \dfrac{\partial}{\partial t}\mathbb{H} \end{cases}$$

$H_{\nu\kappa} = \varepsilon^{\nu\mu\lambda} S_{\mu\lambda\kappa}$: $E_{\lambda\kappa} = S_{0\lambda\kappa}$

anelasticity

$$\frac{d\, ds^2}{dt} = 2\, a_{\lambda\kappa}\, dx^\lambda dx^\kappa$$

$$\partial_t\, a_{\lambda\kappa} = K_{\lambda 0 \kappa 0}$$

Finsler Geometry of ferromagnetic material

torsion S and spin: interaction

Certain Arithmetic Quasicrystals

砂田利一, Toshikazu Sunada
明治大学 総合数理学部
Graduate School of Advanced Mathematical Sciences, Meiji University

In this talk, motivated by the 31st entry dated 1796 September 6 in Gauss's Mathematisches Tagebuch (Mathematical Diary), I will deal with a class of discrete sets defined arithmetically in the Euclidean space. Asymptotic behaviors of primitive Pythagorean and Eisenstein triples are discussed in connection with the notion of quasicrystals.

References

[1] T. Sunada, Topics on mathematical crystallography, in the proceedings of the symposium "Groups, graphs and random walks", London Mathematical Society Lecture Note Series 436, Cambridge University Press, 2017, 473–513
[2] T. Sunada, Generalized Riemann sums, in "From Riemann to Differential Geometry and Relativity", Editors: Lizhen Ji, Athanase Papadopoulos, Sumio Yamada, Springer (2017), 457–479.

Certain Arithmetic Quasicrystals

11th September, 2018 at Kyushu University

Toshikazu Sunada

Meiji University,
School of Interdisciplinary Mathematical Sciences

ABSTRACT

In this talk, motivated by the 31st entry dated 1796 September 6 in Gauss's Mathematisches Tagebuch (Mathematical Diary), I will deal with a class of discrete sets defined arithmetically in the Euclidean space. Asymptotic behaviors of primitive Pythagorean and Eisenstein triples are discussed in connection with the notion of quasicrystals.

A short history

Gauss's Mathematisches Tagebuch, a record of the mathematical discoveries of C. F. Gauss from 1796 to 1814, contains 146 entries, most of which consist of brief and somewhat cryptical statements. Some of the statements which he never published were independently discovered and published by others often many years later.

The entry we take up among others is the 31st dated 1796 September 6:

> "Numero fractionum inaequalium quorum denomonatores certum limitem non superant ad numerum fractionum omnium quarum num[eratores] aut denom[inatores] sint diversi infra limitem in infinito ut $6 : \pi\pi$"

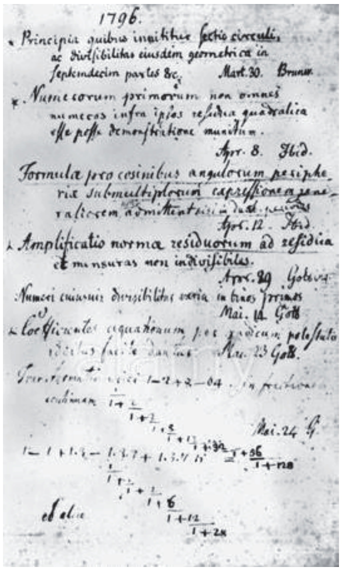
1796.

Principia quibus innititur sectio circuli, ac divisibilitas eiusdem geometrica in septemdecim partes &c. Mart. 30. Brunsv.

Numerorum primorum non omnes numeros infra ipsos residua quadratica esse posse demonstratione munitum. Apr. 8. Ibid.

Formula pro cosinibus angulorum peripheriae submultiplorum expressionem generaliorem non admittentium in duas periodos Apr. 12. Ibid.

Amplificatio normae residuorum ad residua et mensuras non indivisibiles. Apr. 29 Gottingae

Mai. 14 Gott.

Mai. 23 Gott.

Mai. 24 G.

et alia

This vague statement about counting (irreducible) fractions was formulated in an appropriate way afterwards and proved rigorously by Dirichlet (1849) and Ernesto Cesàro (1881). As a matter of fact, because of its vagueness, there are several ways to interpret what Gauss was going to convey.

We should point out that Yagloms refer to the question on the probability of two random integers being coprime as "Chebyshev's problem".

coprime pairs

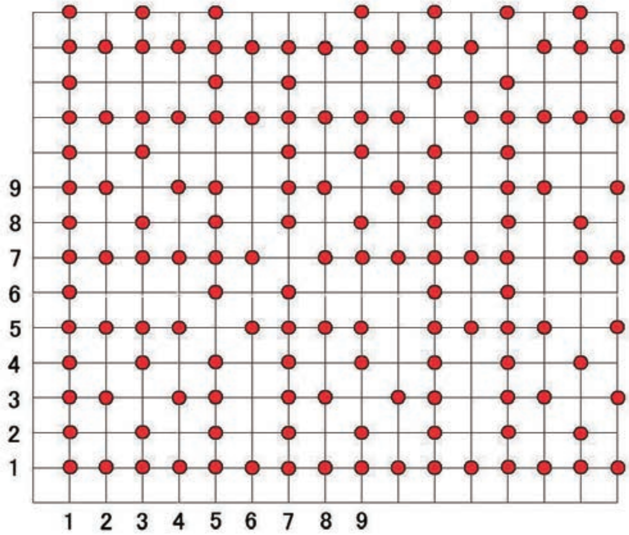

Gauss's theorem

$$\lim_{N\to\infty}\frac{1}{N^2}\left|\{(a,b)\in\mathbb{N}\times\mathbb{N}\,|\,\gcd(a,b)=1,\ a,b\le N\}\right|=\frac{6}{\pi^2}. \qquad (1)$$

In simple words, this theorem says that the frequency for coprime pairs to appear in all pairs of positive integers is $6/\pi^2$. This is also picturesquely stated in the language of probability as

"The probability that two randomly chosen positive integers are coprime is $6/\pi^2$"

Discrete sets with constant density

In general, a weighted discrete subset (Γ, ω) in $\mathbb{R}^d$ is a discrete set $\Gamma \subset \mathbb{R}^d$ with a map $\omega : \Gamma \to \mathbb{C}\backslash\{0\}$. Given a compactly supported function f on $\mathbb{R}^d$, define the Riemann sum associated with (Γ, ω) by setting

$$\sigma_\epsilon(f, \Gamma, \omega) = \sum_{z \in \Gamma} \epsilon^d f(\epsilon z)\omega(z).$$

We say that (Γ, ω) has constant density $c(\Gamma, \omega) \neq 0$ if

$$\lim_{\epsilon \to +0} \sigma_\epsilon(f, \Gamma, \omega) = c(\Gamma, \omega) \int_{\mathbb{R}^d} f(x)dx.$$

holds for any bounded Riemannian integrable function f on $\mathbb{R}^d$ with compact support. In the case $\omega \equiv 1$, we simply say that Γ has constant density $c(\Gamma)$.

Suppose that Γ and Γ' have constant density, and that $\Gamma' \subset \Gamma$. If $c(\Gamma) \neq c(\Gamma')$, then $\Gamma\backslash\Gamma'$ has constant density $c(\Gamma) - c(\Gamma')$.

Example (Motivation)

Let $\Delta = \{D_\alpha\}_{\alpha \in A}$ be a partition of $\mathbb{R}^d$ by bounded domains D_α with piecewise smooth boundaries satisfying

(i) $\mathrm{mesh}(\Delta) := \sup_{\alpha \in A} d(D_\alpha) < \infty$, where $d(D_\alpha)$ is the diameter of D_α,

(ii) there are only finitely many α such that $K \cap D_\alpha \neq \emptyset$ for any compact set $K \subset \mathbb{R}^d$.

We select a point ξ_α from each D_α, and put $\Gamma = \{\xi_\alpha | \ \alpha \in A\}$, and define the weight function ω by setting $\omega(\xi_\alpha) = \mathrm{vol}(D_\alpha)$.

Then (Γ, ω) is a weighted discrete set, and has constant density $c(\Gamma) = 1$. Indeed,

$$\sigma_\epsilon(f, \Gamma, \omega) = \sum_{\alpha \in A} f(\epsilon \xi_\alpha) \mathrm{vol}(\epsilon D_\alpha)$$

is a classical Riemann sum, so that $\lim_{\epsilon \to 0} \sigma_\epsilon(f, \Gamma, \omega) = \int_{\mathbb{R}^d} f(x) dx$

Let $\Gamma \subset \mathbb{R}^d$ be a lattice group, i.e. a subgeroup of $\mathbb{R}^d$ generated by a basis $\mathrm{a}_1, \ldots, \mathrm{a}_d$ of the vector space $\mathbb{R}^d$;

$$\Gamma = \{k_1 \mathrm{a}_1 + \cdots + k_d \mathrm{a}_d |\ k_1, \ldots, k_d \in \mathbb{Z}\}.$$

Then Γ has constant density $c(\Gamma) = \mathrm{vol}(\mathbb{R}^d / \Gamma)^{-1}$.

In particular, $c(\mathbb{Z}^d) = 1$.

Related to Gauss's theorem is counting primitive lattice points.

Let $\mathbb{Z}^d_{\mathrm{prim}}$ is the set of $(x_1, \ldots, x_d) \in \mathbb{Z}^d$ such that $\gcd(|x_1|, \ldots, |x_d|) = 1$.

Theorem 1 $\mathbb{Z}^d_{\mathrm{prim}}$ has constant density $c(\mathbb{Z}^d_{\mathrm{prim}}) = \zeta(d)^{-1}$; that is,

$$\lim_{\epsilon \to +0} \sum_{\mathrm{z} \in \mathbb{Z}^d_{\mathrm{prim}}} \epsilon^d f(\epsilon \mathrm{z}) = \zeta(d)^{-1} \int_{\mathbb{R}^d} f(\mathrm{x}) d\mathrm{x}. \tag{2}$$

Here $\zeta(s) = \sum_{n=1}^{\infty} n^{-s}$ is the zeta function, and $\zeta(2) = \pi^2/6$.

Applying this theorem to the indicator function f for $\{(x, y) \in \mathbb{R}^2 | 0 \leq x, y \leq 1\}$, we get Gauss's theorem.

In connection with Theorem 1, it is perhaps worthwhile to make reference to the Siegel mean value theorem.

Let $g \in \mathrm{SL}_d(\mathbb{R})$. For a bounded Riemann integrable function f on $\mathbb{R}^d$ with compact support, we consider

$$\Phi(g) = \sum_{\mathrm{z}\in\mathbb{Z}^d\setminus\{0\}} f(g\mathrm{z}), \quad \Psi(g) = \sum_{\mathrm{z}\in\mathbb{Z}^d_{\mathrm{prim}}} f(g\mathrm{z}).$$

Both functions Φ and Ψ are $\mathrm{SL}_d(\mathbb{Z})$-invariant with respect to the right action of $\mathrm{SL}_d(\mathbb{Z})$ on $\mathrm{SL}_d(\mathbb{R})$, so that these are identified with functions on the coset space $\mathrm{SL}_d(\mathbb{R})/\mathrm{SL}_d(\mathbb{Z})$. Recall that $\mathrm{SL}_d(\mathbb{R})/\mathrm{SL}_d(\mathbb{Z})$ has finite volume with respect to the measure dg induced from the Haar measure on $\mathrm{SL}_d(\mathbb{R})$. We assume $\int_{\mathrm{SL}_d(\mathbb{R})/\mathrm{SL}_d(\mathbb{Z})} 1\ dg = 1$. Then the Siegel theorem asserts

$$\int_{\mathrm{SL}_d(\mathbb{R})/\mathrm{SL}_d(\mathbb{Z})} \Big(\sum_{\mathrm{z}\in\mathbb{Z}^d\setminus\{0\}} f(g\mathrm{z})\Big) dg = \int_{\mathbb{R}^d} f(\mathrm{x})d\mathrm{x},$$

$$\int_{\mathrm{SL}_d(\mathbb{R})/\mathrm{SL}_d(\mathbb{Z})} \Big(\sum_{\mathrm{z}\in\mathbb{Z}^d_{\mathrm{prim}}} f(g\mathrm{z})\Big) dg = \zeta(d)^{-1} \int_{\mathbb{R}^d} f(\mathrm{x})d\mathrm{x}.$$

Pythagorean triples and Eisenstein triples

Using the notion of constant density, we can investigate the asymptotic behaviors of Pythagorean triple and Eisenstain triple.

A Pythagorean triple is a triple of positive integers (x, y, z) satisfying the equation $x^2 + y^2 = z^2$. The name stems from the Pythagorean theorem for right triangles, have a long history since the Old Babilonian period in Mesopotamia nearly 4000 years ago.

An Eisenstain triple is a triple of positive integers (x, y, z) satisfying the equation $x^2 + xy + y^2 = z^2$.

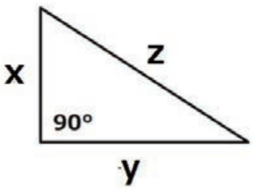

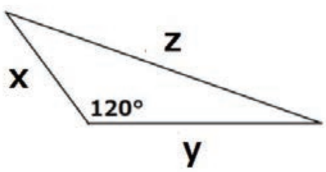

The list of 15 Pythagorean triples exhibited implicitly in the tablet with four columns and fifteen rows, which was written about 1800 BC in cuneiform ("wedge shaped") script.

1. (119, 120, 169)
2. (3367, 3456, 4825)
3. (4601, 4800, 6649)
4. (12709,13500,18541)
5. (65, 72, 97)
6. (319, 360, 481)
7. (2291, 2700, 3541)
8. (799, 960, 1249)
9. (481, 600, 769)
10. (4961, 6480, 8161)
11. (45, 60, 75) $**$
12. (1679, 2400, 2929)
13. (161, 240, 289)
14. (1771, 2700, 3229)
15. (90, 56, 106) $**$

A Pythagorean triple (x, y, z) is called primitive if x, y, z are coprime, i.e. their greatest common divisor is 1, or equivalently they are pair wise coprime. "Primitive" is so named because any Pythagorean triple is generated trivially from the primitive one, i. e., if (x, y, z) is Pythagorean, there are a positive integer ℓ and a primitive (x_0, y_0, z_0) such that $(x, y, z) = (\ell x_0, \ell y_0, \ell z_0)$.

The way to produce primitive Pythagorean triples (PPT) is described as follows: If (x, y, z) is a PPT, then there exist positive integers a, b such that

(i) $a > b$,

(ii) a and b are coprime,

(iii) $a - b \not\equiv 0 \pmod 2$ (i.e. a and b have different parity),

(iv) $(x, y, z) = (a^2 - b^2, 2ab, a^2 + b^2)$ or

$(x, y, z) = (2ab, a^2 - b^2, a^2 + b^2)$.

Conversely, if m and n satisfy (i), (ii), (iii), then $(a^2 - b^2, 2ab, a^2 + b^2)$ and $(2ab, a^2 - b^2, a^2 + b^2)$ are PPTs.

In the table below, due to M. Somos, of PPTs (x, y, z) enumerated in ascending order with respect to z, (x_n, y_n, z_n) is the n-th PPT (we do not discriminate between (x, y, z) and (y, x, z)).

n	x_n	y_n	z_n
1	3	4	5
2	5	12	13
3	15	8	17
4	7	24	25
5	21	20	29
6	35	12	37
7	9	40	41
8	45	28	53
9	11	60	61
10	63	16	65

n	x_n	y_n	z_n
11	33	56	65
12	55	48	73
13	77	36	85
14	13	84	85
15	39	80	89
16	65	72	97
17	99	20	101
18	91	60	109
19	15	112	113
20	117	44	125

$\cdots$

n	x_n	y_n	z_n
1491	4389	8300	9389
1492	411	9380	9389
1493	685	9372	9397
1494	959	9360	9409
1495	9405	388	9413
1496	5371	7740	9421
1497	9393	776	9425
1498	7503	5704	9425
1499	6063	7216	9425
1500	1233	9344	9425

Likewise, one has the notion of primitive Eisenstein triple (PET), and may show that (x, y, z) is a PET if and only if there exist positive integers a, b such that

1. $a > b$,
2. $\gcd(a, b) = 1$,
3. $a - b \not\equiv 0 \pmod 3$,
4. $(x, y, z)) = (a^2 - b^2, a^2 + 2ab, a^2 + ab + b^2)$ or $(a^2 + 2ab, a^2 - b^2, a^2 + ab + b^2)$

Table for PETs

N	x	y	z	N	x	y	z		N	x	y	z
1	3	5	7	11	40	51	79		1991	11481	4760	14461
2	8	7	13	12	11	85	91		1992	3864	12155	14479
3	5	16	19	13	80	19	91		1993	139	14421	14491
4	24	11	31	14	55	57	97		1994	8576	8155	14491
5	7	33	37	15	77	40	103	$\cdots$	1995	695	14137	14497
6	35	13	43	16	24	95	109		1996	5167	10848	14497
7	16	39	49	17	13	120	127		1997	6800	9847	14497
8	9	56	61	18	65	88	133		1998	12032	4063	14497
9	45	32	67	19	120	23	133		1999	973	13992	14503
10	63	17	73	20	91	69	139		2000	1529	13696	14521

What we have interest in is the asymptotic behavior of PPTs (x, y, z) (with respect to z). The numerical observation for PPTs tells us

$$\frac{1}{65}|\{(x,y,z)\ \text{PPT};\ z \le 65\}| = \frac{10}{65} = 0.1538,$$
$$\frac{1}{125}|\{(x,y,z)\ \text{PPT};\ z \le 125\}| = \frac{20}{125} = 0.16,$$
$$\frac{1}{9425}|\{(x,y,z)\ \text{PPT};\ z \le 9425\}| = \frac{1500}{9425} = 0.1591$$

which convinces us that $\frac{1}{N}|\{(x,y,z)\ \text{PPT};\ z \le N\}|$ exists (though the speed of convergence is very slow), and the limit is expected to be equal to $1/2\pi = 0.15915\cdots$.

This is actually true (D. N. Lehmer, 1900), though his proof is by no means easy.

Theorem (Lehmer)

$$\lim_{N\to\infty}\frac{1}{N}|\{(x,y,z)\ \text{PPT};\ z\le N\}| = \frac{1}{2\pi}.$$

For PETs, we have

Theorem (小野公亮; M2)

$$\lim_{N\to\infty}\frac{1}{N}|\{(x,y,z)\ \text{PET};\ z\le N\}| = \frac{\sqrt{3}}{4\pi}.$$

Idea

The above two theorems are consequences of the fact that Γ_2 (resp. Γ_3) has constant density $c(\Gamma_2) = 2/\pi^2$ (resp. $c(\Gamma_3) = 3/2\pi^2$), where

$$\begin{aligned}
\Gamma_1 &= \mathbb{Z}^2_{\text{prim}} = \{(a,b)\in\mathbb{Z}^2 |\, \gcd(a,b)=1\},\\
\Gamma_2 &= \{(a,b)\in\Gamma_1 |\ a-b\equiv 0 \pmod 2\},\\
\Gamma_3 &= \{(a,b)\in\Gamma_1 |\ a-b\equiv 0 \pmod 3\}.
\end{aligned}$$

What we should notice here is that

$$\begin{aligned}
\{(a,b)\in\mathbb{Z}^2 |\, \gcd(a,b)=1,\ a-b\not\equiv 0 \pmod 2\} &= \Gamma_1\backslash\Gamma_2,\\
\{(a,b)\in\mathbb{Z}^2 |\, \gcd(a,b)=1,\ a-b\not\equiv 0 \pmod 3\} &= \Gamma_1\backslash\Gamma_3,
\end{aligned}$$

so that

$$\begin{aligned}
c(\Gamma_1\backslash\Gamma_2) &= c(\Gamma_1)-c(\Gamma_2) = \frac{4}{\pi^2},\\
c(\Gamma_1\backslash\Gamma_3) &= c(\Gamma_1)-c(\Gamma_3) = \frac{9}{2\pi^2}.
\end{aligned}$$

Theorem (Sunada)

$$\lim_{\epsilon \to +0} \sum_{z \in \Gamma_1 \setminus \Gamma_2} \epsilon^2 f(\epsilon z) = \frac{4}{\pi^2} \int_{\mathbb{R}^2} f(x) dx.$$

Theorem (Ono)

$$\lim_{\epsilon \to +0} \sum_{z \in \Gamma_1 \setminus \Gamma_3} \epsilon^2 f(\epsilon z) = \frac{9}{2\pi^2} \int_{\mathbb{R}^2} f(x) dx.$$

In the case of PPT, we apply the theorem to the indicator function f for the set $\{(x,y) \in \mathbb{R}^2 |\ x \geq y \geq 0,\ x^2 + y^2 \leq 1\}$. Then

$$\sum_{z \in \Gamma} \epsilon^2 f(\epsilon z) = \epsilon^2 \big| \{(a,b) \in \mathbb{N}^2 |\ \gcd(a,b) = 1,\ a > b,\ a^2 + b^2 \leq \epsilon^{-2},\ a - b \not\equiv 0 \pmod 2\} \big|.$$

Therefore we obtain

$$\lim_{k \to \infty} \frac{1}{N} | \{(a,b) \in \mathbb{N}^2 |\ \gcd(a,b) = 1,\ a > b,\ a^2 + b^2 \leq N,\ a - b \not\equiv 0 \pmod 2\} \big| = \frac{4}{\pi^2} \cdot \frac{\pi}{8} = \frac{1}{2\pi}.$$

Note that $\big| \{(a,b) \in \mathbb{N}^2 |\ \gcd(a,b) = 1,\ a > b,\ a^2 + b^2 \leq N,\ a - b \not\equiv 0 \pmod 2\} \big|$ coincides with the number of PPT (x,y,z) with $z \leq N$. This observation leads us to $\lim_{N \to \infty} \frac{1}{N} |\{(x,y,z) \text{ PPT};\ z \leq N\} = \frac{1}{2\pi}$.

Corollary For a rational point $(p,q) \in S^1(\mathbb{Q})(= S^1 \cap \mathbb{Q}^2)$, define the height $h(p,q)$ to be the minimal positive integer h such that $(hp, hq) \in \mathbb{Z}^2$. Then for any arc A in S^1, we have

$$\left|\{(p,q) \in A \cap \mathbb{Q}^2 |\ h(p,q) \leq h\}\right| \sim \frac{2 \cdot \mathrm{length}(A)}{\pi^2} h \quad (h \to \infty),$$

and hence rational points are equidistributed on the unit circle, i. e.

$$\lim_{h\to\infty} \frac{\left|\{(p,q) \in A \cap \mathbb{Q}^2 |\ h(p,q) \leq h\}\right|}{\left|\{(p,q) \in S^1 \cap \mathbb{Q}^2 |\ h(p,q) \leq h\}\right|} = \frac{\mathrm{length}(A)}{2\pi}.$$

This theorem is stated in Duke's paper published in Ramanujan Journal, 7(2003). He suggests that this can be proved by using tools from the theory of L-functions combined with Weyl's famous criterion for equidistribution on the circle.

In the case of PET, we take the indicator function f for the set $\{(x,y) \in \mathbb{R}^2 |\ x \geq y \geq 0,\ x^2 + xy + y^2 \leq 1\}$. Then

$$\sum_{\mathrm{z}\in\Gamma} \epsilon^2 f(\epsilon \mathrm{z}) = \epsilon^2 \big|\{(a,b) \in \mathbb{N}^2 |\ \gcd(a,b) = 1,\ a > b,$$
$$a^2 + ab + b^2 \leq \epsilon^{-2},\ a - b \not\equiv 0 \pmod 3\}\big|.$$

Therefore we obtain

$$\lim_{k\to\infty} \frac{1}{N} \big|\{(a,b) \in \mathbb{N}^2 |\ \gcd(a,b) = 1,\ a > b,\ a^2 + ab + b^2 \leq N,$$
$$a - b \not\equiv 0 \pmod 3\}\big| = \frac{9}{2\pi^2} \cdot \frac{\pi}{6\sqrt{3}} = \frac{\sqrt{3}}{4\pi}.$$

Note that $\big|\{(a,b) \in \mathbb{N}^2 |\ \gcd(a,b) = 1,\ a > b,\ a^2+ab+b^2 \leq N,\ a-b \not\equiv 0 \pmod 3\}\big|$ coincides with the number of PET (x,y,z) with $z \leq N$. This observation leads us to Ono's theorem.

Summation formulae

I gave three examples of discrete sets $\mathbb{Z}^d_{\mathrm{prim}}$, Γ_2, Γ_3 with constant density. The proof that these discrete sets have constant density relies on the summation formulae derived from the so-called Inclusion-Exclusion Principle (IEP).

To state the formulae, we need the Möbius function $\mu(k)$ defined by

$$\mu(k) = \begin{cases} 1 & (k = 1) \\ (-1)^r & (k = p_{i_1} \cdots p_{i_r};\ i_1 < \cdots < i_r) \\ 0 & (\text{otherwise}), \end{cases}$$

where $p_1 < p_2 < \cdots$ are all primes enumerated into ascending order. This is related to the zeta function by the formula

$$\zeta(s)^{-1} = \sum_{k=1}^{\infty} \frac{\mu(k)}{k^s}.$$

$$\sum_{\mathrm{z} \in \mathbb{Z}^d_{\mathrm{prim}}} f(\mathrm{z}) = \sum_{k=1}^{\infty} \mu(k) \sum_{\mathrm{w} \in \mathbb{Z}^d \setminus \{0\}} f(k\mathrm{w}) \quad (\text{classical}),$$

$$\sum_{\mathrm{z} \in \Gamma_2} f(\mathrm{z}) = \sum_{k=1}^{\infty} \mu(k) \sum_{h=0}^{\infty} \sum_{\mathrm{w} \in (2\mathbb{Z}+1)^2} f(k2^h\mathrm{w}) \quad (\text{Sunada}),$$

$$\sum_{\mathrm{z} \in \Gamma_3} f(\mathrm{z}) = \sum_{k=1}^{\infty} \mu(k) \sum_{h=0}^{\infty} \sum_{\mathrm{w} \in (3\mathbb{Z}+1)^2 \coprod (3\mathbb{Z}-1)^2} f(k3^h\mathrm{w}) \quad (\text{Ono}).$$

where f is a function on $\mathbb{R}^d$ with compact support (thus both sides are finite sums).

Inclusion-Exclusion Principle

Inclusion-Exclusion Principle (IEP) is a powerful tool to approach general counting problems involving aggregation of things that are not mutually exclusive.

It is a generalization of the obvious equality

$$
\begin{aligned}
&|A_1 \cup A_2 \cup A_3| \\
= \; &|A_1| + |A_2| + |A_3| \\
&-|A_1 \cap A_2| - |A_2 \cap A_3| - |A_3 \cap A_1| \\
&+|A_1 \cap A_2 \cap A_3|
\end{aligned}
$$

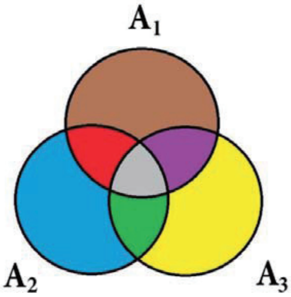

We now formulate the IEP from a general viewpoint.

Let $\{A_i\}_{i=1}^{\infty}$ be a family of subsets of a set X where X and A_i are not necessarily finite.

Let f be a real-valued function with finite support defined on X (in the practice, we consider a family of functions). We assume that there exists N such that if $i > N$, then $A_i \cap \operatorname{supp} f = \emptyset$, i.e. $f(x) = 0$ for $x \in A_i$.

From now on, for a subset A of X, we use the symbol A^c, meaning the complement of A in X.

Theorem (IEP)

$$\sum_{x\in\bigcap_{i=1}^{\infty} A_i^c} f(x) = \sum_{h=0}^{\infty}(-1)^h \sum_{i_1<\cdots<i_h} \sum_{x\in A_{i_1}\cap\cdots\cap A_{i_h}} f(x) \tag{3}$$

$$\left(= \sum_{h=0}^{N}(-1)^h \sum_{i_1<\cdots<i_h} \sum_{x\in A_{i_1}\cap\cdots\cap A_{i_h}} f(x) \right),$$

where, for $h = 0$, the term $\displaystyle\sum_{i_1<\cdots<i_h} \sum_{x\in A_{i_1}\cap\cdots\cap A_{i_h}} f(x)$ should be understood as $\displaystyle\sum_{x\in X} f(x)$.

In applying this theorem to the summation formulae, we need tricky choices of X and $\{A_i\}_{i=1}^{\infty}$.

The proof for $\mathbb{Z}^d_{\mathrm{prim}}$ goes as follows. Consider the case that

$$X = \mathbb{Z}^d\backslash\{0\}, \quad A_h = \{(x_1,\ldots,x_d)\in X|\ p_h|x_1,\ldots,p_h|x_d\}.$$

Then $\displaystyle\bigcap_{h=1}^{\infty} A_h^c = \mathbb{Z}^d_{\mathrm{prime}}$. We also easily observe

$$A_{h_1}\cap\cdots\cap A_{h_k} = p_{h_1}\cdots p_{h_k}X.$$

Applying the theorem above to this case, we have

$$\begin{aligned}\sum_{\mathrm{z}\in\mathbb{Z}^d_{\mathrm{prime}}} f(\mathrm{z}) &= \sum_{k=0}^{\infty}(-1)^k \sum_{h_1<\cdots<h_k} \sum_{\mathrm{w}\in\mathbb{Z}^d\backslash\{0\}} f(p_{h_1}\cdots p_{h_k}\mathrm{w}) \\ &= \sum_{k=1}^{\infty}\mu(k) \sum_{\mathrm{w}\in\mathbb{Z}^d\backslash\{0\}} f(k\mathrm{w}).\end{aligned}$$

Are $\mathbb{Z}^d_{\text{prim}}$, Γ_2, Γ_3 quasicrystals?

Answer: From the summatin formulae, it follows that

(1) Γ_2 and Γ_3 are quasicrystals, and

(2) $\mathbb{Z}^d_{\text{prim}}$ is a near quasicrystal.

Conjecture Let p be a prime, and let $a_1, \ldots, a_d$ be integers satisfying

$$\gcd(a_1, \ldots, a_d) = 1 \text{ and } p \not| a_i \quad (i = 1, \ldots, d)$$

Then

$$\{(x_1, \ldots, x_d) \in \mathbb{Z}^d \,|\, a_1x_1 + \cdots + a_dx_d \equiv 0 \ (\mathrm{mod}\, p)\}$$

is a quasicrystal.

What are quasicrystals and "near"-quasicrystals?

A quasicrystals is a form of solid matter whose atoms are arranged like those of a crystal but assume patterns that do not exactly repeat themselves.

The interest in quasicrystals arose when in 1984 Schechtman and others discovered materials whose X-ray diffraction spectra had sharp spots indicative of long range order. Soon after the announcement of their discovery, material scientists began intensive studies of quasicrystals from empirical and theoretical sides. On the other hand, the theoretical discovery of quasicrystal structures was already made by R. Penrose in 1973.

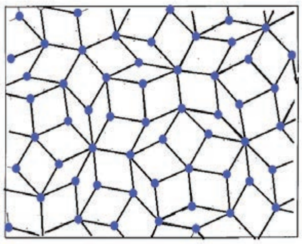

At the moment, there are several ways to define quasicrystals mathematically. As a matter of fact, an official nomenclature has not yet been agreed upon.

Definition

We adopt the following definition for quasicrystals.

Formal definition: (1) A discrete set $\Gamma \subset \mathbb{R}^d$ is said to be a quasicrystal if a generalized Poisson summation formula holds for Γ; namely there exist a countable subset $\Lambda \subset \mathbb{R}^d$ and a sequence $\{a(\xi)\}_{\xi\in\Lambda}$ such that

$$\sum_{z\in\Gamma} f(z) \sim \sum_{\xi\in\Lambda} a(\xi)\hat{f}(\xi) \tag{4}$$

for every $f \in C_0^\infty(\mathbb{R}^d)$. Here $\hat{f}$ is the Fourier transform of f:

$$\hat{f}(\xi) = \int_{\mathbb{R}^d} f(x)e^{-2\pi\sqrt{-1}\langle x,\xi\rangle}dx.$$

(2) Γ is said to be a near-quasicrystal provided that (4) holds for every function f in a "large" proper subspace of $C_0^\infty(\mathbb{R}^d)$

Caution: Λ is not necessarily discrete. Thus the right-hand side may not converge in the ordinary sense. The issue is how to justify the formula (4).

Classical Poisson summation formula: Let Γ be a lattice group. Poisson summation formula tells us

$$\sum_{z\in\Gamma} f(z) = \mathrm{vol}(\mathbb{R}^d/\Gamma)^{-1}\sum_{\xi\in\Lambda} \hat{f}(\xi). \tag{5}$$

Here $\Lambda = \{\xi\in\mathbb{R}^d \mid \langle\xi, z\rangle \in \mathbb{Z} \text{ for every } z \in \Gamma\}$, the dual lattice of Γ.

Generalized Poisson summation formula: We say that a generalized Poisson summation holds for a discrete set Γ if there exist a family of discrete subsets $\{\Lambda_N\}_{N=1}^\infty$ of Λ and functions $a_N(\xi)$ defined on Λ_N such that

(i) $\displaystyle\bigcup_{N=1}^\infty \Lambda_N = \Lambda,$

(ii) $\displaystyle\sum_{\xi\in\Lambda_N} a_N(\xi)\hat{f}(\xi)$ converges absolutely.

(iii) $\displaystyle\lim_{N\to\infty} a_N(\xi) = a(\xi),$

(iv) $\displaystyle\sum_{z\in\Gamma} f(z) = \lim_{N\to\infty}\sum_{\xi\in\Lambda_N} a_N(\xi)\hat{f}(\xi).$

Quasicrystals constructed by the cut and project method

Let L be a lattice in $\mathbb{R}^N = \mathbb{R}^d \times \mathbb{R}^{N-d}$ $(N > d)$, and let W be a compact domain (called a window) in $\mathbb{R}^{N-d}$. We denote by p_d and p_{N-d} the orthogonal projections of $\mathbb{R}^N$ onto $\mathbb{R}^d$ and $\mathbb{R}^{N-d}$, respectively. We assume that $p_{N-d}(L)$ is dense, and p_d is invertible on $p_d(L)$. Then the model set Γ associated with L and W is defined to be $p_d\big(L \cap (\mathbb{R}^d \times W)\big)$.

We put $\Lambda = p_d(L^*)$. It should be remarked that for each $\xi \in \Lambda$, there exists a unique $\xi' \in \mathbb{R}^{N-d}$ such that $(\xi, \xi') \in L^*$. Having this in mind, we define

$$a(\xi) = \mathrm{vol}(D_L)^{-1}\widehat{\chi_W}(\xi') \quad (\xi \in \Lambda,\ (\xi, \xi') \in L^*).$$

We then get

$$\sum_{z\in\Gamma} f(z) \sim \sum_{\xi\in\Lambda} a(\xi)\hat{f}(\xi).$$

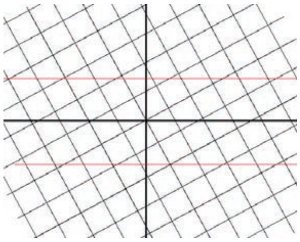

$\mathbb{Z}^d_{\mathrm{prim}}$ is a near quasicrystal

Let $V = \{f \in C_0^\infty(\mathbb{R}^d);\ f(0) = 0\}$. Applying the classical Poisson formula, we obtain

$$\sum_{z\in\mathbb{Z}^d_{\mathrm{prime}}} f(z) = \sum_{k=1}^{\infty}\mu(k) \sum_{w\in\mathbb{Z}^d\setminus\{0\}} f(kw) = \sum_{k=1}^{\infty}\mu(k)\sum_{w\in\mathbb{Z}^d} f(kw)$$

$$= \sum_{k=1}^{N}\mu(k)k^{-d}\sum_{\substack{\xi\in\mathbb{Q}^d\\ n_\xi | k}} \hat{f}(\xi)$$

for $f \in V$, where $\mathrm{supp}\, f \subset B_N(x)$.

For $\xi \in \mathbb{Q}^d$, we write $\xi = \left(\frac{b_1}{a_1}, \dots, \frac{b_d}{a_d}\right)$ with $a_i > 0$, $b_i \in \mathbb{Z}$, and $\gcd(a_i, b_i) = 1$. Put

$$n_\xi = \mathrm{lcm}(a_1, \dots, a_d).$$

To transform further this, we put

$$a_N(\xi) = \frac{\mu(n(\xi))}{n(\xi)^d} \sum_{\substack{1 \le \ell \le N/n(\xi) \\ \gcd(\ell, n(\xi))=1}} \frac{\mu(\ell)}{\ell^d}, \quad \Lambda_N = \{\xi \in \mathbb{Q}_N^d \mid \mu(n(\xi)) \neq 0\}.$$

Then

$$\sum_{z \in \mathbb{Z}^d_{\mathrm{prim}}} f(z) = \sum_{\xi \in \Lambda_N} a_N(\xi) \hat{f}(\xi).$$

Furthermore, if we put

$$\Lambda = \{\xi \in \mathbb{Q}^d | \mu(n(\xi)) \neq 0\}, \quad a(\xi) = \frac{\mu(n_\xi)}{n(\xi)^d} \zeta(d)^{-1} \prod_{p | n(\xi)} \left(1 - p^{-d}\right)^{-1} \quad (\xi \in \Lambda),$$

then

$$\Lambda = \bigcup_{N=1}^{\infty} \Lambda_N, \qquad \lim_{N \to \infty} a_N(\xi) = \frac{\mu(n(\xi))}{n(\xi)^d} \sum_{\substack{\ell=1 \\ \gcd(\ell, n(\xi))=1}}^{\infty} \frac{\mu(\ell)}{\ell^d} = a(\xi).$$

Thus $\mathbb{Z}^d_{\mathrm{prim}}$ is a near-quasicrystal.

In the case of Γ_2 and Γ_3, we note that $(2\mathbb{Z}+1)^2$ and $(3\mathbb{Z} \pm 1)^2$ are lattices. Thus one may apply directly the classical Poisson formula to obtain

$$\sum_{z \in \Gamma_2} f(z) = \sum_{\xi \in \mathbb{Q}^2_{2N}} \Big(\sum_{\substack{k \ge 1, h \ge 0 \\ n(\xi) | k 2^{h+1}}}^{k 2^h \le N} \frac{\mu(k)}{k^2} \frac{1}{2^{2h+2}} e^{\pi i k 2^{h+1} \langle \xi, 1 \rangle} \Big) \hat{f}(\xi),$$

where supp $f \subset B_N(0)$ and $1 = (1, 1)$. This implies that Γ_2 is a quasicrystal. One can check that Γ_2 is a quasicrystal as well.

Counting things is a great favorite of children, and mathematicians as well, whatever the things are

Thanks a lot !

「マス・フォア・インダストリ研究」シリーズ刊行にあたり

本シリーズは，平成 23 年 4 月に設立された九州大学マス・フォア・ インダストリ研究所(IMI)が，平成 25 年 4 月に共同利用・共同研究拠点「産業数学の先進的・基礎的共同研究拠点」として，文部科学大臣より認定を受けたことにともない刊行するものである．本シリーズでは，主として，マス・フォア・インダストリに関する研究集会の会議録，共同研究の成果報告等を出版する．各巻はマス・フォア・インダストリの最新の研究成果に加え，その新たな視点からのサーベイ及びレビューなども収録し，マス・フォア・インダストリの展開に資するものとする．

平成 30 年 10 月

マス・フォア・インダストリ研究所

所長 佐伯　修

結晶転位の先進数理解析

マス・フォア・インダストリ研究 No.11, IMI, 九州大学

ISSN 2188-286X

発行日　2019 年 1 月 7 日

編　集　松谷 茂樹，佐伯 修，中川 淳一，濱田 裕康，上坂 正晃

発　行　九州大学マス・フォア・インダストリ研究所

〒819-0395 福岡市西区元岡 744

九州大学数理・IMI 事務室

TEL 092-802-4402　FAX 092-802-4405

URL http://www.imi.kyushu-u.ac.jp/

印　刷　社会福祉法人　福岡コロニー

〒811-0119　福岡県糟屋郡新宮町緑ケ浜 1 丁目 11 番 1 号

TEL 092-962-0764　FAX 092-962-0768

シリーズ既刊

Issue	Author／Editor	Title	Published
マス・フォア・インダストリ研究　No.1	穴田 啓晃 安田 貴徳 Xavier Dahan 櫻井 幸一	Functional Encryption as a Social Infrastructure and Its Realization by Elliptic Curves and Lattices	26 February 2015
マス・フォア・インダストリ研究　No.2	滝口 孝志 藤原 宏志	Collaboration Between Theory and Practice in Inverse Problems	12 March 2015
マス・フォア・インダストリ研究　No.3	筧 三郎	非線形数理モデルの諸相：連続，離散，超離散，その先 (Various aspects of nonlinear mathematical models : continuous, discrete, ultra-discrete, and beyond)	24 March 2015
マス・フォア・インダストリ研究 No.4	穴田　啓晃 安田　貴徳 櫻井　幸一 寺西　勇	Next-generation Cryptography for Privacy Protection and Decentralized Control and Mathematical Structures to Support Techniques	29 January 2016
マス・フォア・インダストリ研究 No.5	藤原　宏志 滝口　孝志	Mathematical Backgrounds and Future Progress of Practical Inverse Problems	1 March 2016
マス・フォア・インダストリ研究 No.6	松谷　茂樹 佐伯　修 中川　淳一 上坂　正晃 濵田　裕康	結晶のらせん転位の数理	10 January 2017
マス・フォア・インダストリ研究 No.7	滝口　孝志 藤原　宏志	Collaboration among mathematics, engineering and industry on various problems in infrastructure and environment	1 March 2017
マス・フォア・インダストリ研究 No.8	藤原　宏志 滝口　孝志	Practical inverse problems based on interdisciplinary and industry-academia collaboration	20 February 2018
マス・フォア・インダストリ研究 No.9	阿部　拓郎 高島　克幸 縫田　光司 安田　雅哉	代数的手法による数理暗号解析 Workshop on analysis of mathematical cryptography via algebraic methods	1 March 2018
マス・フォア・インダストリ研究 No.10	阿部　拓郎 落合　啓之 高島　克幸 縫田　光司 安田　雅哉	量子情報社会に向けた数理的アプローチ Mathematical approach for quantum information society	26 December 2018

Institute of Mathematics for Industry
Kyushu University

九州大学マス・フォア・インダストリ研究所

〒819-0395 福岡市西区元岡744
URL http://www.imi.kyushu-u.ac.jp/